



**WYDZIAŁ BIOLOGII
i OCHRONY ŚRODOWISKA**
Uniwersytet Łódzki

Stacjonarne Studia Doktoranckie Genetyki Molekularnej,
Cytogenetyki i Biofizyki Medycznej

Kamila Białkowska

**Opracowanie i wdrożenie metod
badawczych do oceny wpływu
materiałów na komórki hodowane
w hodowlach 3D, na przykładzie
wykorzystania dendrymerów jako
nośnika siRNA**

Development and implementation of research
methods for evaluation of the impact of materials on
cells cultured in 3D, on the example of the use of
dendrimers as a carrier of siRNA

Praca doktorska
wykonana w Katedrze Biofizyki Ogólnej
Instytutu Biofizyki

Promotor: dr hab. Katarzyna Miłowska, prof. UŁ
Promotor pomocniczy: dr inż. Piotr Komorowski

→ Łódź, 2022

*Składam serdeczne podziękowania Pani Promotor **dr hab. Katarzynie Miłowskiej prof. UŁ** za wszystkie owocne i merytoryczne rozmowy, za poświęcony czas, nawet w dni wolne, oraz za cierpliwość i wyrozumiałość.*

*Dziękuję również **dr inż. Piotrowi Komorowskiemu** za wsparcie w pogodzeniu obowiązków zawodowych z realizacją doktoratu wdrożeniowego.*

*Szczególne podziękowania dla Pani **prof. dr hab. Marii Bryszewskiej** za pomoc w dopełnieniu formalności umożliwiających realizację doktoratu wdrożeniowego.*

*Dziękuję **koleżankom i kolegom** z „Bionanoparku” za wiarę we mnie i zapewnienie, „że dam radę”, kiedy myślałam, że „nie dam rady”.*

*Dziękuję **koleżankom i kolegom** z Katedry Biofizyk Ogólnej za współpracę i pomoc.*

*Dziękuję również moim **bliskim** za wsparcie.*

Praca wykonana w ramach projektu Ministerstwa Nauki i Szkolnictwa Wyższego (obecnie Ministerstwa Edukacji i Nauki) pt. „*Doktorat wdrożeniowy*”.



Ministerstwo
Edukacji i Nauki

Praca wykonana we współpracy z:

- firmą „*Bionanopark*” Sp. z o. o. (<http://bionanopark.pl/>)

BIONANOPARK

- Katedrą Chemii Organicznej i Nieorganicznej Uniwersytetu Alcala (Hiszpania)



Spis treści

Dorobek naukowy	5
1. Wstęp	8
2. Cele pracy.....	11
3. Opracowanie metod pozwalających na określenie wpływu substancji/materiałów/związków na komórki hodowane w 3D.....	13
3.1. Materiały i metody.....	13
3.2. Optymalizacja warunków hodowli 3D.....	13
3.3. Ocena przydatności popularnych testów cytotoksyczności w badaniach na hodowłach 3D	19
3.3.1. Testy XTT i MTT.....	19
3.3.2. Test uszkodzeń DNA.....	20
3.4. Hodowla 3D na płytkach 96-dółkowych	20
4. Omówienie prac wchodzących w zakres rozprawy doktorskiej.....	21
5. Podsumowanie	24
6. Wniosek	25
7. Streszczenie	26
8. Abstract	28
9. Bibliografia.....	30
Prace wchodzące w skład rozprawy doktorskiej.....	34
Oświadczenia współautorów	82

Dorobek naukowy

- **Artykuły naukowe wchodzące w skład rozprawy doktorskiej**

W skład rozprawy doktorskiej wchodzi 3 prace opublikowane w recenzowanych czasopismach: jedna publikacja przeglądowa i dwie doświadczalne:

1. **Białkowska K.***, Komorowski P., Bryszewska M., Miłowska K., Spheroids as a Type of Three-Dimensional Cell Cultures—Examples of Methods of Preparation and the Most Important Application, *Int. J. Mol. Sci.*, 2020, 21(17):6225

➔ Praca przeglądowa

➔ Impact factor: 5,924

➔ Punkty MEiN: 140

2. **Białkowska K.***, Miłowska K., Michlewska S., Sokołowska P., Komorowski P., Lozano-Cruz T., Gomez-Ramirez R., de la Mata F.J., Bryszewska M., Interaction of Cationic Carbosilane Dendrimers and Their siRNA Complexes with MCF-7 Cells, *Int. J. Mol. Sci.*, 2021, 22(13):7097

➔ Praca oryginalna

➔ Impact factor: 5,924

➔ Punkty MEiN: 140

3. **Białkowska K.***, Komorowski P., Gomez-Ramirez R., de la Mata F.J., Bryszewska M., Miłowska K. Interaction of Cationic Carbosilane Dendrimers and Their siRNA Complexes with MCF-7 Cells Cultured in 3D Spheroids; *Cells*, 2022, 11: 1697

➔ Praca oryginalna

➔ Impact factor: 6,600

➔ Punkty MEiN: 140

* autor korespondencyjny

Łączny IF prac wchodzących w skład rozprawy doktorskiej: **18,448**.

Suma punktów MEiN: **420**.

- **Pozostałe artykuły**

1. Siatkowska M., Sokołowska P., **Białkowska K.**, Zimon A., Grala M., Rosowski M., Kądzioła-Długołęcka K., Komorowski P., Makowski K., Reda D., Walkowiak B. Impact of micron-sized diamond particles on barrier cells of the human small intestine, *Diam. Relat. Mater.*, 2021, 114:108307;

- ➔ Praca oryginalna;

- ➔ Impact factor: 3,315;

- ➔ Punkty MEiN: 100.

2. Sokołowska P., Siatkowska M., **Białkowska K.**, Rosowski M., Komorowski P., Walkowiak B., Osteosarcoma cells in early and late stages as cancer *in vitro* progression model for assessing the responsiveness of cells to silver nanoparticles, *J. Biomed. Mater. Res. B Appl. Biomater.*, 2022, 110:1319-1334;

- ➔ Praca oryginalna;

- ➔ Impact factor: 3,368;

- ➔ Punkty MEiN: 140.

- **Komunikaty zjazdowe**

1. **Białkowska K.**, Sokołowska P., Siatkowska M., Działoszyńska K., Rosowski M., Żak W., Wasiak T., Komorowski P., Makowski K., Walkowiak B., Ocena wrażliwości komórek nowotworowych na nanocząstki srebra na przykładzie komórek kostniakomięsaka linii Saos-2 w pasażach niskich i wysokich, IV Ogólnopolska Konferencja Doktorantów Nauk o Życiu „Bioopen”, 24-25.05.2018, Łódź, Polska; wystąpienie ustne;

2. **Białkowska K.**, Komorowski P., Michlewska S., Miłowska K., Therapeutic use of siRNA complexed with dendrimers, Imaging of Diagnostic and Therapeutic Biomarkers in Oncology, 25-28.09.2019, Le Bono, Francja; wystąpienie ustne;

3. **Białkowska K.**, Komorowski P., Miłowska K., Zastosowanie trójwymiarowych hodowli komórkowych (3D) w badaniach biologicznych, Ogólnopolska Konferencja Interdyscyplinarna Eureka, 09-10.01.2020, Krzyżowa, Polska; wystąpienie ustne;

4. **Białkowska K.**, Komorowski P., Miłowska K., Kompleksy dendrymerów z siRNA jako potencjalne narzędzie do walki z nowotworami, Interdyscyplinarna Konferencja Naukowa TYGIEL, 24-27-09.2020, on-line; wystąpienie ustne;

5. **Białkowska K.**, Komorowski P., Miłowska K., Wpływ dendrymerów karbokrzemowych oraz ich kompleksów z siRNA na komórki raka piersi (MCF-7) hodowane w 3D, I Międzynarodowa Multidyscyplinarna Konferencja Doktorantów Uniwersytetu Szczecińskiego MKDUS 2.0, 23-25.06.2021, on-line; wystąpienie ustne.

- **Staż zagraniczny**

1. Staż naukowy w ramach Projektu PROM na Uniwersytecie Łódzkim finansowanego przez Narodową Agencję Wymiany Akademickiej, Uniwersytet w Atenach, Ateny, Grecja, 10-28.06.2019.

- **Nagrody**

1. Wyróżnienie abstraktu i nagroda w postaci dofinansowania udziału w konferencji Imaging of Diagnostic and Therapeutic Biomarkers in Oncology, 25-28.09.2019, Le Bono, Francja.

- **Udział w projektach**

1. Projekt w ramach konkursu Program Badań Stosowanych III (PBS) „Innowacyjna technologia chirurgiczna z urządzeniem implantowanym (IP) rozszerzająca efektywne leczenie kręgosłupa degeneracyjnego – badania modelowe”, 2015 – 2018;
2. Projekt w ramach konkursu Programu Operacyjnego Inteligentny Rozwój „Projektowanie i wytwarzanie spersonalizowanych implantów medycznych” akronim Custom-ITAP, 2018 – 2021.

- **Działalność promocyjna**

3. Uczestnictwo w „Nocy Biologów” w latach 2018-2019;
4. Uczestnictwo w „Instytucie Kreatywnej Biologii” w latach 2019-2020.

1. Wstęp

Hodowle komórkowe są znane od lat 40-tych XX w. (Goodman i wsp., 2008) i są wykorzystywane do badań nad biologią komórki czy mechanizmów komórkowych (do Amaral i wsp., 2011). Komórki mogą być pozyskiwane do hodowli bezpośrednio z tkanek i po odpowiednim przygotowaniu umieszczone w sztucznym środowisku hodowlanym lub zakupione jako linie komórkowe, już wcześniej pozyskane przez badaczy. Komórki są hodowane w medium zawierającym wymagane składniki odżywcze, czynniki wzrostu czy hormony, w specjalnych naczyniach umieszczonych w inkubatorach, wewnątrz których utrzymywane są ściśle kontrolowane warunki temperatury, która najczęściej wynosi 37 °C, a także wilgotności i stężenia CO₂ (Antoni i wsp., 2015). Komórki są przytwierdzone do płaskiej powierzchni naczynia, szklanego lub z tworzywa sztucznego, w dwuwymiarowym środowisku, tworząc tzw. monowarstwy. Taka metoda hodowli jest najbardziej powszechna. Przez wiele lat była nieoceniona jako model przeróżnych chorób (Andersen i wsp., 2015; Centeno i wsp., 2018). Ten rodzaj hodowli ma jednak pewne ograniczenia. Wzrost komórek na płaskich powierzchniach może zmieniać ich metabolizm i funkcjonowanie (Andersen i wsp., 2015). W dwuwymiarowym środowisku ograniczone są interakcje pomiędzy komórkami oraz pomiędzy komórkami a macierzą zewnątrzkomórkową (ECM, ang. *extracellular matrix*) (do Amaral i wsp., 2011; Lee i wsp., 2009). Ponadto, środowisko komórek może zmieniać ich fenotyp, a co za tym idzie wpływać na ich odpowiedź na badane substancje, jak np. leki (Goodman i wsp., 2008).

Komórki w organizmach funkcjonują w środowisku trójwymiarowym, co jest kluczowe dla ich metabolizmu i wzrostu. Fenotyp i funkcje komórek są zależne od interakcji z sąsiadującymi komórkami, z macierzą zewnątrzkomórkową oraz białkami (Lee i wsp., 2009). Wspomniane interakcje komórka-komórka oraz komórka-ECM różnią się pomiędzy hodowlami 2D i 3D oraz pomiędzy warstwami w hodowli trójwymiarowej, a to z kolei może wpływać, np. na wyniki cytotoksyczności podczas badania przeróżnych substancji (Moshksayan i wsp., 2018). To powoduje, że testowanie toksyczności materiałów i substancji na hodowlach 2D nie pozwala na uzyskanie rezultatów, które można odnieść do tych mogących wystąpić w organizmie (Edmondson i wsp., 2014; Lee i wsp., 2009).

Hodowle 3D zdecydowanie lepiej odzwierciedlają naturalne mikrośrodowisko funkcjonowania komórek. Morfologia i fizjologia komórek w hodowlach 3D różni się

w porównaniu do hodowli dwuwymiarowych, w testach wykazując odpowiedzi, które są zbliżone do tych uzyskiwanych *in vivo* (Edmondson i wsp., 2014).

Trójwymiarowe hodowle komórkowe są wykorzystywane w badaniu procesów zachodzących w komórkach nowotworowych, w badaniu różnicowania komórek, w ocenie cytotoksyczności substancji i efektywności potencjalnych leków (Kitel i wsp., 2013). Z tego powodu hodowle 3D wydają się być obiecującym narzędziem, wypełniającym lukę pomiędzy eksperymentami z użyciem hodowli 2D a eksperymentami na zwierzętach (Lv i wsp., 2017). Udowodniono, że trójwymiarowe hodowle komórkowe wykazują zwiększony poziom tkankowo specyficznych markerów, przejawiają charakterystyczne dla tkanek funkcje oraz różnią się profilem ekspresji genów względem hodowli 2D (Vantangoli i wsp., 2015). Porównano komórki raka piersi linii MCF-7 hodowane w systemach 2D i 3D. Wykazano, że w modelu 3D ma miejsce zwiększona ekspresja mRNA (z ang. *messenger RNA*) dla keratyny 8 i keratyny 19, oraz zmniejszona ekspresja keratyny 14 i wimentyny (Vantangoli i wsp., 2015). Hodowle 3D w postaci sferoidów, podobnie do guzów litych, ze względu na swoją budowę, tworzą barierę, przez którą muszą przedostać się testowane substancje (Sant i Johnston, 2017).

W związku z powyższym, do badań wykonanych w niniejszej pracy wykorzystano komórki raka piersi linii MCF-7 hodowane w 3D, w postaci sferoidów, co odzwierciedlało warunki funkcjonowania guza. W badaniach testowano dwa rodzaje dendrymerów karbokrzemowych: CBD-1 oraz CBD-2, jako nośników dla pro-apoptotycznych siRNA (z ang. *small interfering RNA*): Mcl-1 oraz Bcl-2. Dendrymery zostały zsyntezowane w Katedrze Chemii Organicznej i Nieorganicznej Uniwersytetu Alcala (Hiszpania).

siRNA jest małym, dwuniciowym kwasem nukleinowym, mającym zdolność do wyciszenia ekspresji wybranych genów (Tokatlian i Segura, 2010). Wyciszenie genów jest możliwe dzięki mechanizmowi tzw. interferencji RNA (RNAi, ang. *RNA interference*). W trakcie tego procesu dochodzi do degradacji docelowego mRNA (Ambesajir i wsp., 2012; Angart i wsp., 2013; Dzitruk i wsp., 2015): siRNA jest wbudowane do kompleksu białkowego RISC (ang. *RNA-induced silencing complex*), co prowadzi do jego aktywacji, a następnie do rozpoznania i degradacji docelowego mRNA (Tokatlian i Segura, 2010).

Mechanizm RNAi może być wykorzystany w terapii genowej, będącej jedną z najbardziej obiecujących metod leczenia nowotworów, które są najczęstszą przyczyną zgonów na świecie (Białkowska i wsp., 2020; Dubé i Cournoyer, 1995; Giacca i Zacchigna, 2012; Ionov i wsp., 2015; Mulligan, 1993; Pędziwiatr-Werbicka i wsp., 2020). Terapia genowa polega na naprawie materiału genetycznego m.in. poprzez korektę

zmutowanego genu, za pomocą terapeutycznego genu transportowanego do chromosomów docelowych tkanek lub komórek, co skutkuje regulacją lub wymianą uszkodzonych genów (Gonçalves i Paiva, 2017; Misra, 2012; Shi i wsp., 2017). Błona komórkowa jest silną barierą dla genów w postaci wielkocząsteczkowych kwasów nukleinowych o ujemnych ładunkach (Giacca i Zacchigna, 2012). Z tego powodu możliwość zastosowania terapii genowej jest uzależniona od technologii, które umożliwią dostarczenie genów do komórek, tkanek, czy organów (Verma i Weitzman, 2005). Możliwość wdrożenia terapii genowej zależy od rozwoju nośników dla kwasów nukleinowych, które jednocześnie będą bezpieczne dla zdrowych tkanek (Matthews i Curiel, 2007; Verma i Weitzman, 2005). Najbardziej obiecujące w tym obszarze są dendrymery, syntetyczne polimery charakteryzujące się dużą liczbą grup funkcyjnych, które mogą przyłączać m.in. kwasy nukleinowe (Białkowska i wsp., 2021; Michlewska i wsp., 2018; Wang i wsp., 2010).

W niniejszej pracy oceniano tworzenie kompleksów dendrymerów z siRNA (tzw. dendrypleksów) oraz ich wpływ na komórki linii MCF- hodowane zarówno w 2D jak i 3D.

Praca doktorska składa się z dwóch części: opisowej, obejmującej omówienie optymalizacji warunków hodowli 3D w postaci sferoidów oraz z **trzech publikacji**: pracy przeglądowej oraz dwóch prac oryginalnych. Artykuły opublikowano w czasopismach o międzynarodowym zasięgu, znajdujących się na liście Ministerstwa Edukacji i Nauki.

Dodatkowo, w pracy doktorskiej opisano podjęte próby badań na hodowlach 3D, które nie przyniosły oczekiwanych rezultatów i nie były kontynuowane oraz próbę wykorzystania płytek 96-dołkowych do hodowli 3D.

2. Cele pracy

W pracy można wyróżnić dwa główne cele: wdrożeniowy i badawczy oraz cele szczegółowe.

a) Cel wdrożeniowy:

Opracowanie metod pozwalających na określenie wpływu substancji/materiałów/związków na komórki hodowane w 3D:

- opracowanie i optymalizacja metody hodowli komórek w postaci sferoidów;
- opracowanie i optymalizacja metod pozwalających na pomiary wpływu substancji/materiałów/związków na komórki hodowane w 3D;
- wdrożenie hodowli 3D do oferty usług „Bionanoparku” Sp. z o. o.

Cel wdrożeniowy został osiągnięty poprzez:

- wybór metody do hodowli 3D;
- wysiewanie różnej liczby komórek na żel i wybór optymalnych warunków;
- testowanie odczynników zrywających połączenia międzykomórkowe w celu otrzymania zawiesiny pojedynczych komórek do testów cytometrycznych (roztwory trypsyna-EDTA w różnych stężeniach, odczynnik TrypLE);
- obserwacje mikroskopowe otrzymanych sferoidów;
- opracowanie metody przygotowania komórek do obserwacji przy użyciu mikroskopu konfokalnego.

b) Cel badawczy:

Ocena wpływu badanych dendrymerów i ich kompleksów z siRNA na komórki:

- ocena zdolności badanych dendrymerów do tworzenia kompleksów z siRNA;
- określenie toksyczności dendrymerów i ich kompleksów z siRNA wobec komórek linii MCF-7 (komórki raka piersi) hodowanych w 2D i 3D;
- porównanie zdolności badanych dendrymerów do transportowania siRNA do komórek.

Cel badawczy został osiągnięty poprzez:

- pomiary potencjału zeta;
- przeprowadzenie badań metodą dichroizmu kołowego;
- przeprowadzenie testu z bromkiem etydyny;
- przeprowadzenie elektroforezy kompleksów;
- określenie żywotności komórek hodowanych w 2D testem XTT oraz testem live-dead za pomocą cytometru przepływowego;
- określenie transportu dendrypleksów do komórek hodowanych w 2D za pomocą mikroskopu konfokalnego oraz analizy HCA (ang. *high content analysis*; analiza za pomocą mikroskopu automatycznego);
- określenie żywotności komórek hodowanych w 3D testem live-dead za pomocą cytometru przepływowego;
- wykrywanie apoptozy w komórkach hodowanych w 3D testem z aneksyną V za pomocą cytometru przepływowego;
- określenie transportu dendrypleksów do komórek hodowanych w 3D za pomocą mikroskopu konfokalnego oraz cytometru przepływowego.

Hipoteza badawcza:

Dendrymery CBD-1 oraz CBD-2 transportują siRNA (Mcl-1 i Bcl-2) do komórek MCF-7 hodowanych w 3D, co prowadzi do śmierci komórek nowotworowych.

3. Opracowanie metod pozwalających na określenie wpływu substancji/materialów/związków na komórki hodowane w 3D

3.1. Materiały i metody

- ludzkie komórki raka piersi linii MCF-7 (ATCC, nr kat. HTB-22™)
- komórki ludzkiego kostniakomięsaka linii Saos-2 (ATCC, nr kat. HTB-85™)
- ludzkie komórki śródbłónka linii EA.hy926 (ATCC, nr kat. CRL-2922™)
- formy do przygotowania hydrożeli (Microtissues Inc., nr kat. 12-256)
- agaroz (Blirt, nr kat. AG41-010)
- TrypLE (Gibco, nr kat. 12563029)
- odczynniki do hodowli: medium hodowlane DMEM (Biowest, nr kat. L0104-500), płodowa surowica bydlęca (Biowest, nr kat. S181H-500), antybiotyki penicylina-streptomycyna (Biowest, nr kat. L0022-100)
- roztwór trypsyny-EDTA (Biowest, nr kat. L0931-100, Corning, nr kat. 25-053-C1)
- 96-dołkowe płytki do hodowli 3D firmy PHC Europe BV, z dnem w kształcie wrzeciona

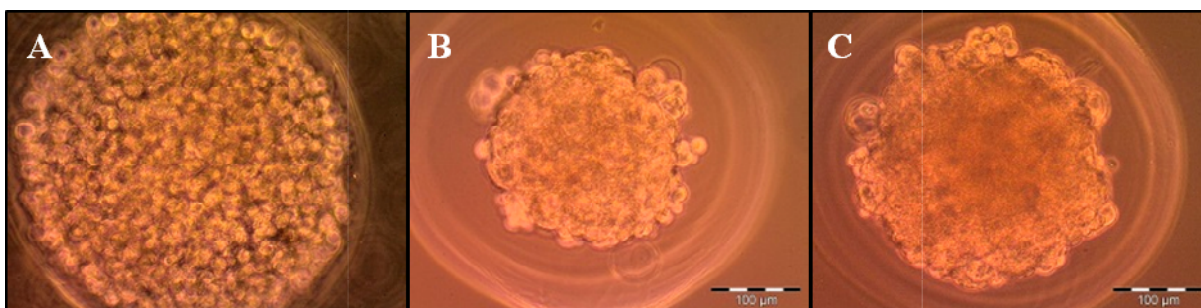
3.2. Optymalizacja warunków hodowli 3D

Do otrzymania hodowli 3D w postaci tzw. sferoidów, wybrano metodę z zastosowaniem hydrożeli. Hydrożele przygotowano z agarozy z użyciem specjalnych form z firmy Microtissues Inc. (ryc. 1).

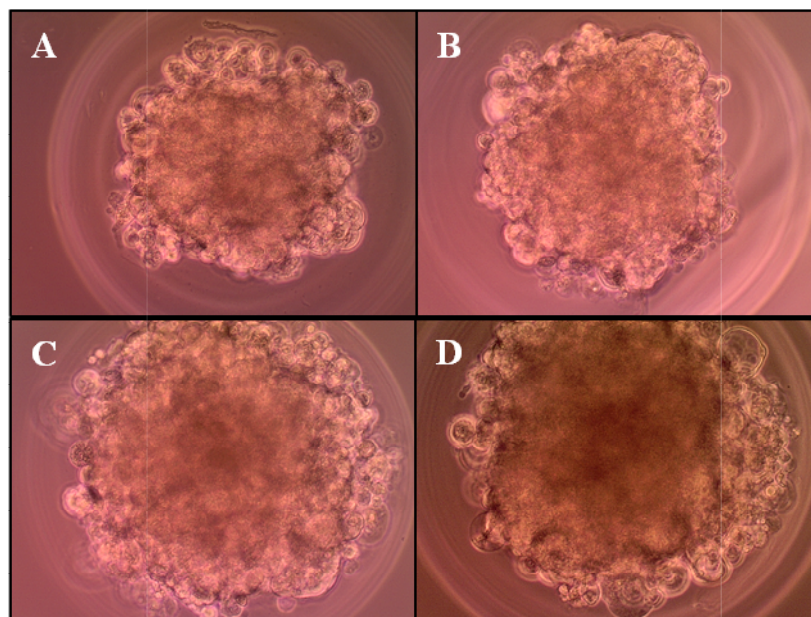


Ryc. 1. Formy do przygotowania żeli firmy Microtissues Inc. i gotowe żele; A – puste formy; B – żele wylane na formy; C – gotowe żele. Zdjęcia wykonano za pomocą AI Quad Camera.

Przed rozpoczęciem części eksperymentalnej, przeprowadzono optymalizację metody hodowli 3D, określając czas hodowli sferoidu przed dodaniem testowanych substancji oraz liczbę komórek MCF-7 wysiewanych na żel. Sferoidy tworzyły się po ok. 24 godzinach od wysiania komórek (ryc. 2), ale jako optymalny czas hodowli wybrano 7 dni. Po siedmiu dniach od wysiania do komórek podawano badane związki, a komórki poddawano analizie cytometrycznej lub mikroskopowej. Liczbę komórek wysianych na żel wybrano na podstawie obserwacji mikroskopowej po wysianiu 100 000, 110 000, 120 000, 130 000, 140 000, 150 000, 170 000 oraz 190 000 komórek/żel. Przykładowe zdjęcia sferoidów po wysianiu różnej liczby komórek przedstawia ryc. 3. Jako najbardziej optymalny wariant wybrano opcję 100 000 komórek/żel.

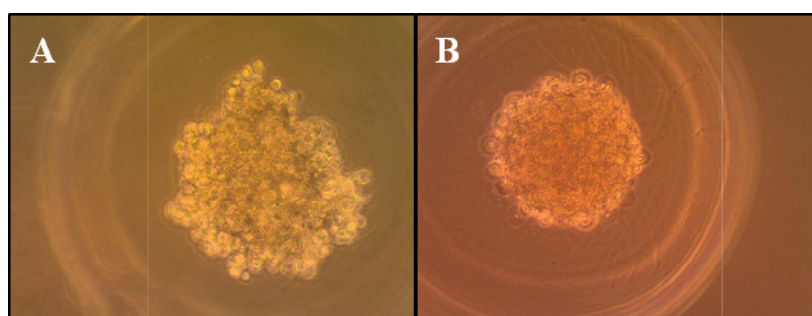


Ryc. 2. Etapy tworzenia sferoidu z komórek MCF-7; A – komórki 10 minut po wysianiu; B – komórki ok. 24 godz. po wysianiu; C – komórki 4 dni po wysianiu. Zdjęcia wykonano za pomocą mikroskopu Olympus CKX41; pow. 10x.



Ryc. 3. Zdjęcia sferoidów uzyskanych po wysianiu różnej liczby komórek linii MCF-7 na żel po 7 dniach hodowli: A – 100 000 komórek/żel; B – 110 000 komórek/żel; C – 120 000 komórek/żel; D – 140 000. Zdjęcia wykonano za pomocą mikroskopu Olympus CKX41; pow. 10x.

Dodatkowo, aby sprawdzić zdolność komórek innych linii do tworzenia sferoidów, na żełe wysiewano również komórki ludzkiego kostniakomięsa linii Saos-2 oraz ludzkie komórki śródbłonna linii EA.hy926. W każdym przypadku komórki agregowały tworząc sferoidy (ryc. 4).



Ryc. 4. Sferoidy utworzone na hydrożelach z komórek dwóch linii: A – Saos-2; B – EA.hy926. Zdjęcia wykonano za pomocą mikroskopu Olympus CKX41; pow. 10x.

W celu uzyskania zawiesiny pojedynczych komórek do badań cytometrycznych testowano różne odczynniki pozwalające na rozerwanie połączeń międzykomórkowych (TrypLE, roztwory trypsyna-EDTA w różnych stężeniach). Dla komórek linii MCF-7

najlepszym wariantem okazał się odczynnik TrypLE, natomiast dla komórek linii Saos-2 i EA.hy926 – roztwór trypsyny-EDTA (0,25%/2,21 mM).

Określano również czas inkubacji z wybranym odczynnikiem, potrzebny do zerwania połączeń międzykomórkowych, testując następujące warianty: 10 min. inkubacji + mieszanie pipetą, 10 min. inkubacji + mieszanie pipetą + 10 min. inkubacji, 10 min. bez mieszania pipetą. Wybrano ostatni z wariantów, czyli 10 min. inkubacji z odczynnikiem bez mieszania pipetą. Testowano również możliwość mechanicznego pozyskania zawiesiny: komórki mieszano za pomocą pipety automatycznej, jednak ta metoda nie była wystarczająco efektywna i powodowała zbyt duże uszkodzenia komórek.

OPRACOWANA METODA HODOWLI

Przygotowanie żeli

- Do zlewki o pojemności 100 ml odważano 1 g agarozy;
- Do agarozy dodawano 50 ml roztworu PBS;
- Zakrywano wlot zlewki folią aluminiową i sterylizowano w autoklawie;
- Po zakończeniu procesu sterylizacji wylewano po 0,5 ml agarozy na formy;
- Po kilku minutach żele (ryc. 1C) przenoszono do dołków płytki 12-dołkowej;
- Do każdego z żeli dodawano po 2 ml medium, tak aby na powierzchni żeli nie powstały pęcherzyki powietrza;
- Żele inkubowano w medium co najmniej 15 min. w temperaturze pokojowej;
- Delikatnie odciągano medium;
- Inkubację z medium powtarzano łącznie 3-krotnie.

Wysiewanie komórek

- Zawiesinę komórek rozcieńczano w taki sposób, aby otrzymać stężenie 100 000 kom./190 μ l medium;
- Na każdy żel podawano po 190 μ l zawiesiny komórek, w taki sposób, aby komórki były wysiane równomiernie na całym żelu;
- Pozostawiano komórki na co najmniej 10 minut, pozwalając im opaść na dno żelu;
- Do każdego dołka z żelem z wysianymi komórkami, delikatnie dodawano po 2 ml pełnego medium hodowlanego;
- Płytki umieszczano w inkubatorze w warunkach 37 °C, 5% CO₂.

Przygotowanie komórek do pomiarów cytometrycznych

- Żele wraz z wysianymi komórkami przepłukiwano 2-krotnie roztworem PBS;
- Do płytek 12-dołkowych dodawano po 0,5 ml odczynnika TrypLE;

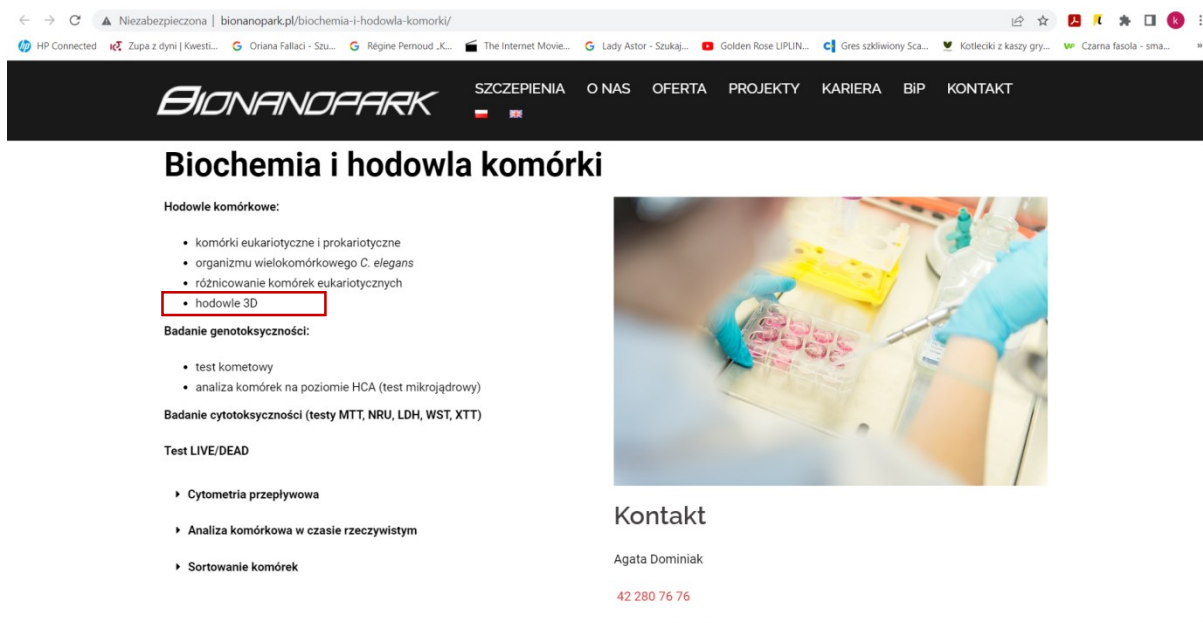
- Każdy żel przenoszono na nową płytkę 12-dółkową z wcześniej przygotowanym odczynnikiem TrypLE, w taki sposób, aby komórki były zwrócone do dna płytki i aby uniknąć tworzenia się pęcherzyków powietrza;
- Płytki wirowano przez 5 min., 500 rpm;
- Po odwirowaniu usuwano żele;
- Komórki umieszczano w inkubatorze w warunkach 37 °C, 5% CO₂ na ok. 10 min.;
- Po inkubacji do komórek dodawano po 0,25 ml 10% roztworu FBS w HBSS;
- Komórki delikatnie mieszano za pomocą pipety automatycznej, aby rozbić ewentualne agregaty komórkowe;
- Przenoszono po 0,5 ml zawiesiny do próbek cytometrycznych, jednocześnie filtrując za pomocą filtrów o średnicy otworów 70 µm;
- Przygotowana zawiesina była poddawana dalszej preparatyce, zgodnie z wytycznymi producenta dla danego testu.

Przygotowanie komórek do analizy na mikroskopie konfokalnym

- Żele wraz z wysianymi komórkami przepłukiwano 2-krotnie roztworem PBS;
- Na każdy żel podawano po 190 µl 3,7% roztworu formaldehydu i inkubowano przez 1 godz.;
- Po upływie czasu inkubacji komórki 3-krotnie przepłukiwano roztworem PBS, za każdym razem po 20 min.;
- Komórki wybarwiano mieszaniną znaczników fluorescencyjnych przez 1 godz. (190 µl/żel);
- Po zakończeniu etapu wybarwiania do komórek dodawano po ok. 2 ml roztworu PBS/żel.
- Wybarwione komórki poddawano analizie mikroskopowej.

Opracowane metody hodowli 3D i analizy komórek pozwalają na uzyskanie wiarygodnych wyników i zostały wdrożone do oferty handlowej „Bionanoparku” Sp. z o. o. (ryc. 5).

Link do strony internetowej z ofertą: <http://bionanopark.pl/biochemia-i-hodowla-komorki/>.



Ryc. 5. Wycinek strony internetowej „Bionanoparku” Sp. z o. o. Na czerwono zaznaczono informację o prowadzeniu hodowli 3D.

3.3. Ocena przydatności popularnych testów cytotoksyczności w badaniach na hodowlach 3D

3.3.1. Testy XTT i MTT

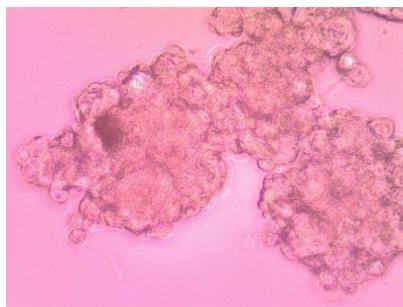
W pracy podjęto próby zaadaptowania testów cytotoksyczności wykorzystywanych na hodowlach 2D, do warunków hodowli 3D, przeprowadzając testy XTT oraz MTT na komórkach na hydrożelach. Jako kontrolę negatywną (KN) stosowano komórki nietraktowane, natomiast jako kontrolę pozytywną dendrymery w różnych stężeniach. Wyniki przeprowadzonych testów uznano za niewiarygodne, ponieważ nie zaobserwowano obniżenia wartości absorbancji dla komórek traktowanych dendrymerami w porównaniu do wartości absorbancji dla kontroli negatywnej, co było niezgodne z wynikami testów cytometrycznych. Ponadto, w przypadku testu MTT utrudnione było wypłukanie kryształów formazanu z żeli.

3.3.2. Test uszkodzeń DNA

W celu wykrycia uszkodzeń DNA wykonano test z wykorzystaniem zestawu odczynników Apoptosis, DNA Damage and Cell Proliferation Kit (Becton Dickinson). Procedura obejmuje wiele etapów wirowania oraz usuwania supernatantu, co prowadzi do usuwania części komórek z próbki. Ponadto, komórki silnie agregowały w trakcie wykonywania procesu przygotowania próbek, co wiązało się z utraceniem części komórek podczas filtrowania. W związku z powyższym, nie kontynuowano eksperymentów z wykorzystaniem tego testu.

3.4. Hodowla 3D na płytkach 96-dołkowych

Do utworzenia sferoidów wykorzystano również płytki 96-dołkowe do hodowli 3D firmy PHC Europe BV, z dnem w kształcie wrzeciona. Wysiewano 6 000 kom./dołek, a po 7 dniach hodowli, dodawano roztwór nadtlenu wodoru (H_2O_2) w różnych stężeniach (1, 2 i 3 mM). Po 24 godzinach przeprowadzono test XTT. Wyniki nie były zadowalające, ponieważ wyniki absorbancji mierzonej dla H_2O_2 były równe wartościom absorbancji dla komórek nietraktowanych (kontrola negatywna). W związku z tym wyniki uznano za niewiarygodne i nie kontynuowano badań z wykorzystaniem płytek. Ponadto, kształty sferoidów nie były równomierne (ryc. 6), co mogło wpływać na powtarzalność wyników.



Ryc. 6. Sferoidy utworzone z komórek MCF-7 na płytce 96-dołkowej. Zdjęcia wykonano za pomocą mikroskopu Olympus CKX41; pow. 10x.

4. Omówienie prac wchodzących w zakres rozprawy doktorskiej

Praca przeglądowa *Spheroids as a Type of Three-Dimensional Cell Cultures—Examples of Methods of Preparation and the Most Important Application* (**praca nr 1**) stanowi wprowadzenie w zagadnienie hodowli 3D. Opisuje różnice pomiędzy hodowlami 2D oraz 3D oraz wskazuje na czym polega przewaga hodowli 3D. Praca jest podzielona na dwie główne części. Pierwsza część opisuje mechanizm tworzenia się tzw. sferoidów oraz najbardziej popularne metody hodowli pozwalające na ich otrzymanie. Druga część opisuje najważniejsze zastosowania hodowli komórek w postaci sferoidów.

Praca oryginalna *Interaction of Cationic Carbosilane Dendrimers and Their siRNA Complexes with MCF-7 Cells* (**praca nr 2**) przedstawia ocenę tworzenia kompleksów badanych dendrymerów z siRNA (dendrypleksów) oraz wpływ badanych dendrymerów i dendrypleksów na żywotność komórek hodowanych w 2D. W pracy zaprezentowano również wyniki pomiarów jakościowych oraz ilościowych, otrzymane na podstawie badań mikroskopowych, udowadniające, że dendrypleksy są transportowane do wnętrza komórek.

Tworzenie kompleksów CBD-1 oraz CBD-2 z każdym z siRNA oceniono poprzez pomiary potencjału zeta, badania metodą dichroizmu kołowego, test z bromkiem etydyny oraz elektroforezę kompleksów (CBD-2/siRNA). Zastosowane testy wykazały, że każdy z dendrymerów tworzy kompleksy zarówno z Mcl-1 jak i z Bcl-2. Ponadto, badania elektroforetyczne wykazały działanie ochronne dendrymerów na siRNA w obecności RNazy. Dodatkowo, na podstawie wykresów zmian potencjału zeta określono ile cząsteczek dendrymeru przyłącza się do jednej cząsteczki siRNA; liczba ta wynosiła 15 dla CBD-1/Mcl-1, 16 dla CBD-1/Bcl-2, 9 dla CBD-2/Mcl-1 i 11 dla CBD-2/Bcl-2.

Oceny wpływu dendrymerów i dendrypleksów na komórki dokonano za pomocą testu XTT. Badania rozpoczęto na komórkach linii MCF-7 hodowanych w 2D, aby wybrać zakres stężeń, w których dendrymery będą wykorzystane na etapie badań na komórkach hodowanych w 3D. Wyniki testu XTT wskazują, że wpływ dendrymerów na komórki jest zależny od stężenia, przy czym im wyższe stężenie dendrymerów tym większy efekt cytotoksyczny. Dendrymer CBD-1 jest bardziej toksyczny w stosunku do komórek linii MCF-7 hodowanych w 2D niż CBD-2. Przyłączenie siRNA do dendrymerów powoduje

większy spadek liczby żywych komórek w porównaniu do działania samych dendrymerów. Szczególnie jest to widoczne w przypadku dendrymeru CBD-1.

W celu sprawdzenia, czy dendrypleksy wnikają do komórek wykonano obrazy za pomocą mikroskopu konfokalnego. Kompleksy każdego z dendrymerów były widoczne w cytoplazmie komórek. Do analizy ilościowej wykorzystano kompleksy CBD-2/siRNA, ponieważ dendrymer CBD-2 był mniej toksyczny. Analiza wykazała, że ok. 40% komórek miało w swojej cytoplazmie kompleksy CBD-2/Mcl-1 i ok. 60% komórek miało w swojej cytoplazmie kompleksy CBD-2/Bcl-2.

Podsumowując, dendrymery CBD-1 oraz CBD-2 tworzą kompleksy z Mcl-1 oraz Bcl-2. Ponadto, badane dendrymery chronią siRNA przed degradacją przez RNazę. Dendrymery i ich kompleksy z siRNA wpływają na żywotność komórek MCF-7, zmniejszając liczbę żywych komórek wraz ze wzrostem stężenia. Każdy z dendrymerów transportuje siRNA do komórek.

W pracy oryginalnej *Interaction of Cationic Carbosilane Dendrimers and Their siRNA Complexes with MCF-7 Cells Cultured in 3D Spheroids* (**praca nr 3**) opisano wpływ dendrymerów i dendrypleksów na komórki hodowane w postaci sferoidów oraz zdolność dendrymerów do transportu siRNA do komórek w takiej hodowli.

Badania rozpoczęto od przeprowadzenia testu live-dead za pomocą cytometru przepływowego na komórkach MCF-7 hodowanych w 2D. Testy te potwierdziły, że dendrymer CBD-1 jest bardziej toksyczny wobec komórek niż dendrymer CBD-2.

Następnie przeprowadzono szereg testów cytometrycznych na komórkach hodowanych w 3D po inkubacji z dendrymerami lub dendrypleksami.

Aby określić wpływ dendrymerów, przeprowadzono test live-dead za pomocą cytometru przepływowego po 24-godzinnej inkubacji komórek z dendrymerami. Co ciekawe, wyniki pokazują, że odwrotnie niż w przypadku hodowli 2D, dla komórek hodowanych w postaci sferoidu, bardziej toksyczny jest dendrymer CBD-2, a obniżenie liczby żywych komórek, jest tym większe, im wyższe jest stężenie dendrymeru.

Do dalszych badań wybrano dendrymery w stężeniach 5 i 10 μM , ponieważ w tych stężeniach dendrymery nie były toksyczne wobec komórek. Wykonano test live-dead po 24-godzinnej inkubacji z dendrypleksami. Statystycznie istotne obniżenie liczby żywych komórek jest widoczne dla kompleksów CBD-1/Bcl-2, CBD-2/Mcl-1, CBD-2/Bcl-2, w których stężenie dendrymeru wynosiło 10 μM , ale liczba żywych komórek utrzymywała się powyżej 90%. W związku z powyższym wydłużono czas inkubacji z dendrypleksami do 48 godzin, stosując dendrymery w stężeniu 10 μM . Istotne statystycznie obniżenie

liczby żywych komórek jest widoczne w przypadku kompleksów CBD-2/siRNA, jednak liczba żywych komórek nadal wynosiła powyżej 90%.

Annexin V-FITC Apoptosis Detection Kit pozwala na wykrywanie apoptozy w komórkach. Po traktowaniu komórek MCF-7 dendrymerem CBD-2 oraz jego kompleksami z siRNA istotny statystycznie wzrost poziomu komórek apoptotycznych obserwowano tylko dla kompleksu CBD-2/Bcl-2.

Przeprowadzono również jakościowe i ilościowe oznaczenie wnikania dendrypleksów do komórek. Do oznaczenia jakościowego posłużył mikroskop konfokalny, który pozwolił na obserwację kompleksów z przyłączonym znacznikiem fluorescencyjnym (fluoresceina). Na obrazach mikroskopowych są widoczne dendrypleksy w postaci zielonych punktów. Analiza cytometryczna pozwoliła na analizę ilościową. Wyniki wskazują, że od ok. 4 do 8% komórek miało w swojej cytoplazmie dendrypleksy.

W związku z tym, że po 24 i 48-godzinnej inkubacji komórek z dendrypleksami liczba żywych komórek utrzymywała się na poziomie ok. 90%, zaprojektowano eksperyment, w którym podano trzy dawki dendrymerów lub dendrypleksów w odstępach 48-godzinnych. Statystycznie istotne obniżenie liczby żywych komórek jest widoczne dla każdej z testowanych grup związków. Najwyższy spadek jest widoczny dla grup CBD-1/Mcl-1 i CBD-1/Bcl-2, gdzie liczba żywych komórek znacznie spadła.

Uzyskane wyniki potwierdzają tworzenie się kompleksów dendrymer/siRNA. Każdy z badanych dendrymerów transportuje siRNA do komórek, zarówno w hodowli 2D jak i 3D, przy czym w przypadku hodowli 3D, transport jest znacznie mniej efektywny. Ponadto, badane dendrymery chronią siRNA przed degradacją przez RNazę. Dendrymer CBD-1 jest bardziej toksyczny dla komórek hodowanych w 2D, natomiast dla komórek hodowanych w 3D bardziej toksyczny jest dendrymer CBD-2. Różnice w działaniu dendrymerów mogą wynikać z różnic w ich budowie: oba dendrymery zawierają 8 powierzchniowych grup kationowych, które są uważane za przyczynę cytotoksycznego działania dendrymerów, jednak charakter tych ugrupowań jest inny. CBD-1 zawiera trzeciorzędowe grupy amoniowe (RNHMe_2Cl), które są zależne od pH, podczas gdy w strukturze CBD-2 obserwuje się stabilne niezależnie od pH czwartorzędowe grupy amoniowe (RNMe_3I). Inna subtelna różnica jest związana z hydrofobowością — dendrymer zakończony (RNMe_3I) jest bardziej hydrofobowy.

Z punktu widzenia terapeutycznego wykorzystania dendrymerów, najkorzystniejsze wyniki otrzymano po dodaniu do komórek w hodowli 3D trzech dawek kompleksów CBD-1/siRNA w odstępach 48-godzin.

5. Podsumowanie

- Opracowano metodę hodowli 3D w postaci sferoidów oraz metody do badania wpływu związków/materiałów/substancji na komórki w hodowli 3D i wdrożono je do oferty badań „Bionanoparku” Sp. z o. o.
- Każdy z badanych dendrymerów tworzy kompleksy z siRNA oraz ma zdolność transportowania siRNA do komórek.
- Wpływ badanych dendrymerów na komórki MCF-7 hodowane w 2D i 3D jest zależny od stężenia – im wyższe stężenie tym większy efekt cytotoksyczny.
- Efekt cytotoksyczny w przypadku komórek hodowanych w 2D jest widoczny przy niższych stężeniach dendrymerów niż w przypadku komórek hodowanych w 3D.
- Kompleksy dendrymer karbokrzemowy/siRNA tylko w niewielkim stopniu obniżają żywotność komórek MCF-7 w hodowli 3D po 24 i 48 godz. inkubacji.
- Najlepszy efekt terapeutyczny (znaczne obniżenie żywotności komórek nowotworowych) uzyskano po podaniu do hodowli trzech dawek kompleksów CBD-1/siRNA.

6. Wniosek

Dendrymer CBD-1 jest lepszym nośnikiem dla siRNA, ponieważ sam nie jest cytotoksyczny dla komórek hodowanych w 3D, natomiast dostarcza siRNA, które po zastosowaniu trzech dawek kompleksów doprowadza do śmierci komórek nowotworowych MCF-7, co jest istotne z punktu widzenia przeciwnowotworowej terapii genowej.

7. Streszczenie

Hodowle komórkowe są bardzo ważnym narzędziem pozwalającym na testowanie różnych substancji, materiałów lub leków, a także na poznawanie biologii komórki i mechanizmów komórkowych. Najbardziej popularnym modelem hodowli komórkowych są hodowle w monowarstwie, czyli hodowle dwuwymiarowe (2D), które jednak nie odzwierciedlają w sposób wystarczający fizjologicznych warunków funkcjonowania komórek. Komórki w hodowlach 2D są pozbawione interakcji komórka-komórka oraz komórka-macierz zewnątrzkomórkowa (ECM). O wiele lepszym modelem są hodowle trójwymiarowe (3D), dlatego też jednym z celów pracy było opracowanie metody hodowli 3D oraz metod badawczych do oceny wpływu materiałów na komórki hodowane w 3D. Ponadto, badano wpływ dwóch rodzajów dendrymerów karbokrzemowych (CBD-1 oraz CBD-2) oraz ich kompleksów z pro-apoptycznymi siRNA (Mcl-1 oraz Bcl-2) na komórki MCF-7 hodowane zarówno w 2D jak i w 3D.

Jako metodę pozyskiwania sferoidów wybrano hodowlę na hydrożelach. Pierwszy etap badań obejmował optymalizację procesu hodowli. Po wykonaniu szeregu badań wstępnych, ostatecznie wysiewano po 100 000 komórek/żel, a hodowlę, przed podaniem badanych związków, prowadzono przez 7 dni.

W celu sprawdzenia, czy tworzą się kompleksy pomiędzy badanymi dendrymerami i siRNA wykonano pomiary potencjału zeta, dichroizmu kołowego, fluorescencyjne z bromkiem etydyny oraz przeprowadzono elektroforezę kompleksów w żelu agarozowym (CBD-2/siRNA). Każdy z przeprowadzonych testów potwierdził tworzenie się kompleksów dendrymer/siRNA. Ponadto, badanie elektroforetyczne potwierdziły ochronny wpływ dendrymerów przed degradacją siRNA przez RNazę.

Kolejnym etapem badań była ocena wpływu dendrymerów lub dendrypleksów na komórki MCF-7 hodowane w 2D. Przeprowadzono testy XTT oraz live-dead (analiza cytometryczna), które wykazały, że stosowane dendrymery wpływają na żywotność komórek, przy czym im wyższe stężenie dendrymeru tym niższa żywotność. Przyłączenie siRNA zwiększało efekt cytotoksyczny. Bardziej toksyczny okazał się dendrymer CBD-1.

Określono również transport dendrypleksów do komórek. Do tego celu wykorzystano mikroskop konfokalny (analiza jakościowa) oraz mikroskop automatyczny INCell Analyser 2000 wraz z analizą HCA (analiza ilościowa). Analizy mikroskopowe wykazały, że zarówno CBD-1 jak i CBD-2 transportują siRNA do komórek.

Następnie wykonano analizy cytometryczne (test live-dead) określające wpływ dendrymerów i dendrypleksów na komórki hodowane w 3D. Pomiary wykonywano po 24 lub 48 godzinach inkubacji z wybranymi próbkami oraz po podaniu trzech dawek badanych związków. W przypadku hodowli 3D bardziej toksyczny okazał się dendrymer CBD-2. Najlepsze wyniki z punktu widzenia zastosowania dendrymerów jako nośników siRNA w terapii genowej otrzymano po podaniu trzech dawek CBD-1 w kompleksach z siRNA.

Analiza jakościowa za pomocą mikroskopu konfokalnego oraz ilościowa za pomocą cytometru przepływowego potwierdziły transport dendrypleksów do komórek hodowanych w 3D, ale był on mniej efektywny, niż w przypadku komórek hodowanych w monowarstwie.

8. Abstract

Cell cultures are very important for testing materials and drugs, and in the examination of cell biology and cell mechanisms. The most popular models of cell culture are two-dimensional (2D) as monolayers, but this does not mimic the natural cell environment. Cells are then deprived of cell–cell and cell–extracellular matrix interactions. A much better *in vitro* model is three-dimensional (3D) culture. For this reason, one goal of this work was to develop a model of 3D cell culture and methods which allow to estimate influence of materials on cells in 3D. Moreover, two types of dendrimers (CBD-1 and CBD-2) and their complexes with pro-apoptotic siRNA (Mcl-1 and Bcl-2) were tested on MCF-7 cells cultured both in 2D and 3D.

For spheroid formation the method using hydrogels was chosen. First, the culture method was optimized. After a series of preliminary studies, 100,000 cells/gel were finally seeded and cultured for 7 days prior to addition of the test compounds.

In order to examine whether complexes are formed between the studied dendrimers and siRNAs, the following tests were performed: measurement of the zeta potential, circular dichroism, fluorescence with ethidium bromide and electrophoresis of the complexes (CBD-2/siRNA). Each of the tests confirmed the formation of dendrimer/siRNA complexes. Moreover, electrophoresis of dendriplexes confirmed the protective effect of dendrimers against siRNA degradation by RNase.

The next step of the research was evaluation of the effect of dendrimers or dendriplexes on MCF-7 cells grown in 2D. XTT and live-dead tests (cytometric analysis) were carried out, which showed that the dendrimers affect the viability of cells and the higher concentration of dendrimer, the lower viability was observed. The attachment of siRNA increased the cytotoxic effect. The CBD-1 dendrimer was more toxic.

Transport of dendriplexes into cells was also determined. For this purpose, a confocal microscope (qualitative analysis) and an automatic INCell Analyzer 2000 microscope with HCA analysis (quantitative analysis) were used. Microscopic analysis showed that both CBD-1 and CBD-2 transport siRNA into cells.

Then, cytometric analysis (live-dead test) was performed to determine the effect of dendrimers and dendriplexes on cells grown in 3D. Measurements were made after 24 or 48 hours of incubation with the selected samples and after administration of 3 doses of test compounds. In the case of 3D culture, the CBD-2 dendrimer turned out to be more toxic.

The best results in terms of the use of dendrimers as siRNA carriers in gene therapy were obtained after addition of 3 doses of CBD-1 in complexes with siRNA.

Qualitative analysis with a confocal microscope and quantitative analysis with a flow cytometer confirmed the transport of dendriplexes into cells cultured in 3D, but it was less efficient than with cells grown in a monolayer.

9. Bibliografia

- Ambesajir, A., Kaushik, A., Kaushik, J. J., Petros, S. T. (2012). RNA interference: A futuristic tool and its therapeutic applications. *Saudi J. Biol. Sci.* **19**, 395–403. <https://doi.org/10.1016/j.sjbs.2012.08.001>
- Andersen, T., Auk-Emblem, P., Dornish, M. (2015). 3D Cell Culture in Alginate Hydrogels. *Microarrays* **4(2)**, 2. <https://doi.org/10.3390/microarrays4020133>
- Angart, P., Vocelle, D., Chan, C., Walton, S. P. (2013). Design of siRNA Therapeutics from the Molecular Scale. *Pharmaceuticals* **6**, 440–468. <https://doi.org/10.3390/ph6040440>
- Antoni, D., Burckel, H., Josset, E., Noel, G. (2015). Three-Dimensional Cell Culture: A Breakthrough in Vivo. *Int. J. Mol. Sci.* **16(3)**, 3. <https://doi.org/10.3390/ijms16035517>
- Białkowska, K., Komorowski, P., Bryszewska, M., Miłowska, K. (2020). Spheroids as a Type of Three-Dimensional Cell Cultures—Examples of Methods of Preparation and the Most Important Application. *Int. J. Mol. Sci.* **21(6225)**, 6225. <https://doi.org/10.3390/ijms21176225>
- Białkowska, K., Miłowska, K., Michlewska, S., Sokołowska, P., Komorowski, P., Lozano-Cruz, T., Gomez-Ramirez, R., de la Mata, F. J., Bryszewska, M. (2021). Interaction of Cationic Carbosilane Dendrimers and Their siRNA Complexes with MCF-7 Cells. *Int. J. Mol. Sci.* **22(7097)**, 7097. <https://doi.org/10.3390/ijms22137097>
- Centeno, E. G. Z., Cimarosti, H., Bithell, A. (2018). 2D versus 3D human induced pluripotent stem cell-derived cultures for neurodegenerative disease modelling. *Mol. Neurodegener.* **13(1)**, 27. <https://doi.org/10.1186/s13024-018-0258-4>
- do Amaral, J., Rezende-Teixeira, P., Freitas, V., Machado-Santelli, G. (2011). MCF-7 Cells as a Three-Dimensional Model for the Study of Human Breast Cancer. *Tissue Eng. Part C Methods* **17(11)**, 1097–1107. <https://doi.org/10.1089/ten.tec.2011.0260>
- Dubé, I. D., Cournoyer, D. (1995). Gene therapy: here to stay. *Can. Med. Assoc. J.* **152(10)**, 10.

- Dzmitruk, V., Szulc, A., Shcharbin, D., Janaszewska, A., Shcharbina, N., Łaźniewska, J., Novopashina, D., Buyanova, M., Ionov, M., Klajnert-Maculewicz, B., Gomez-Ramirez, R., Mignani, S., Majoral, J. P., Muñoz-Fernández, M. A., Bryszewska, M. (2015). Anticancer siRNA cocktails as a novel tool to treat cancer cells. Part (B). Efficiency of pharmacological action. *Int. J. Pharm.* **485**, 288–294. <https://doi.org/10.1016/j.ijpharm.2015.03.034>
- Edmondson, R., Broglie, J. J., Adcock, A. F., Yang, L. (2014). Three-Dimensional Cell Culture Systems and Their Applications in Drug Discovery and Cell-Based Biosensors. *Assay Drug Dev. Technol.* **12**, 207–218. <https://doi.org/10.1089/adt.2014.573>
- Giacca, M., Zacchigna, S. (2012). Virus-mediated gene delivery for human gene therapy. *J. Control Release* **161**, 377–388. <https://doi.org/10.1016/j.jconrel.2012.04.008>
- Gonçalves, G. A. R., Paiva, R. de M. A. (2017). Gene therapy: advances, challenges and perspectives. *Einstein (Sao Paulo)* **15(3)**, 369–75. <https://doi.org/10.1590/S1679-45082017RB4024>
- Goodman, T. T., Ng, C. P., Pun, S. H. (2008). 3-D Tissue Culture Systems for the Evaluation and Optimization of Nanoparticle-Based Drug Carriers. *Bioconjugate Chem.* **19(10)**, 1951–1959. <https://doi.org/10.1021/bc800233a>
- Ionov, M., Łaźniewska, J., Dzmitruk, V., Halets, I., Loznikova, S., Novopashina, D., Apartsin, E., Krasheninina, O., Venyaminova, A., Miłowska, K., Nowacka, O., Gomez-Ramirez, R., de la Mata, F. J., Majoral, J.-P., Shcharbin, D., Bryszewska, M. (2015). Anticancer siRNA cocktails as a novel tool to treat cancer cells. Part (A). Mechanisms of interaction. *Int. J. Pharm.* **485**, 261–269. <https://doi.org/10.1016/j.ijpharm.2015.03.024>
- Kitel, R., Czarnecka, J., Rusin, A. (2013). Trójwymiarowe hodowle komórek—Zastosowania w badaniach podstawowych i inżynierii tkankowej. *Post Biochem.* **59(305–314)**, 305–314.
- Lee, J., Lilly, G. D., Doty, R. C., Podsiadlo, P., Kotov, N. A. (2009). In vitro Toxicity Testing of Nanoparticles in 3D Cell Culture. *Small* **5**, 1213–1221. <https://doi.org/10.1002/sml.200801788>

- Lv, D., Hu, Z., Lu, L., Lu, H., Xu, X. (2017). Three-dimensional cell culture: A powerful tool in tumor research and drug discovery (Review). *Oncol. Lett.* **14(6)**, 6999–7010. <https://doi.org/10.3892/ol.2017.7134>
- Matthews, Q. L., Curiel, D. T. (2007). Gene therapy: human germline genetic modifications--assessing the scientific, socioethical, and religious issues. *South. Med. J.* **100(1)**, 98–100. <https://doi.org/10.1097/smj.0b013e31802e645f>
- Michlewska, S., Ionov, M., Maroto-Díaz, M., Szwed, A., Ihnatsyeyu-Kachan, A., Loznikova, S., Shcharbin, D., Maly, M., Gomez-Ramirez, R., de la Mata, F. J., Bryszewska, M. (2018). Ruthenium dendrimers as carriers for anticancer siRNA. *J. Inorg. Biochem.* **181**, 18–27. <https://doi.org/10.1016/j.jinorgbio.2018.01.001>
- Misra, S. (2012). Human gene therapy: a brief overview of the genetic revolution. *J. Assoc. Physicians India* **61(2)**, 127–33.
- Moshksayan, K., Kashaninejad, N., Warkiani, M. E., Lock, J. G., Moghadas, H., Firoozabadi, B., Saidi, M. S., Nguyen, N.-T. (2018). Spheroids-on-a-chip: Recent advances and design considerations in microfluidic platforms for spheroid formation and culture. *Sens. Actuators B Chem.* **263**, 151–176. <https://doi.org/10.1016/j.snb.2018.01.223>
- Mulligan, R. C. (1993). The Basic Science of Gene Therapy. *Science* **260(5110)**, 926–932. <https://doi.org/10.1126/science.8493530>
- Pędziwiatr-Werbicka, E., Gorzkiewicz, M., Horodecka, K., Abashkin, V., Klajnert-Maculewicz, B., Peña-González, C. E., Sánchez-Nieves, J., Gomez-Ramirez, R., de la Mata, F. J., Bryszewska, M. (2020). Silver Nanoparticles Surface-Modified with Carbosilane Dendrons as Carriers of Anticancer siRNA. *Int. J. Mol. Sci.* **21(4647)**, 4647. <https://doi.org/10.3390/ijms21134647>
- Sant, S., Johnston, P. A. (2017). The production of 3D tumor spheroids for cancer drug discovery. *Drug Discov. Today Technol.* **23(27–36)**, 27–36. <https://doi.org/10.1016/j.ddtec.2017.03.002>
- Shi, B., Zheng, M., Tao, W., Chung, R., Jin, D., Ghaffari, D., Farokhzad, O. C. (2017). Challenges in DNA Delivery and Recent Advances in Multifunctional Polymeric DNA Delivery Systems. *Biomacromolecules* **18**, 2231–2246. <https://doi.org/10.1021/acs.biomac.7b00803>

- Tokatlian, T., Segura, T. (2010). siRNA applications in nanomedicine. *Wiley Interdiscip. Rev. Nanomed. Nanobiotechnol.* **2(3)**, 305–315. <https://doi.org/10.1002/wnan.81>
- Vantangoli, M. M., Madnick, S. J., Huse, S. M., Weston, P., Boekelheide, K. (2015). MCF-7 Human Breast Cancer Cells Form Differentiated Microtissues in Scaffold-Free Hydrogels. *PLOS ONE* **10(8)**, e0135426. <https://doi.org/10.1371/journal.pone.0135426>
- Verma, I. M., Weitzman, M. D. (2005). Gene Therapy: Twenty-First Century Medicine. *Annu. Rev. Biochem.* **74**, 711–38. <https://doi.org/10.1146/annurev.biochem.74.050304.091637>
- Wang, J., Lu, Z., Wientjes, M. G., Au, J. L.-S. (2010). Delivery of siRNA Therapeutics: Barriers and Carriers. *AAPS J.* **12(4)**, 4. <https://doi.org/10.1208/s12248-010-9210-4>

Prace wchodzące w skład rozprawy doktorskiej



Review

Spheroids as a Type of Three-Dimensional Cell Cultures—Examples of Methods of Preparation and the Most Important Application

Kamila Białkowska ^{1,2,*}, Piotr Komorowski ^{2,3}, Maria Bryszewska ¹ and Katarzyna Miłowska ¹

¹ Department of General Biophysics, Faculty of Biology and Environmental Protection, University of Lodz, 141/143 Pomorska St. Building D, 90-236 Lodz, Poland; maria.bryszewska@biol.uni.lodz.pl (M.B.); katarzyna.milowska@biol.uni.lodz.pl (K.M.)

² Molecular and Nanostructural Biophysics Laboratory, “Bionanopark” Ltd., 114/116 Dubois St., 93-465 Lodz, Poland; p.komorowski@bionanopark.pl

³ Department of Biophysics, Institute of Materials Science, Lodz University of Technology, 1/15 Stefanowskiego St., 90-924 Lodz, Poland

* Correspondence: kamila.bialkowska1@unilodz.eu

Received: 8 July 2020; Accepted: 26 August 2020; Published: 28 August 2020



Abstract: Cell cultures are very important for testing materials and drugs, and in the examination of cell biology and special cell mechanisms. The most popular models of cell culture are two-dimensional (2D) as monolayers, but this does not mimic the natural cell environment. Cells are mostly deprived of cell–cell and cell–extracellular matrix interactions. A much better in vitro model is three-dimensional (3D) culture. Because many cell lines have the ability to self-assemble, one 3D culturing method is to produce spheroids. There are several systems for culturing cells in spheroids, e.g., hanging drop, scaffolds and hydrogels, and these cultures have their applications in drug and nanoparticles testing, and disease modeling. In this paper we would like to present methods of preparation of spheroids in general and emphasize the most important applications.

Keywords: 3D cell culture; spheroids; drug testing

1. Introduction

Cells have been cultured since the 1940s [1], and are generally in use to examine cell biology and molecular mechanisms [2]. Cells are taken directly from a tissue and, after suitable preparation, transferred into an artificial environment or they are obtained from a cell line already adopted by others. Cells grow in a medium containing the required nutrients, growth factors, and hormones, in an incubator. Cultures are kept in special dishes placed in strictly controlled temperature conditions, normally a 37 °C [3]. Cells are attached to a flat surface as a substrate, glass or plastic, mainly in two dimensions, as monolayers. This method of cell culturing is most popular because it is simple and convenient; it has been an invaluable method providing important knowledge as models of variety diseases [4,5]. However, forcing cells to grow on flat surfaces can change their metabolism and functioning [4]. In 2D cell cultures, the cell–cell and cell–extracellular matrix interactions are reduced, and the level of cellular responsiveness is limited [2,6]. Moreover, cell culture environment can have an effect on the phenotype of cells and hence affect the cellular response to added substances, e.g., drugs [1]. All cells in the body live in 3D environment, which is crucial for their metabolism and growth. The phenotype and functions of each cell are highly dependent on elaborated interactions with neighboring cells, the extracellular matrix (ECM) and proteins [6]. Those cell–cell and cell–ECM interactions differ from 2D to 3D cultures and also between cell layers in spheroids structures, and this

can affect cytotoxicity results [7]. For these reasons, testing the toxicity of materials and substances on 2D cell cultures is not exactly predictive of that which might be expected in the body [6,8]. 3D cell cultures more precisely mimic the natural cell microenvironment. The morphology and physiology of cells in 3D cultures are different from cells in 2D cultures, showing responses that correspond in some ways more like in vivo behavior [8]. In 2D models, molecules can be secreted into the culture medium, and, therefore, changing the medium will remove these substances and might disturb some analysis. For example, in 2D models of Alzheimer disease, removing the medium will mean that secreted amyloid beta (A β) is discarded and, therefore, change the analysis of A β aggregation. 3D cell cultures can limit the diffusion of A β into the culture medium [5].

Three-dimensional cell cultures are widely used in investigations of cancer cells, intracellular interactions and cell differentiation, evaluation of substance toxicity and efficacy of potential drugs [9], and therefore show promise in filling the gap between 2D culturing and experiments with animals [10]. It has been shown that 3D cell cultures exhibit increased levels of tissue-specific markers, regain tissue-specific functions and have various profiles of gene expression compared to 2D cultured cells [11]. The authors compared 3D and 2D MCF-7 human breast cancer cells, and showed that cells cultured in 3D systems had a higher mRNA expression of the luminal epithelial markers keratin 8 and keratin 19, and a lower expression of basal marker keratin 14 and the mesenchymal marker vimentin [11]. The 3D spheroids, as in solid tumors, have permeability barriers through which some substances or agents under test have to penetrate [12]. Table 1 shows the most important differences between 2D and 3D cell cultures.

Table 1. Comparing of 2D and 3D cell cultures.

2D	3D
<ul style="list-style-type: none"> • Cell-cell contact is limited [13]; • Cell-flat, plastic surface contact is dominating [9]; • Contact with ECM only on one surface [9]; • No gradient [9]; • Co-culture cannot create a microenvironment [17]; • No resistance for anticancer drug [19]; 	<ul style="list-style-type: none"> • Cell-cell contact is dominating [14,15]; • Cells remain in contact with ECM [14,15]; • Diffusion gradient of nutrients, waste, oxygen and drugs [9,16]; • Co-culture can mimic microenvironment [18]; • Resistant to anticancer drugs (mimic tumor morphology) [20].

There are a number of formats and materials available that help the culturing of cells in 3D. For example, there are some hydrogel substrates, e.g., beads, injectable gels, moldable gels, and macroporous structures. Other techniques are also available that help prepare 3D cultures, e.g., hanging drop, low-binding plastic, pyramid plates. There are also macroporous scaffolds, e.g., meshes, foams or fibrous patches that allow spatial organization of cells and seeding cells throughout the thickness of the matrix, but they have cell-matrix interactions closer to 2D cell cultures (and are therefore called semi-3D or 2.5D cultures). This is characteristic of polystyrene-based 3D cell culture materials [4].

Polymer hydrogels seem to be suitable for 3D cell cultures because of their similarity to physiological extracellular matrix. Synthetic materials that could be applied as hydrogels are polyethylene glycol (PEG), polyvinyl alcohol (PVA), poly(hydroxyethyl methacrylate) (polyHEMA), and polycaprolactone (PCL). Furthermore, natural polymers and proteins can form hydrogels, e.g., alginate, collagen, chitosan, hyaluronan, dextran, and fibrin. Alginate hyaluronan (a product of bacterial fermentation) and dextran are non-animal derived materials [4].

In this paper we would like to outline the methods of spheroid preparation and focus on the most important applications.

2. Spheroids as a Type of 3D Cell Cultures

2.1. Spheroids

Spheroids (Figure 1) are cell aggregates, self-assembling in an environment that prevents attachment to a flat surface [9,12]. Spheroid formulation is possible because of membrane proteins

(integrins) and extracellular matrix proteins [9]. During spheroids formation three steps could be defined: (i) dispersed cells aggregate due to long-chain ECM fibers consisting RGD motifs that allow to bind cell-surface integrin and this leads to upregulated cadherin expression, (ii) cadherin accumulates on the surface of cell membrane, (iii) the hemophilic cadherin–cadherin binding between neighboring cells allows to tighten connections between cells and spheroids are formed [14,21]. Moreover, integrins are involved in activation of focal adhesion kinase (FAK), which is a cytoplasmic tyrosine kinase. Invasive phenotype of tumor, increased tumor growth, and poor patient prognosis are associated with overexpression of FAK. Knockout of FAK in mouse tumor models leads to prevention of some aspects of initiation and progression of breast carcinoma tumor [22]. FAK is involved in cell adhesion, migration, and also growth. FAK influences the rearrangement of the cytoskeleton (actin filaments) and microtubules, and this affects cell adhesion and migration. Moreover, FAK transmits extracellular signals associated with integrins [23]. Cytoskeleton proteins are responsible for the mechanical integrity [9]. Actin cytoskeleton is crucial in adhesion, mediation of cell shape, migration, and spreading. Furthermore, actin skeleton plays an important role in spheroids formation. Blocking polymerization of actin filaments reduces aggregation of T47D, HC11, and 4T1 cells strongly. Microtubules also take part in cell aggregation and the growth of spheroids. Interference with the polymerization of microtubules slows down the aggregation of cells or results in the decrease of compaction of spheroids in HC11 cells [23]. Oxygen supply to 3D cell culture is a very important factor limiting cell viability during culturing cells. Anada et al. (2012) showed that after 10 days in culture, spheroids stopped growing on non-oxygen-permeable chips and the diameter remained constant at approximately 360 μm . They tested 3D culture chips made of gas-permeable polydimethylsiloxane (PDMS) and noticed, that after 14 days in culture, spheroids on those PDMS chips continued growing until approximately 600 μm [24]. During culturing, cells may be of different sizes; cells within spheroid are smaller than cells on the outside [9]. Cells remaining on the periphery of the spheroid proliferate more actively [25]. Several techniques are used to form spheroids.

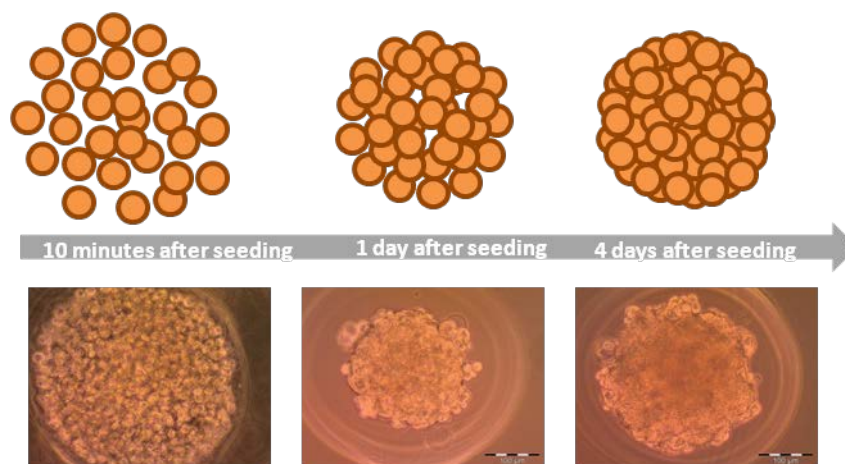


Figure 1. Formation of spheroids on MCF-7 cell line.

2.1.1. Hanging Drop

Hanging drop (Figure 2) is one method of obtaining scaffold-free cell cultures [11]. This technique has some limitations, including low throughput, spherical geometry, and a high shear force environment [26]. Some manipulations, e.g., changing the medium and adding of compounds can be complicated and time-consuming [11]. Some cell lines do not form compact spheroids using this method [25]. This method, however, does not require specialized equipment [27], but involves small volumes of cell suspension (usually 20 μL). Cell density depends on the required size of the spheroid. The cell suspension can be placed into the well of a special plate, which is turned upside

down so that the cell suspension becomes a hanging drop held by surface tension [28]. Cells remain in direct contact with each other and with the ECM [27].

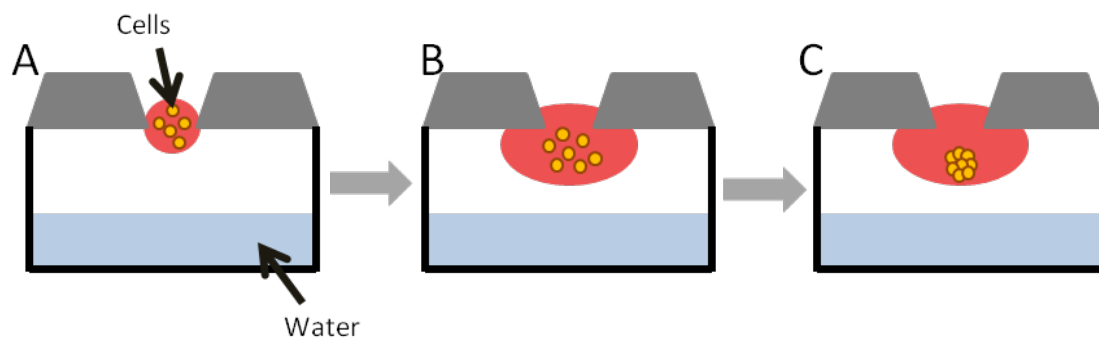


Figure 2. Spheroid formation in hanging drop method: (A)—cell suspension dispensed; (B)—cells in hanging drop; (C)—cells aggregate to form spheroid [29].

The simplest way to obtain cell culture in hanging drop is to put a drop with a cell suspension onto the inside of a lid of a culture plate. After reversing, microgravity concentrates cells at the bottom of the drop [9]. The hanging drop method could be used also to co-culture several cell lines [27].

Tung et al. (2010) described a hanging drop culture plate in 384-well format that can be adapted to high-throughput screening (HTS) instruments available to 2D cultures, e.g., liquid handling robots. The plate is made of polystyrene and contains 16 rows and 24 columns. On the edges of the plate a water reservoir is located. When it is filled with water it avoids an evaporation. A small volume of culture media causes its rapid evaporation and changes in its osmolality, which should be stable during long period of cell culturing. For this reason, the 384-hanging drop array plate is surrounded by a plate lid from the top and by 96-well plate filled with water from the bottom. On the top of every well of the 384-hanging drop array plate there is an access hole through which cells are seeded and medium is exchanged. During culturing the whole system is wrapped with Parafilm. To obtain a spheroid, 15 μL of cell suspension was added to access hole to create a hanging drop. To change a medium 5 μL of liquid was taken and then 7 μL of a fresh growth medium was added [30].

Osmolality of culture media was investigated, and the results showed that it was in the optimal range of 300 to 360 mmol/kg. The authors used cell lines: African green monkey kidney fibroblasts (COS7), murine embryonic stem cells (ES-D3), and human epithelial carcinoma cells (A431.H9) that stably express mesothelin [30].

A431.H9 cells in hanging drop cell culture were treated with 2 types of anticancer drugs and the viability was measured. After incubation with tested drugs alamarBlue was added and fluorescence was measured using plate reader. Due to the possibility of using liquid handling robots and popular plate readers, the 384-hanging drop array plate enables to perform HTS [30].

2.1.2. Hydrogels

Among the systems for spheroid culturing there are non-adhesive agarose hydrogels that do not have the influence of an ECM. This type of cell culturing has some advantages, ease of maintenance, the possibility of controlling the microtissue size, and a large amount of microtissues per plate [11]. In this technique, cells are seeded on hydrogel with recesses where cells sink and can self-assemble into 3D spheroid microtissues. Without any influence from the ECM, cells in homogenous suspension can self-assemble spheroids, and cells in heterogeneous suspension self-segregate and form multilayered structures [26]. Napolitano et al. (2007) cultured different types of cell lines to show the versatility of the technique using MCF-7 human breast cancer cells, human umbilical vein endothelial cells (HUVEC), normal human fibroblasts (NHF), rat hepatoma cells (H35) and rat glioblastoma cells (RG2). With the aid of computer-assisted design, they created special molds including a cell-seeding chamber, recesses for cell aggregation, and ports for exchanging medium. Those micromolds were filled with sterilized

agarose to form the right substrate for cell culturing [26]. Because the substrate was non-adhesive, cell-to-cell binding was favored, and cells self-assembled in spheroids. These cell-to-cell interactions were maximized because of the shape of the bottom hydrogels. They showed that use of hydrogel gives versatility for controlled microtissue production [26]. Some cell lines require ECM proteins in culture medium to create shapely spheroids [9].

Some micromolds for preparation of hydrogels are commercially available. For example, Vantangoli et al. (2015) used them to prepare agarose hydrogel, for MCF-7 cell testing [11].

2.1.3. Rotary Cell Cultures

One of the methods of obtaining spheroids is cell culture in a bottle with an agitator (Figure 3). In these conditions, cells cannot attach to the substrate, and start aggregating and self-assembling. It is one of the simplest methods to produce spheroids on a large scale. This method has certain disadvantages e.g., longevity of cultures, variation in spheroid size, and mechanical damages of cells. One variation of this method is a system with a flask rotating around a horizontal axis. Simulation of microgravity with minimal hydrodynamic forces does not destroy cells, such that this method allows the formation of bigger spheroids than in a bottle with an agitator. Morphological differences between spheroids are also smaller than in the first method [9].

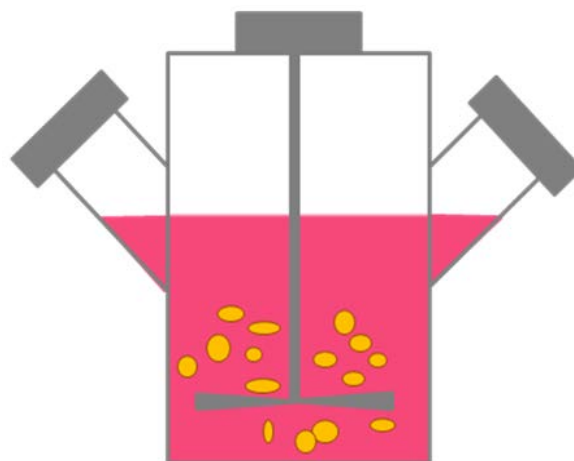


Figure 3. Cell culture in bottle with agitator. Cells start aggregating and self-assembling [9].

2.1.4. Cell Suspension with the Addition of Nanofibers

This method of producing spheroids is by the addition of polymer nanofibers to a suspension of adherent cells. Shin et al. (2012) added poly(lactic-co-glycolic acid) (PLGA) nanofibers to a suspension of human embryonic kidney 293 cells (HEK) and human dermal fibroblasts (HDFs), although this could be for all types of adherent cells [31].

Nanofibers increase spheroid production and reduce cell death due to cell non-adherence. In a cell suspension lacking nanofibers, neighboring cells interact because of cadherins. When nanofibers are added, spheroid formation is promoted also by the interaction of cells with them [31]. Cell binding to nanofibers may be due to the action of vitronectin and fibronectin from the serum in the medium [32]. Those proteins when added to the culture medium adsorb on the nanofibers and then cells attach to those nanofibers forming spheroids [31].

2.1.5. Magnetic Levitation Method

Magnetic levitation is one of the methods to produce scaffold-free 3D cell cultures. Thanks to magnetic levitation cells associate into 3D cell culture and produce ECM, keeping cellular activity. In this technique the magnetic force overcomes the gravitational force [33]. Cells are treated with paramagnetic iron oxide nanoparticles overnight, which allows for their uptake by cells. Cell culture is

washed and then treated with trypsin solution and seeded into low-adhesive plates. Finally, the magnet is placed on a top of the plate lid that leads to pulling labeled cells up under magnetic forces. Spheroids are created within few hours [29].

Türker et al. (2018) investigated the levitation platform using gadolinium(III) chelates (GD(III) chelates), which are paramagnetic agents. They suspended cells in capillary channels and the cell medium was paramagnetized using various Gd(III) chelates. After placement, the capillary channel into the magnetic levitation platform the cells levitated to a levitation height (z) or equilibrium height. Because the environment was paramagnetized, the cells reached the levitation height, migrating from a higher magnetic field region to a lower magnetic field region. The 3D cell culture formation took place at the levitation height, where the cells interacted and assembled [33]. The authors tested viability of the NIH 3T3 mouse fibroblasts after incubation with three types of gadolinium agents (Gadobutrol, Gadoteric acid and Gadodiamide) using MTT and Live/Dead assays. The data showed that cells after treatment with Gadobutrol exhibited higher viability compared to other agents [33].

Souza et al. (2010) proposed a model of 3D cell culture using magnetic levitation combined with hydrogels with gold and magnetic iron oxide (MIO) nanoparticles and filamentous bacteriophage. Hydrogels were obtained via mixing the solution of gold nanoparticles with MIO nanopowder (magnetite [Fe_3O_4]). Then, the solution was mixed with phage solution of equal volume and, finally, put at 4 °C overnight, to allow to form hydrogel. Preparing levitated cell culture consisted of treatment of the cells with hydrogel (1 $\mu\text{L}/1 \text{ cm}^2$ of surface area) and incubation overnight. Then cells were detached using trypsin-EDTA solution in PBS and seeded into a culture Petri dish. The cell line used in this study was human glioblastoma cells, genetically modified. Cells were grown for 8 days, and during this period the fluorescence of mCherry protein was observed confirming the viability of the cells in the 3D structures. Within 30 min. after seeding, the cells were collected together. Spheroids were obtained after 3–8 days [34].

Souza et. al. (2010) investigated molecular similarity of 3D cell cultures obtained using magnetic levitation to orthotopic human tumor xenografts from immunodeficient mice. They measured expression of transmembrane protein, N-cadherin. The expression of this protein in the 3D culture showed that magnetic levitation exhibits some features similar to the in vivo model. This suggests that 3D cell cultures based on magnetic levitation method could be a cheaper substitute for expensive and labor-intensive method based on human tumor xenografts from immunodeficient mice [34].

2.1.6. Microfluidic Systems

The described methods are non-microfluidic methods. They play an important role in the formation and investigation of spheroids, but they have also some limitations. Some disadvantages of these methods (e.g., hanging drop method) are differences in spheroids' diameters, low-throughput, or labor intensity. The non-microfluidic environment causes reduction of oxygen and nutrients and the increase of osmolality and level of metabolites. To overcome those limitations the microfluidics systems are created. The device with microfluidic flow is made of microwells which are connected by microfluidic channels, from simple to more sophisticated arrays of microchannels. Microchannels are prepared through etching or forming on the surface of using neutral materials, e.g., silicon, glass or polydimethylsiloxane (PDMS). The cells are cultured above layers made of matrix coated porous membrane and with direct contact with endothelial cells. Additionally, immune cells and tumor cells flow through the microchannels [29].

Very important advantages of microfluidic systems are controlled mixing, chemical concentration gradients, lower consumption of reagents, control of shear stress and pressure on cells, and also constant perfusion. Microfluidic chips provide dynamic environment for better reflection of tissue environment [7]. The sizes of spheroids are homogenous [35]. Viability of hepatocytes cultured in spheroids in flow conditions is higher than in static model [7,36]. Cancer spheroids cultured in a microwell plate in dynamic conditions exhibit higher resistance for drugs than in no-flow conditions [7,35].

2.1.7. Spheroids Based on Co-Cultures

The tumor microenvironment is heterogenous; therefore, the biology of tumor is the result of mutual influence between cancer cells and their environment. For example, fibronectin, one of the ECM protein, takes part in the regulation of tumor stiffness, promotes the growth of the tumor and resistance for drugs. Interactions between cancer cells and surrounding fibroblasts and also immune and endothelial cells are connected to regulation of tumor progression. Fibroblasts are involved in metastasis of the tumor and also in tumor development. During tumor vascularization the migration and the proliferation of endothelial cells takes place and they depend on interactions between ECM proteins, fibroblasts, and cancer cells. Such complex systems need reflection in an appropriate in vitro model, to better mimic tumor environment [37]. For this reason, Lazzari et al. (2018), proposed a spheroid model of pancreatic tumor, based on a triple co-culture of pancreatic cancer cells (PANC-1) together with fibroblasts (MRC-5) and endothelial cells (HUVEC). The authors proved that in complex environment cancer cells are less sensitive to chemotherapy [37].

Xin et al. (2019) distinguished two platforms for 3D cell co-cultures: co-cultures with the cell-cell contact and co-cultures without the cell-cell contact. Co-cultures with the cell-cell contact allow to evaluate interactions between cancer cells and stromal cells, mediated by adhesion. Among those methods there is a co-culture with direct contact, where cancer and stromal cells are mixed to form heterogenous spheroids, and co-culture with the semi-contact, where homogeneous cancer cells spheroids are seeded into 3D scaffolds combined with stromal cells. Cells in non-contact co-cultures are not allowed to contact and adhere together, because they are kept in distinct layers or chambers. In those methods interactions between cancer and stromal cells could be assigned to chemical mediators [38].

2.1.8. Bioprinting

Simple structure and low vascularization potential are the main limits in using current 3D cultures models. The lack of vascularization limits the spheroids size and probably does not mimic later stages of tumors very well. In most of the models of 3D cultures the spatial distribution of cancer cells and ECM composition is not well arranged [39]. The solution to lack of vascularization and designing scaffolds for better reflection of tumor microenvironment and heterogeneity could be bioprinting technology [40]. Bioprinting includes variety of approaches consisting of distributing of biological materials and cells in a spatially defined way [39]. In other words, the bioprinting technique could be defined as a technology in which cell layers and supporting biological materials are positioned precisely to mimic functions of the tissue or organ [41]. There are few strategies of bioprinting: inkjet printing, extrusion-based printing, laser-assisted printing and stereolithography [39]. In the inkjet bioprinting the droplets made of bioink (cell-laden) filling the cartridge are generated and deposited on a scaffold precisely. A computer program controls the deposition of the droplets and it leads to the creation of 3D structures. This method is relatively fast and not expensive and provides high viability of cells [39,40]. In the extrusion-based bioprinting the bioink is moved through the nozzle with pneumatic or mechanical pressure. This method is also quite cheap and fast. In the laser-assisted bioprinting laser stimulation leads to a response of the donor layer which absorbs energy and generates a high-pressure bubble that leads to pushing a droplet of the bioink onto the substrate. Some disadvantages of this method are expensive equipment and poor choice of bioinks. In the stereolithography an array of programmed mirrors generates a digital mask, which is projected to reservoir with bioink to photo-crosslink patterns layer by layer. This method is characterized by high resolution and fast speed [39].

3. Applications of 3D Cell Cultures

3.1. Drug Testing and Nanoparticles Examination

3.1.1. Drug Testing

A generation of new cancer drugs is based on three approaches, referred to as: (i) high throughput drug screening (HTS), (ii) expansion of analogs of existing drugs, and (iii) rational drug design. These involve assays based on measuring cell viability, proliferation, and clonogenicity in an in vitro environment [42]. Cell cultures help assess drug safety and indicate their possible mechanism of action. Test substances are added to the culture medium and their activity investigated [43]. Presently, 2D cell cultures remain very useful in drug investigation. However, as already mentioned, 2D models do not mimic well the physiological environment of living cells [34]. For instance, cells of the colon cancer cell line, HCT-116 wt, cultured as spheroids were more resistant to some of the tested drugs compared with them cultured as a monolayer [42,44].

Cells grown in 3D cultures can be maintained longer than as 2D monolayers. The 3D aggregates can be kept for 4 weeks, whereas cells in 2D cultures last approximately 1 week before reaching confluence. For this reason, 3D cell cultures make a better model for studying long-term effects of drugs. Tumor cells in a monolayer proliferate faster than in 3D aggregates and are more sensitive to agents used during chemotherapy or radiation therapy [3].

Karlson et al. (2012) used 96-well NanoCulture[®] plate to form spheroids from the human colon cancer cell lines HCT-116 wt, HCT-116 wt/GFP and HCT-116 HRP EGFP (hypoxia-responsive promoter enhanced green fluorescent protein) cell lines. 3- and 6-day spheroids were tested, using standard drugs in the treatment of colon cancer, including 5-FU, oxaliplatin and irinotecan (Table 2). They also used melphalan (Table 2), used clinically in treating some cancers. They also used topoisomerase inhibitors, acriflavine, and VLX50, which is now in an early phase of evolution. Cells were incubated for 72 h with each drug. After preliminary experiments on monolayers, these authors selected three suitable concentrations of each drug. HCT116 wt and HCT116 wt/GFP cell lines cultured as monolayers were equally highly sensitive to 5-FU, oxaliplatin, irinotecan, and melphalan, which indicated that GFP-labeling does not influence the phenotype. For this reason, GFP-labeled cells were used to following experiments on drug cytotoxicity. The results showed that 3-day old spheroids were more resistant to four standard drugs and 6-day old spheroids were almost totally resistant to these drugs. The fact that cells cultured in 3D systems were more resistant to these drugs is closely related to geno- and pheno-typical changes caused by spheroid formation [42].

Table 2. Comparison of drug testing results on 2D and 3D cultures.

Cell Cultures	Drugs	2D	3D
HCT-116 wt HCT-116 wt/GFP	5-FU, oxaliplatin, irinotecan, melphalan	equally and highly sensitive to 5-FU, oxaliplatin, irinotecan and melphalan	resistant or almost totally resistant to 4 standard drugs
NHEK	gefitinib	antiviral activity in concentrations too high for in vivo applications	gefitinib at concentration 0.5 μ M was sufficient to induce meaningful reduction of replication and spreading of virus
SW1353	DXR, CIS, CQ	cell viability in 2D cultures were lower than in 3D cell cultures	cell viability in spheroid cultures were higher than in 2D cell cultures
	SAL	similar results for monolayers and 3D cell cultures	

Koban et al. (2018) tested gefitinib (Table 2), a specific inhibitor of the epidermal growth factor receptor (EGFR), and used as a treatment for non-small-cell lung cancer. They used it as

antiviral compound for treating primary human keratinocytes (NHEK) kept in a 3D ECM-based cell culture. The results were then compared to the effects on analogous 2D cell culture [19]. The morphology of NHEK cells grown in 3D systems more closely mimic *in vivo* physiology than traditional monolayers. In 2D cell cultures, gefitinib showed antiviral activity at concentrations too high for *in vivo* application [14,45]. Significant reduction of virus replication occurred at 25 μM gefitinib, which was cytotoxic. In 3D cell culture, 0.5 μM gefitinib was sufficient to induce a clear reduction of the replication and spread of the virus. Near total inhibition of viral replication and EGFR phosphorylation were reached at 5 μM , without any obvious cytotoxic effects [19].

Orthopoxviruses (OPV) are double-stranded DNA viruses which replicate in host-cell cytoplasm. Virus spread and replication are supported by some proteins encoded by OPV, e.g., growth factor proteins. One of these proteins, epidermal growth factor (EGF)-like protein, activates EGFR, which enhances host cell proliferation and inhibits apoptosis [19].

The reason that viral replication and also cell proliferation at low concentrations of gefitinib were lower in 3D cell than in 2D systems might be that proliferation in the former is generally much less, even in non-infectious conditions. Viral infection may be an impulse for cell proliferation due to expression of the EGF homologue cowpox growth factor (CGF). Expression of this factor is significantly higher in infected cells in 3D models than in 2D models 48 h post-infection (p.i.). Moreover, expression of EGFR on the surface of cells in 3D cultures is clearly lower than on their counterparts in 2D culture [19,46]. As a result, in 3D cultures inhibition of only a small part of EGFR on the cell surface could be stronger and more crucial in reducing cell proliferation than in 2D cultures [19].

Perut et al. (2018) compared the effects of anticancer drugs on human chondrosarcoma (SW1353) and osteosarcoma (MG-63DXR30 cell line obtained from parental MG-63) cell lines [20].

Chondrosarcoma is a bone (cartilage) sarcoma of adults. It is resistant to chemotherapy and radiotherapy, and is, therefore, treated only by surgery [20,47]. Resistance is probably caused by the poor proliferation potential [47]. New drugs are now being tested that target this tumor. Several possible targets have been discovered, but this has failed to develop effective therapies for patients [48]. Failure in the search for rewarding therapy probably is a result of weakness of the monolayer tumor model—2D cell cultures do not mimic tumor structure adequately [20]. Perut et al. (2018) used a spheroid cell culture (hanging drop method) to test several anticancer drugs, anti-mitogenic DXR, cisplatin (CIS) and salinomycin (SAL; Table 2). They have investigated the anti-autophagic chloroquine (CQ) because of reports suggesting a role for autophagy in tumor resistance [20,49]. Autophagy is a degradation process of proteins and organelles, which can be reused to by cell [50].

SW1353 cells grown in 2D and 3D cell cultures were treated with DXR and CIS. After 72 h, cell viability in spheroid cultures was higher than in 2D cultures, with similar effects being seen with CQ. The only drug which gave similar results for monolayers and 3D cell cultures was SAL [20].

Resistance of 3D chondrosarcoma cultures to anticancer drugs could also be explained by a characteristic structure of 3D culture. In the 3D spheroid, an important role is played not only by cell-cell interactions, but also by internal or external biochemical signals that are part of the tumor microenvironment, e.g., hypoxia, limited access to nutrients, or acidosis [20]. As chondrosarcoma is a tumor with rather low vascularity and is highly hypoxic, it is important to establish low pH and low oxygen tension conditions [20,51]. Perut et al. (2018) measured the expression of a marker of hypoxia, CA IX, and found that the level was remarkably higher in spheroids than in monolayers [20].

3.1.2. Nanoparticle Examination

Testing of nanomaterials and their effects on cells is important because of possible therapeutic application. Nanomaterials are considered as safe gene carriers in gene therapy. Gene therapy is a potential method for fighting diseases, such as cancer, when traditional treatment is poor [52].

Because of the lack of the nanoparticle (NP) transport through cell layers in 2D cell cultures, 3D cell culture offers a better model. Techniques used for testing nanoparticle toxicity are the same as the methods for drug examination, although the toxic mechanism can be different [6].

Lee et al. (2009) have introduced 3D spheroid-culture-based NP toxicity testing system (Figure 4) using human hepatocarcinoma (HepG2) cells, because the liver is the main organ for NP accumulation. As a substrate, they used transparent and nonadhesive polyacrylamide hydrogel to measure the toxic effects of cadmium telluride (CdTe) and gold (Au) nanoparticles. Morphology, metabolic activity, membrane activity, and mechanism of cell death were explored, comparing the results from 3D cultures with those from 2D cultures. Cell number and spheroid diameter were crucial parameters to get repeatable results. They also showed that the activity of a spheroid depends on its size. They found significant differences between the morphology of cells in 2D and 3D cell cultures after treatment with CdTeNPs, with more death in 2D than in 3D cultures. Cell toxicity assays also confirmed that the toxic effects of NPs were reduced in 3D compared to 2D cultures [6].

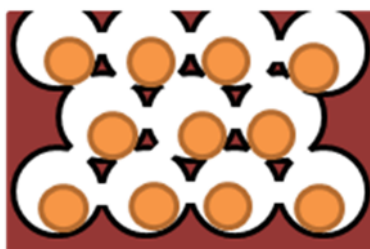


Figure 4. Model of hydrogel inverted colloidal crystal (ICC) scaffold [6].

Zeng et al. (2016) examined the effects of polyamidoamine (PAMAM) dendrimers on human neural progenitor cells in 3D neurosphere systems imitating the nervous system. Cells were treated with dendrimers from G4 group at 0.3, 1, 3, and 10 $\mu\text{g}/\text{mL}$. Fluorescent-labeled dendrimers aided measurement of their biodistribution, and microarray analysis were used to investigate gene expression [53].

Dendrimers are highly branched, synthetic molecules of spherical shape [54,55]. PAMAM dendrimers have a characteristic structure with a 2-carbon ethylenediamine core surrounded by functional groups [53]. These authors demonstrated that PAMAM dendrimers could get through external cells of neurospheres and penetrate them. Some groups of dendrimers inhibited cell proliferation and neuronal migration. They found 32 genes related to toxicity caused by dendrimers [53].

Goodman et al. (2007), evaluated the impact of nanoparticle size and collagenase treatment on the diffusion of carboxylated polystyrene nanoparticles into spheroid cell culture [56]. ECM is considered a factor involved in the resistance to therapeutic agents because it prevents penetration into the tumor [57]. Diffusion of molecules depends on tumor type and its localization [58]. Penetration of particles (such as viruses) increases after injections of protease enzymes into tumors. Immobilization of collagenase on the surface of nanoparticles leads to digestion of ECM proteins and also increases delivery of nanoparticles into a spheroid [56].

According to Goodman et al. (2007) particles <100 nm penetrate poorly into a spheroid core. Treatment of spheroids with nanoparticles coated with collagenase influences penetration of smaller nanoparticles (up to 100 nm) more than particles >100 nm. This means that coating nanoparticles with enzymes degrading proteins of the ECM could improve delivering them into solid tumors [56].

3.2. Models for Neurodegenerative Diseases

The 3D cell cultures are widely used in medical studies [3], e.g., research on neurodegenerative diseases [59].

Neurodegenerative diseases are a group of congenital or acquired disorders of the nervous system, characterized by progressive degeneration of neural cells, leading to their death. Neurons show pathological changes resulting in the formation of aggregates of modified proteins that are neurotoxic and resistant to proteolytic enzymes. Among these abnormal proteins are β -amyloid (A β) in Alzheimer's disease (AD), α -synuclein in Parkinson's disease (PD), and the huntingtin protein in Huntington's disease (HD). Those proteins disturb the functions of neurons and eventually lead to necrosis or apoptosis [59–61].

3.2.1. Alzheimer Disease

The most widespread neurodegenerative disease in the world is Alzheimer Disease (AD), for which there is no effective therapy, only some symptomatic treatment [62,63]. It is characterized by a progressive cognitive decline and involves memory deterioration. Orientation, judgments, and reasoning are also disturbed [64]. There are two characteristic features of AD, namely plaques of β -amyloid and neurofibrillary tangles of tau protein [59,63,65]. A β is generated from amyloid precursor protein (APP) during the process caused by two enzymes, β -secretase and γ -secretase [62]. The hypothesis that A β accumulation is the initial event in AD, leading to the next pathological events is called the “amyloid cascade hypothesis” [66].

Transgenic mice have now been used as models for studies on AD, but unfortunately, they do not exhibit important features occurring in humans [63]. Additional phenotypes of mice can also occur, which are not related to AD [67]. For these reasons, therapies for AD that are effective in mouse models probably do not work on humans [63,68]. In transgenic mice, there is also no amyloid cascade [66,69]. According to Choi et al. (2016) the Matrigel-based 3D cell culture system is a more appropriate model for AD testing as A β plaques are present, and these are not present in the mouse model [63].

SH-SY5Y is a neuronal-like cell line that is artificially differentiated to neural cells. This cell line came from the bone marrow of a patient with neuroblastoma [59]. Characteristic features of the cells are activities of dopamine- β -hydroxylase and tyrosine hydroxylase, some level of noradrenaline (NA) release, and the presence of choline acetyltransferase, acetylcholinesterase, and butyrylcholinesterase [70]. Seidel et al. (2012) used spheroids of human neuroblastoma cell line (SH-SY5Y) which overexpress EGFP-fused tau as a model to study the pathologies of tau protein in AD. They obtained 3 variants of SH-SY5Y over expressing tau (0N4R), namely wild type (WT), a variant with single point mutation P301L (which is used in common) and K280Q (which is 4-fold gene mutation in the tau protein gene DK280, P301L, V337M, R406W), which was used to enhance tauopathy. Generally, differentiation of SH-SY5Y cells took place by using several agents, e.g., phorbol esters and retinoic acid, growth factors (like brain derived neurotrophic factor, BDNF), nerve growth factor (NGF) or cholesterol [71]. However, differentiation agents influence cell metabolism and could probably affect the induction of tauopathy. The 3D cell cultures might help in eliminating the problem with differentiation agents [72].

3.2.2. Parkinson Disease

Parkinson disease (PD) is a neurodegenerative illness characterized by a loss of cells in the substantia nigra in the midbrain. The loss of these dopaminergic neurons is related to motor dysfunction [73,74], resting tremors, bradykinesia, postural instability and rigidity [75,76]. There is no representative in vitro model to study this neurodegenerative dysfunction. Animal models are not sufficient to predict responses occurring in humans [73]. Since there is the possibility of obtaining most major cell types from the human brain during differentiating induced-pluripotent stem cells—iPSCs [77], this research model seems to show promise as an accurate human model for PD [73].

Moreno et al. (2015) obtained human neuroepithelial cells from iPSCs and finally differentiated them as receiving dopaminergic neurons, cultured within 3D microfluidic cell culture bioreactors. After 30 days, those neurons had characteristic features of dopaminergic neurons and were active [78]. The 3D culture bioreactors were described by Trietsch et al. (2013), who proposed a platform that mimics tissue and perfusion excluding spatial separation [79]. Neighboring lanes of gels and liquids reproduced tissue heterogeneity. A single bioreactor is made from a row of cells settled in hydrogel, and one or more neighboring lanes of liquid flowing laminarily (Figure 5). To shape liquids flowing into the bioreactor, each pair of lanes is separated using a phaseguide. Phaseguide technology makes it possible to control the filling and emptying of a range of types of microfluidic constructions [80,81]. Cells are mixed with replacement ECM, which is subsequently distributed into a well plugged to the phaseguide delimited lane. Finally, the fresh portion of medium is added to the well, which is combined with the medium lane neighboring with cells in hydrogel [78]. Moreno et al. (2015) confirmed

that using this technique allows them to obtain dopaminergic neurons and proved its usefulness in calcium imaging and immunofluorescence. Moreover, analysis of 3D images showed neurons with long neurites [78].

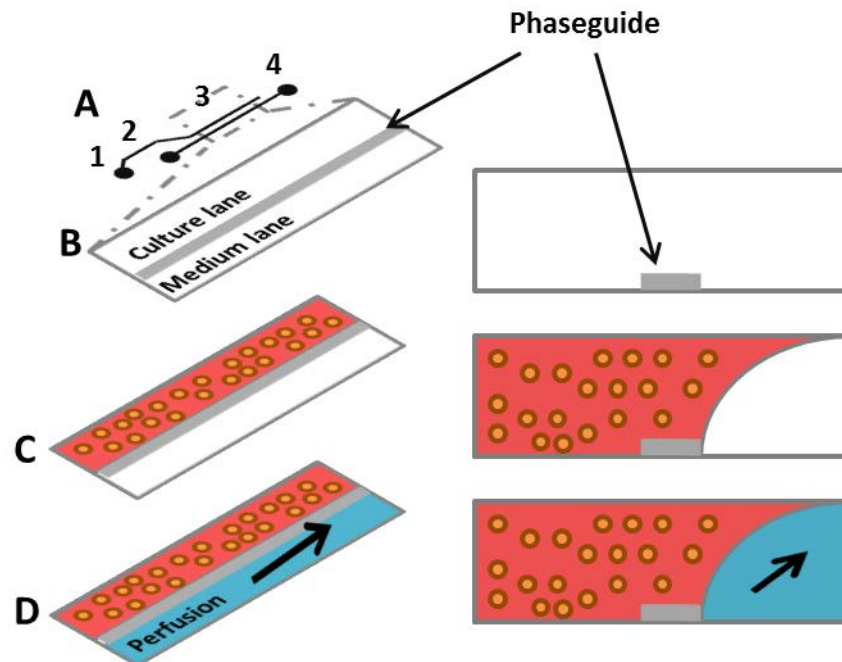


Figure 5. (A) A single 2-lane bioreactor scheme composed of: 1—a gel inlet; 2—a perfusion inlet; 3—an optical readout window; 4—a perfusion outlet; (B) the readout window and its cross section (horizontal view); a phaseguide separates a 2-lane chamber and allows to selective gel patterning; (C) melted gel with cells is loaded and selectively patterned by the phaseguide; (D) after gelation the medium is provided in the perfusion lane and gravitational leveling leads to perfusion between the perfusion inlet and the perfusion outlet wells [78].

3.3. Hepatocyte Spheroids as A Model for Studying Liver Functions and Diseases

Primary human hepatocyte (PHH) spheroid system is a promising tool to investigate liver diseases, functions, long-term drug-induced liver injury, and drug testing, since monolayers seem to be useless due to their rapid de-differentiation. Culturing PHH spheroids in serum-free and chemically specific conditions makes them similar to liver *in vivo*. Furthermore, some inter-individual variability could be observed. Moreover, morphology, viability, and some functions specific for hepatocytes could be noticed after a minimum 5 weeks of culturing. Spheroids remain phenotypically stable. PHH cells could be co-cultured with non-parenchymal cells e.g., Kupffer cells and biliary or stellate cells and this supports their long-term viability [82].

Bell et al. (2016) performed proteome analysis of PHH cells cultured in spheroids (7 days spheroids) as described above and cells from the same donor cultured as monolayers (after 24 h and 7 days) with livers from which they came from. The rapid changes were observed in 2D monolayers cultures. Measurements after 24 h showed that expression of 457 proteins was changed. After 7 days the differences in expression were seen for 358 proteins and expression of 282 of them were changed also after 24 h. After spheroids measurements it was observed that fewer proteins showed altered expression. Moreover, in spheroids cells retained inter-individual differences, what was proved when compared to the corresponding liver pieces from which they were obtained [82].

Analysis of albumin secretion exhibited that hepatocyte-specific functions in the PHH spheroid were kept during prolonged culture, and the secretion was stable [82].

PHH spheroids seem to be a good model for testing liver pathologies. Exposing spheroids to chlorpromazine led to notable accumulation of bile acid, which suggested disturbances in bile acid

transport characteristic for cholestasis. Moreover, treatment of the PHH spheroids with cyclosporine A caused increase of neutral lipids which is associated with steatosis. This indicates that the PHH spheroid model could recreate steatotic pathologies *in vitro*. Furthermore, this model is appropriate for studying the underlying mechanisms of this disease and for drug screening [82].

4. Conclusions

The 3D cell cultures seem to be a suitable tool to improve on the imitations of the simpler 2D cell cultures, which do not simulate the physiological environment precisely as studies on animals. The 3D culture models have the potential for drug testing and discoveries and the examination of nanoparticles. They could also be used as models for diseases, e.g., neurodegenerative diseases or tumors, since animal models do not have some of the relevant and important features that are found in humans, which limit applicability.

The 3D cell cultures offer more in cell–cell and cell–ECM interactions compared to the more traditional use of monolayers (2D cultures), and can have structures more similar to those found *in vivo*.

Author Contributions: Writing—original draft preparation, K.B.; writing—review and editing, P.K., M.B., K.M. All authors have read and agreed to the published version of the manuscript.

Funding: This research received no external funding.

Acknowledgments: This review is written as a part of the first edition of the Ministry of Science and Higher Education program called “Doktoraty wdrozeniowe”.

Conflicts of Interest: The authors declare no conflict of interest.

Abbreviations

2D	two-dimensional
3D	three-dimensional
AD	Alzheimer’s disease
APP	amyloid precursor protein
A β	amyloid beta
Au	gold
CdTe	cadmium telluride
CGF	cowpox growth factor
CIS	cisplatin
CQ	chloroquine
ECM	extracellular matrix
EGFR	epidermal growth factor receptor
FAK	focal adhesion kinase
HD	Huntington’s disease
HTS	high-throughput screening
iPSCs	induced-pluripotent stem cells
NA	noradrenaline
NGF	nerve growth factor
NPs	nanoparticles
OPV	Orthopoxviruses
PAMAM	polyamidoamine
PCL	polycaprolactone
PD	Parkinson’s disease
PDMS	polydimethylsiloxane
PEG	polyethylene glycol
PLGA	poly(lactic-co-glycolic acid)
polyHEMA	poly(hydroxyethyl methacrylate)
PVA	polyvinyl alcohol
RGD	the tripeptide Arg-Gly-Asp consists of Arginine, Glycine, and Aspartate
SAL	salinomycin
WT	wild type

References

1. Goodman, T.T.; Ng, C.P.; Pun, S.H. 3-D tissue culture systems for the evaluation and optimization of nanoparticle-based drug carriers. *Bioconjug. Chem.* **2008**, *19*, 1951–1959. [[CrossRef](#)] [[PubMed](#)]
2. Do Amaral, J.B.; Rezende-Teixeira, P.; Freitas, V.M.; Machado-Santelli, G.M. MCF-7 cells as a three-dimensional model for the study of human breast cancer. *Tissue Eng. Part C Methods* **2011**, *17*, 1097–1107. [[CrossRef](#)]
3. Antoni, D.; Burckel, H.; Josset, E.; Noel, G. Three-dimensional cell culture: A breakthrough in vivo. *Int. J. Mol. Sci.* **2015**, *16*, 5517–5527. [[CrossRef](#)] [[PubMed](#)]
4. Andersen, T.; Auk-Emblem, P.; Dornish, M. 3D cell culture in alginate hydrogels. *Microarrays* **2015**, *4*, 133–161. [[CrossRef](#)] [[PubMed](#)]
5. Centeno, E.G.Z.; Cimarosti, H.; Bithell, A. 2D versus 3D human induced pluripotent stem cell-derived cultures for neurodegenerative disease modeling. *Mol. Neurodegener.* **2018**, *13*, 27. [[CrossRef](#)] [[PubMed](#)]
6. Lee, J.; Lilly, G.D.; Doty, R.C.; Podsiadlo, P.; Kotov, N.A. *In vitro* toxicity testing of nanoparticles in 3D cell culture. *Small* **2009**, *5*, 1213–1221. [[CrossRef](#)]
7. Moshksayan, K.; Kashaninejad, N.; Warkiani, M.E.; Lock, J.G.; Moghadas, H.; Firoozabadi, B.; Saidi, M.S.; Nguyen, N.T. Spheroids-on-a-chip: Recent advances and design considerations in microfluidic platforms for spheroid formation and culture. *Sens. Actuators B Chem.* **2018**, *263*, 151–176. [[CrossRef](#)]
8. Edmondson, R.; Broglie, J.J.; Adcock, A.F.; Yang, L.J. Three-dimensional cell culture systems and their applications in drug discovery and cell-based biosensors. *Assay Drug Dev. Technol.* **2014**, *12*, 207–218. [[CrossRef](#)]
9. Kitel, R.; Czarnecka, J.; Rusin, A. Trójwymiarowe hodowle komórek—Zastosowania w badaniach podstawowych i inżynierii tkankowej. *Post Biochem.* **2013**, *59*, 305–314.
10. Lv, D.; Hu, Z.; Lu, L.; Lu, H.; Xu, X. Three-dimensional cell culture: A powerful tool in tumor research and drug discovery (Review). *Oncol. Lett.* **2017**, *14*, 6999–7010. [[CrossRef](#)]
11. Vantangoli, M.M.; Madnick, S.J.; Huse, S.M.; Weston, P.; Boekelheide, K. MCF-7 human breast cancer cells form differentiated microtissues in scaffold-free hydrogels. *PLoS ONE* **2015**, *10*, e0135426. [[CrossRef](#)] [[PubMed](#)]
12. Sant, S.; Johnston, P.A. The production of 3D tumor spheroids for cancer drug discovery. *Drug Discov. Today Technol.* **2017**, *23*, 27–36. [[CrossRef](#)] [[PubMed](#)]
13. Kapałczyńska, M.; Kolenda, T.; Przybyła, W.; Zajaczkowska, M.; Teresiak, A.; Filas, V.; Ibbs, M.; Bliźniak, R.; Łuczewski, Ł.; Lamperska, K. 2D and 3D cell cultures—A comparison of different types of cancer cell cultures. *Arch. Med. Sci.* **2018**, *14*, 910–919. [[CrossRef](#)] [[PubMed](#)]
14. Lin, R.Z.; Chang, H.Y. Recent advances in three-dimensional multicellular spheroid culture for biomedical research. *Biotechnol. J.* **2008**, *3*, 1172–1184. [[CrossRef](#)] [[PubMed](#)]
15. Lin, R.Z.; Chou, L.F.; Chien, C.C.M.; Chang, H.Y. Dynamic analysis of hepatoma spheroid formation: Roles of E-cadherin and β 1-integrin. *Cell Tissue Res.* **2006**, *324*, 411–422. [[CrossRef](#)]
16. Hirschhaeuser, F.; Menne, H.; Dittfeld, C.; West, J.; Mueller-Klieser, W.; Kunz-Schughart, L.A. Multicellular tumor spheroids: An underestimated tool is catching up again. *J. Biotechnol.* **2010**, *148*, 3–15. [[CrossRef](#)]
17. Estrada, M.F.; Rebelo, S.P.; Davies, E.J.; Pinto, M.T.; Pereira, H.; Santo, V.E.; Smalley, M.J.; Barry, S.T.; Gualda, E.J.; Alves, P.M.; et al. Modelling the tumour microenvironment in long-term microencapsulated 3D co-cultures recapitulates phenotypic features of disease progression. *Biomaterials* **2016**, *78*, 50–61. [[CrossRef](#)]
18. Kim, J.B. Three-dimensional tissue culture models in cancer biology. *Semin. Cancer Biol.* **2005**, *15*, 365–377. [[CrossRef](#)]
19. Koban, R.; Neumann, M.; Dausgs, A.; Bloch, O.; Nitsche, A.; Langhammer, S.; Ellerbrok, H. A novel three-dimensional cell culture method enhances antiviral drug screening in primary human cells. *Antivir. Res.* **2018**, *150*, 20–29. [[CrossRef](#)]
20. Perut, F.; Sbrana, F.V.; Avnet, S.; De Milito, A.; Baldini, N. Spheroid-based 3D cell cultures identify salinomycin as a promising drug for the treatment of chondrosarcoma. *J. Orthop. Res.* **2018**, *36*, 2305–2312. [[CrossRef](#)]
21. Cui, X.; Hartanto, Y.; Zhang, H. Advances in multicellular spheroids formation. *J. R. Soc. Interface* **2017**, *14*, 20160877. [[CrossRef](#)] [[PubMed](#)]
22. Tancioni, I.; Miller, N.L.G.; Uryu, S.; Lawson, C.; Jean, C.; Chen, X.L.; Kleinschmidt, E.G.; Schlaepfer, D.D. FAK activity protects nucleostemin in facilitating breast cancer spheroid and tumor growth. *Breast Cancer Res.* **2015**, *17*, 47. [[CrossRef](#)] [[PubMed](#)]

23. Smyrek, I.; Mathew, B.; Fischer, S.C.; Lissek, S.M.; Becker, S.; Stelzer, E.H.K. E-cadherin, actin, microtubules and FAK dominate different spheroid formation phases and important elements of tissue integrity. *Biol. Open* **2019**, *8*. [[CrossRef](#)] [[PubMed](#)]
24. Anada, T.; Fukuda, J.; Sai, Y.; Suzuki, O. An oxygen-permeable spheroid culture system for the prevention of central hypoxia and necrosis of spheroids. *Biomaterials* **2012**, *33*, 8430–8441. [[CrossRef](#)]
25. Ong, S.M.; Zhao, Z.; Arooz, T.; Zhao, D.; Zhang, S.; Du, T.; Wasser, M.; van Noort, D.; Yu, H. Engineering a scaffold-free 3D tumor model for *in vitro* drug penetration studies. *Biomaterials* **2010**, *31*, 1180–1190. [[CrossRef](#)]
26. Napolitano, A.P.; Dean, D.M.; Man, A.J.; Youssef, J.; Ho, D.N.; Rago, A.P.; Lech, M.P.; Morgan, J.R. Scaffold-free three-dimensional cell culture utilizing micromolded nonadhesive hydrogels. *Biotechniques* **2007**, *43*, 494–500. [[CrossRef](#)]
27. Foty, R. A Simple Hanging Drop Cell Culture Protocol for Generation of 3D Spheroids. *J. Vis. Exp.* **2011**. [[CrossRef](#)]
28. Breslin, S.; O'Driscoll, L. Three-dimensional cell culture: The missing link in drug discovery. *Drug Discov. Today* **2013**, *18*, 240–249. [[CrossRef](#)]
29. Nath, S.; Devi, G.R. Three-dimensional culture systems in cancer research: Focus on tumor spheroid model. *Pharmacol. Ther.* **2016**, *163*, 94–108. [[CrossRef](#)]
30. Tung, Y.C.; Hsiao, A.Y.; Allen, S.G.; Torisawa, Y.S.; Ho, M.; Takayama, S. High-throughput 3D spheroid culture and drug testing using a 384 hanging drop array. *Analyst* **2011**, *136*, 473–478. [[CrossRef](#)]
31. Shin, J.Y.; Park, J.; Jang, H.K.; Lee, T.J.; La, W.G.; Bhang, S.H.; Kwon, I.K.; Kwon, O.H.; Kim, B.S. Efficient formation of cell spheroids using polymer nanofibers. *Biotechnol. Lett.* **2012**, *34*, 795–803. [[CrossRef](#)] [[PubMed](#)]
32. Ryu, J.H.; Kim, M.S.; Lee, G.M.; Choi, C.Y.; Kim, B.S. The enhancement of recombinant protein production by polymer nanospheres in cell suspension culture. *Biomaterials* **2005**, *26*, 2173–2181. [[CrossRef](#)] [[PubMed](#)]
33. Türker, E.; Demircak, N.; Arslan-Yildiz, A. Scaffold-free three-dimensional cell culturing using magnetic levitation. *Biomater. Sci.* **2018**, *6*, 1745–1763. [[CrossRef](#)] [[PubMed](#)]
34. Souza, G.R.; Molina, J.R.; Raphael, R.M.; Ozawa, M.G.; Stark, D.J.; Levin, C.S.; Bronk, L.F.; Ananta, J.S.; Mandelin, J.; Georgescu, M.M.; et al. Three-dimensional tissue culture based on magnetic cell levitation. *Nat. Nanotechnol.* **2010**, *5*, 291–296. [[CrossRef](#)] [[PubMed](#)]
35. Ruppen, J.; Cortes-Dericks, L.; Marconi, E.; Karoubi, G.; Schmid, R.A.; Peng, R.W.; Marti, T.M.; Guenat, O.T. A microfluidic platform for chemoresistive testing of multicellular pleural cancer spheroids. *Lab Chip* **2014**, *14*, 1198. [[CrossRef](#)]
36. Lee, S.A.; No, D.Y.; Kang, E.; Ju, J.; Kim, D.S.; Lee, S.H. Spheroid-based three-dimensional liver-on-a-chip to investigate hepatocyte-hepatic stellate cell interactions and flow effects. *Lab Chip* **2013**, *13*, 3529. [[CrossRef](#)]
37. Lazzari, G.; Nicolas, V.; Matsusaki, M.; Akashi, M.; Couvreur, P.; Mura, S. Multicellular spheroid based on a triple co-culture: A novel 3D model to mimic pancreatic tumor complexity. *Acta Biomater.* **2018**, *78*, 296–307. [[CrossRef](#)]
38. Xin, X.; Yang, H.P.; Zhang, F.L.; Yang, S.T. 3D cell coculture tumor model: A promising approach for future cancer drug discovery. *Process Biochem.* **2019**, *78*, 148–160. [[CrossRef](#)]
39. Zhang, Y.S.; Duchamp, M.; Oklu, R.; Ellisen, L.W.; Langer, R.; Khademhosseini, A. Bioprinting the Cancer Microenvironment. *ACS Biomater. Sci. Eng.* **2016**, *2*, 1710–1721. [[CrossRef](#)]
40. Hoarau-Vechot, J.; Rafii, A.; Touboul, C.; Pasquier, J. Halfway between 2D and Animal Models: Are 3D Cultures the Ideal Tool to Study Cancer-Microenvironment Interactions? *Int. J. Mol. Sci.* **2018**, *19*, 181. [[CrossRef](#)]
41. Munoz-Abraham, A.S.; Rodriguez-Davalos, M.I.; Bertacco, A.; Wengert, B.; Geibel, J.P.; Mulligan, D.C. 3D Printing of Organs for Transplantation: Where Are We and Where Are We Heading? *Curr. Transpl. Rep.* **2016**, *3*, 93–99. [[CrossRef](#)]
42. Karlsson, H.; Fryknas, M.; Larsson, R.; Nygren, P. Loss of cancer drug activity in colon cancer HCT-116 cells during spheroid formation in a new 3-D spheroid cell culture system. *Exp. Cell Res.* **2012**, *318*, 1577–1585. [[CrossRef](#)] [[PubMed](#)]
43. Amelian, A.; Wasilewska, K.; Megias, D.; Winnicka, K. Application of standard cell cultures and 3D *in vitro* tissue models as an effective tool in drug design and development. *Pharmacol. Rep.* **2017**, *69*, 861–870. [[CrossRef](#)]

44. Fang, Y.; Eglen, R.M. Three-dimensional cell cultures in drug discovery and development. *SLAS Discov.* **2017**, *22*, 456–472. [[CrossRef](#)] [[PubMed](#)]
45. Langhammer, S.; Koban, R.; Yue, C.; Ellerbrok, H. Inhibition of poxvirus spreading by the anti-tumor drug Gefitinib (Iressa™). *Antivir. Res.* **2011**, *89*, 64–70. [[CrossRef](#)]
46. Luca, A.C.; Mersch, S.; Deenen, R.; Schmidt, S.; Messner, I.; Schafer, K.L.; Baldus, S.E.; Huckenbeck, W.; Piekorz, R.P.; Knoefel, W.T.; et al. Impact of the 3D microenvironment on phenotype, gene expression, and EGFR inhibition of colorectal cancer cell lines. *PLoS ONE* **2013**, *8*, e59689. [[CrossRef](#)] [[PubMed](#)]
47. Jamil, N.; Howie, S.; Salter, D.M. Therapeutic molecular targets in human chondrosarcoma. *Int. J. Exp. Pathol.* **2010**, *91*, 387–393. [[CrossRef](#)]
48. De Jong, Y.; van Oosterwijk, J.G.; Kruisselbrink, A.B.; Briaire-de Bruijn, I.H.; Agrogiannis, G.; Baranski, Z.; Cleven, A.H.G.; Cleton-Jansen, A.M.; van de Water, B.; Danen, E.H.J.; et al. Targeting survivin as a potential new treatment for chondrosarcoma of bone. *Oncogenesis* **2016**, *5*, e222. [[CrossRef](#)] [[PubMed](#)]
49. Liu, L.Y.; Yang, M.H.; Kang, R.; Wang, Z.; Zhao, Y.M.; Yu, Y.; Xie, M.; Yin, X.C.; Livesey, K.M.; Lotze, M.T.; et al. DAMP-mediated autophagy contributes to drug resistance. *Autophagy* **2011**, *7*, 112–114. [[CrossRef](#)]
50. Yang, Z.N.J.; Chee, C.E.; Huang, S.B.; Sinicrope, F.A. The role of autophagy in cancer: Therapeutic implications. *Mol. Cancer Ther.* **2011**, *10*, 1533–1541. [[CrossRef](#)]
51. Bovee, J.V.M.G.; Hogendoorn, P.C.W.; Wunder, J.S.; Alman, B.A. Cartilage tumours and bone development: Molecular pathology and possible therapeutic targets. *Nat. Rev. Cancer* **2010**, *10*, 481–488. [[CrossRef](#)] [[PubMed](#)]
52. Wu, J.Y.; Huang, W.Z.; He, Z.Y. Dendrimers as Carriers for siRNA Delivery and Gene Silencing: A Review. *Sci. World J.* **2013**. [[CrossRef](#)] [[PubMed](#)]
53. Zeng, Y.; Kurokawa, Y.; Zeng, Q.; Win-Shwe, T.T.; Nansai, H.; Zhang, Z.Y.; Sone, H. Effects of polyamidoamine dendrimers on a 3-D neurosphere system using human neural progenitor cells. *Toxicol. Sci.* **2016**, *152*, 128–144. [[CrossRef](#)] [[PubMed](#)]
54. Newkome, G.R.; Childs, B.J.; Rourke, M.J.; Baker, G.R.; Moorefield, C.N. Dendrimer construction and macromolecular property modification via combinatorial methods. *Biotechnol. Bioeng.* **1999**, *61*, 243–253. [[CrossRef](#)]
55. Bharatwaj, B.; Mohammad, A.K.; Dimovski, R.; Cassio, F.L.; Bazito, R.C.; Conti, D.; Fu, Q.; Reineke, J.; da Rocha, S.R.P. Dendrimer nanocarriers for transport modulation across models of the pulmonary epithelium. *Mol. Pharm.* **2015**, *12*, 826–838. [[CrossRef](#)]
56. Goodman, T.T.; Olive, P.L.; Pun, S.H. Increased nanoparticle penetration in collagenase-treated multicellular spheroids. *Int. J. Nanomed.* **2007**, *2*, 265–274.
57. Netti, P.A.; Berk, D.A.; Swartz, M.A.; Grodzinsky, A.J.; Jain, R.K. Role of extracellular matrix assembly in interstitial transport in solid tumors. *Cancer Res.* **2000**, *60*, 2497–2503.
58. Pluen, A.; Boucher, Y.; Ramanujan, S.; McKee, T.D.; Gohongi, T.; di Tomaso, E.; Brown, E.B.; Izumi, Y.; Campbell, R.B.; Berk, D.A.; et al. Role of tumor-host interactions in interstitial diffusion of macromolecules: Cranial vs. subcutaneous tumors. *Proc. Natl. Acad. Sci. USA* **2001**, *98*, 4628–4633. [[CrossRef](#)]
59. Słowska, A.; Cymerys, J. Zastosowanie trójwymiarowych hodowli komórek nerwowych w badaniach mechanizmów przebiegu chorób neurodegeneracyjnych. *Postepy Hig. Med. Dośw.* **2017**, *71*, 510–519. [[CrossRef](#)]
60. Szwed, A.; Milowska, K. The role of proteins in neurodegenerative disease. *Postepy Hig. Med. Dośw.* **2012**, *66*, 187–195. [[CrossRef](#)]
61. Ramanan, V.K.; Saykin, A.J. Pathways to neurodegeneration: Mechanistic insights from GWAS in Alzheimer’s disease, Parkinson’s disease, and related disorders. *Am. J. Neurodegener. Dis.* **2013**, *2*, 145–175. [[PubMed](#)]
62. Bertram, L.; Tanzi, R.E. Thirty years of Alzheimer’s disease genetics: The implications of systematic meta-analyses. *Nat. Rev. Neurosci.* **2008**, *9*, 768–778. [[CrossRef](#)] [[PubMed](#)]
63. Choi, S.H.; Kim, Y.H.; Quinti, L.; Tanzi, R.E.; Kim, D.Y. 3D culture models of Alzheimer’s disease: A road map to a “cure-in-a-dish”. *Mol. Neurodegener.* **2016**, *11*, 75. [[CrossRef](#)] [[PubMed](#)]
64. Tanzi, R.E.; Bertram, L. Twenty years of the Alzheimer’s disease amyloid hypothesis: A genetic perspective. *Cell* **2005**, *120*, 545–555. [[CrossRef](#)] [[PubMed](#)]
65. D’Avanzo, C.; Aronson, J.; Kim, Y.H.; Choi, S.H.; Tanzi, R.E.; Kim, D.Y. Alzheimer’s in 3D culture: Challenges and perspectives. *Bioessays* **2015**, *37*, 1139–1148. [[CrossRef](#)]

66. Armstrong, R.A. A critical analysis of the 'amyloid cascade hypothesis'. *Folia Neuropathol.* **2014**, *52*, 211–225. [[CrossRef](#)]
67. Sasaguri, H.; Nilsson, P.; Hashimoto, S.; Nagata, K.; Saito, T.; De Strooper, B.; Hardy, J.; Vassar, R.; Winblad, B.; Saido, T.C. APP mouse models for Alzheimer's disease preclinical studies. *EMBO J.* **2017**, *36*, 2473–2487. [[CrossRef](#)]
68. De Strooper, B. Lessons from a failed gamma-secretase Alzheimer trial. *Cell* **2014**, *159*, 721–726. [[CrossRef](#)]
69. Mudher, A.; Lovestone, S. Alzheimer's disease—Do tauists and baptists finally shake hands? *Trends Neurosci.* **2002**, *25*, 22–26. [[CrossRef](#)]
70. Xicoy, H.; Wieringa, B.; Martens, G.J.M. The SH-SY5Y cell line in Parkinson's disease research: A systematic review. *Mol. Neurodegener.* **2017**, *12*, 10. [[CrossRef](#)]
71. Agholme, L.; Lindstrom, T.; Kagedal, K.; Marcusson, J.; Hallbeck, M. An *in vitro* model for neuroscience: Differentiation of SH-SY5Y cells into cells with morphological and biochemical characteristics of mature neurons. *J. Alzheimer's Dis.* **2010**, *20*, 1069–1082. [[CrossRef](#)]
72. Seidel, D.; Krinke, D.; Jahnke, H.G.; Hirche, A.; Kloss, D.; Mack, T.G.A.; Striggow, F.; Robitzki, A. Induced tauopathy in a novel 3D-culture model mediates neurodegenerative processes: A real-time study on biochips. *PLoS ONE* **2012**, *7*, e49150. [[CrossRef](#)]
73. Bolognin, S.; Fosseppe, M.; Qing, X.B.; Jarazo, J.; Scancar, J.; Moreno, E.L.; Nickels, S.L.; Wasner, K.; Ouzren, N.; Walter, J.; et al. 3D cultures of Parkinson's disease-specific dopaminergic neurons for high content phenotyping and drug testing. *Adv. Sci.* **2018**, *6*, 1800927. [[CrossRef](#)]
74. Mahlke, P.; Seppi, K.; Poewe, W. The concept of prodromal Parkinson's disease. *J. Parkinson's Dis.* **2015**, *5*, 681–697. [[CrossRef](#)]
75. Meissner, W.G.; Frasier, M.; Gasser, T.; Goetz, C.G.; Lozano, A.; Piccini, P.; Obeso, J.A.; Rascol, O.; Schapira, A.; Voon, V.; et al. Priorities in Parkinson's disease research. *Nat. Rev. Drug Discov.* **2011**, *10*, 377–393. [[CrossRef](#)]
76. Antony, P.M.A.; Diederich, N.J.; Kruger, R.; Balling, R. The hallmarks of Parkinson's disease. *FEBS J.* **2013**, *280*, 5981–5993. [[CrossRef](#)]
77. Parr, C.J.C.; Yamanaka, S.; Saito, H. An update on stem cell biology and engineering for brain development. *Mol. Psychiatry* **2017**, *22*, 808–819. [[CrossRef](#)]
78. Moreno, E.L.; Hachi, S.; Hemmer, K.; Trietsch, S.J.; Baumuratov, A.S.; Hankemeier, T.; Vulto, P.; Schwamborn, J.C.; Fleming, R.M.T. Differentiation of neuroepithelial stem cells into functional dopaminergic neurons in 3D microfluidic cell culture. *Lab Chip* **2015**, *15*, 2419–2428. [[CrossRef](#)]
79. Trietsch, S.J.; Israëls, G.D.; Joore, J.; Hankemeier, T.; Vulto, P. Microfluidic titer plate for stratified 3D cell culture. *Lab Chip* **2013**, *13*, 3548–3554. [[CrossRef](#)]
80. Yildirim, E.; Trietsch, S.J.; Joore, J.; van den Berg, A.; Hankemeier, T.; Vulto, P. Phaseguides as tunable passive microvalves for liquid routing in complex microfluidic networks. *Lab Chip* **2014**, *14*, 3334–3340. [[CrossRef](#)]
81. Vulto, P.; Podszun, S.; Meyer, P.; Hermann, C.; Manz, A.; Urban, G.A. Phaseguides: A paradigm shift in microfluidic priming and emptying. *Lab Chip* **2011**, *11*, 1596–1602. [[CrossRef](#)]
82. Bell, C.C.; Hendriks, D.F.G.; Moro, S.M.L.; Ellis, E.; Walsh, J.; Renblom, A.; Puigvert, L.F.; Dankers, A.C.A.; Jacobs, F.; Snoeys, J.; et al. Characterization of primary human hepatocyte spheroids as a model system for drug-induced liver injury, liver function and disease. *Sci. Rep.* **2016**, *6*, 25187. [[CrossRef](#)]





Article

Interaction of Cationic Carbosilane Dendrimers and Their siRNA Complexes with MCF-7 Cells

Kamila Białkowska ^{1,2,*} , Katarzyna Miłowska ¹ , Sylwia Michlewska ³ , Paulina Sokołowska ^{2,4},
Piotr Komorowski ^{2,5} , Tania Lozano-Cruz ^{6,7}, Rafael Gomez-Ramirez ^{6,7} , Francisco Javier de la Mata ^{6,7}
and Maria Bryszewska ¹

- ¹ Department of General Biophysics, Faculty of Biology and Environmental Protection, University of Lodz, 141/143 Pomorska St., 90-236 Lodz, Poland; katarzyna.milowska@biol.uni.lodz.pl (K.M.); maria.bryszewska@biol.uni.lodz.pl (M.B.)
- ² Molecular and Nanostructural Biophysics Laboratory, "Bionanopark" Ltd., 114/116 Dubois St., 93-465 Lodz, Poland; paulina.sokolowska@umed.lodz.pl (P.S.); p.komorowski@bionanopark.pl (P.K.)
- ³ Laboratory of Microscopic Imaging and Specialized Biological Techniques, Faculty of Biology and Environmental Protection, University of Lodz, Banacha12/16, 90-237 Lodz, Poland; sylwia.michlewska@biol.uni.lodz.pl
- ⁴ Department of Pharmacology and Toxicology, Medical University of Lodz, Żeligowskiego St. 7/9, 90-752 Lodz, Poland
- ⁵ Department of Biophysics, Institute of Materials Science, Lodz University of Technology, 1/15 Stefanowskiego St., 90-924 Lodz, Poland
- ⁶ Department of Organic and Inorganic Chemistry, IQAR, University of Alcalá, 28805 Madrid, Spain; tania.lozano@uah.es (T.L.-C.); rafael.gomez@uah.es (R.G.-R.); javier.delamata@uah.es (F.J.d.l.M.)
- ⁷ Networking Research Center on Bioengineering, Biomaterials and Nanomedicine (CIBER-BBN), 28029 Madrid, Spain
- * Correspondence: kamila.bialkowska@edu.uni.lodz.pl



Citation: Białkowska, K.; Miłowska, K.; Michlewska, S.; Sokołowska, P.; Komorowski, P.; Lozano-Cruz, T.; Gomez-Ramirez, R.; de la Mata, F.J.; Bryszewska, M. Interaction of Cationic Carbosilane Dendrimers and Their siRNA Complexes with MCF-7 Cells. *Int. J. Mol. Sci.* **2021**, *22*, 7097. <https://doi.org/10.3390/ijms22137097>

Academic Editor: Giovanni Natile

Received: 17 June 2021

Accepted: 28 June 2021

Published: 1 July 2021

Publisher's Note: MDPI stays neutral with regard to jurisdictional claims in published maps and institutional affiliations.



Copyright: © 2021 by the authors. Licensee MDPI, Basel, Switzerland. This article is an open access article distributed under the terms and conditions of the Creative Commons Attribution (CC BY) license (<https://creativecommons.org/licenses/by/4.0/>).

Abstract: The application of siRNA in gene therapy is mainly limited because of the problems with its transport into cells. Utilization of cationic dendrimers as siRNA carriers seems to be a promising solution in overcoming these issues, due to their positive charge and ability to penetrate cell membranes. The following two types of carbosilane dendrimers were examined: CBD-1 and CBD-2. Dendrimers were complexed with pro-apoptotic siRNA (Mcl-1 and Bcl-2) and the complexes were characterized by measuring their zeta potential, circular dichroism and fluorescence of ethidium bromide associated with dendrimers. CBD-2/siRNA complexes were also examined by agarose gel electrophoresis. Both dendrimers form complexes with siRNA. Moreover, the cellular uptake and influence on the cell viability of the dendrimers and dendriplexes were evaluated using microscopic methods and XTT assay on MCF-7 cells. Microscopy showed that both dendrimers can transport siRNA into cells; however, a cytotoxicity assay showed differences in the toxicity of these dendrimers.

Keywords: siRNA; carbosilane dendrimers; dendriplexes; nanocarriers

1. Introduction

One of the most common causes of death in the world is cancer. Finding new methods of treatment is a big challenge because of heterogeneity and metastasis [1,2]. Tumor development is associated with the dysfunctional regulation of apoptosis, the process responsible for the removal of damaged or infected cells. The main regulators of apoptosis are proteins belonging to the Bcl-2 family, consisting of pro- and anti-apoptotic proteins [3]. Among the proteins that can promote cell death are, e.g., Bax, Bak and Bcl-XS, whereas among the proteins promoting cell survival are Bcl-2, Bcl-XL and Mcl-1 [4]. The inhibition or promotion of apoptosis may be due to an imbalance between these proteins [3]. The transformation of normal cells into cancerous ones leads to their uncontrolled proliferation and inability to initiate apoptosis [4,5]. One possibility for reversing this process and inducing apoptosis is a cellular mechanism that enables selective pro-survival gene

silencing, called RNA interference (RNAi). This mechanism promotes messenger RNA (mRNA) degradation using small interfering RNAs (siRNAs) [6–8]. For this reason, siRNA is under investigation for use in gene therapy [9].

An siRNA is a small double stranded molecule, with the ability to silence genes. It is incorporated in the RISC (RNA-induced silencing complex), which mediates mRNA binding and cleavage [10].

The process of RNA interference was first observed in worms. It is believed that a function of RNAi is to protect the genome against invasive genetic material, such as viruses [10]. However, there are some limitations in using naked siRNA for gene silencing [5,10,11]. One is its inability to penetrate cell membranes due to its anionic charge and repulsion from anionic membrane surfaces [10,11]. Furthermore, siRNA effectiveness in vitro and in vivo is limited because of its low enzymatic resistance. This means that effective gene transport into target cells is the main limitation in gene therapy [5,10,11]. Therefore, the application of new synthetic particles as non-viral gene carriers could be very helpful in transporting siRNAs into cells.

Among the nanomaterials considered for potential use in siRNA transport into cells, the most promising are dendrimers [12]. Dendrimers are synthetic polymers with a diameter of 3–10 nm. The name dendrimer originates from Greek “dendron”, which means a tree and is due to their branched structure. The shape of dendrimers is similar to a sphere [13–15]. Generally, their structure can be divided into the following three parts: (1) a central core, which defines the interior size and the number of branches; (2) repetitive branch units for the regulation of molecular size, generation and flexibility; and (3) the terminal groups, which provide the possibility for interaction with a range of compounds [16]. The characteristic structure of dendrimers allows them to complex with different particles, because of the empty spaces within the dendrimer structure [13–15].

Dendrimers have a lot of advantages as effective gene carriers, e.g., their stability and/or large number of groups for nucleic acid binding [5,17]. Cationic dendrimers can penetrate cell membranes due to the positive charge on their surface, in contrast to anionic or neutral dendrimers. Moreover, cationic dendrimers can bind anionic nucleic acids forming dendriplexes, and this allows genes to be transported into cells effectively [5,17–19].

Many types of dendrimers have been investigated for siRNA transport, including poly(amidoamine) dendrimers (PAMAM), carbosilane dendrimers (CBD), poly(propylene imine) dendrimers, poly(L-lysine) dendrimers, triazine dendrimers, polyglycerol-based dendrimers and nanocarbon-based dendrimers [16]. Carbosilane dendrimers complex siRNA via electrostatic interactions and protect them against RNase degradation. CBD/siRNA complexes transfected lymphocytes and silenced the expression of glyceraldehyde 3-phosphate dehydrogenase (GAPDH), and reduced HIV replication in human leukemia T lymphocytes and primary peripheral blood mononuclear cells (PBMC), with low cytotoxicity. CBD can also transfer siRNA to neurons and block HIF1- α synthesis. These effects were similar to that achieved by viral vectors. Furthermore, the gene silencing by CBD/siRNA complexes occurred even after passing the blood–brain barrier in an in vitro model [16].

The present work shows that the new second generation carbosilane dendrimers can provide a potential delivery system to transport pro-apoptotic siRNA to target (cancer) cells. The two types of dendrimers used in this study, CBD-1 and CBD-2, differ in the type of ammonium group on their surfaces; therefore, the aim has been to verify which one is the better carrier for siRNA transport. Dendrimers were complexed with the following pro-apoptotic siRNAs: Mcl-1 and Bcl-2. The formed complexes were characterized by their zeta potential, circular dichroism (CD) and fluorescence measurements. CBD-2/siRNA complexes were also examined by agarose gel electrophoresis. Additionally, the cytotoxicity of dendrimers and formed complexes on the MCF-7 cell line and the cellular uptake of dendriplexes were investigated.

2. Results

2.1. Zeta Potential

The measurement of zeta potential was used to assess changes in the surface charge of the complexes and interactions between dendrimers and siRNAs. The siRNA concentration was constant at 0.5 μM , whereas dendrimers were added in increasing concentrations. Figure 1 shows the changes in the zeta potential of siRNA after the addition of dendrimers. Both dendrimers affected the zeta potential of the selected siRNAs. The siRNAs had negative zeta potential values (both Mcl-1 and Bcl-2: ~ -12 mV). The dendrimers changed the initial zeta potential values of siRNAs from negative to positive. For CBD-1, the plateau was achieved above +5 mV and for CBD-2 above +20 mV.

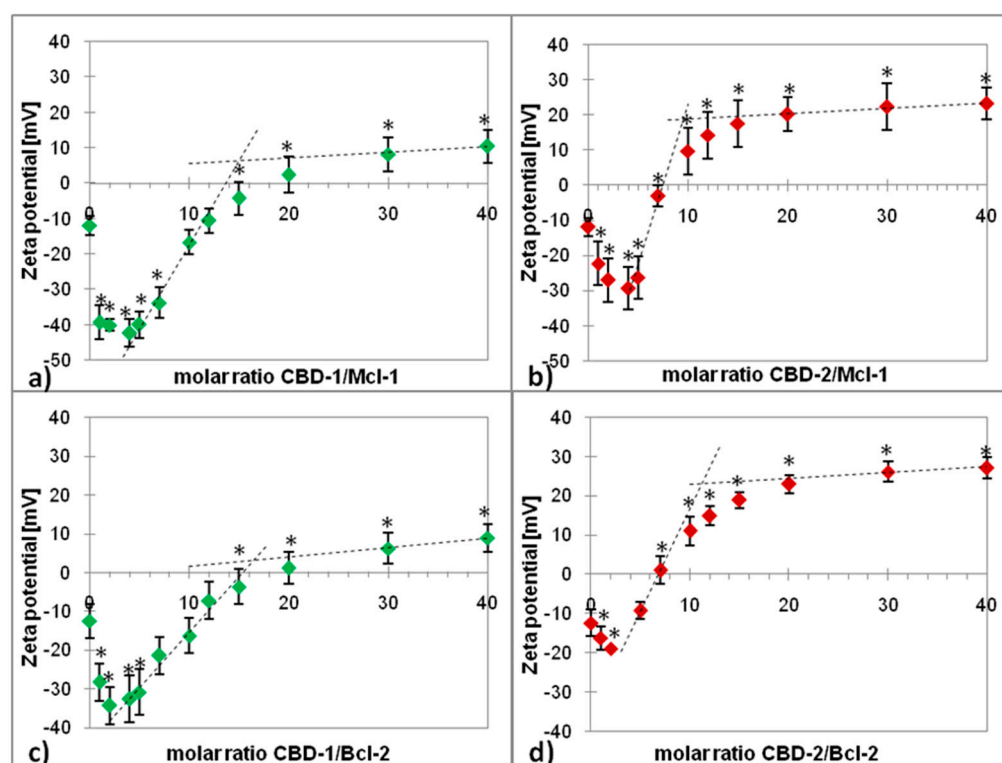


Figure 1. Zeta potential of the Mcl-1 (a,b) and Bcl-2 (c,d) after addition of carboxilane dendrimers CBD-1 or CBD-2 at increasing dendrimer/siRNA molar ratios in 10 mmol/L Na-phosphate buffer, pH 7.4. Results are presented as mean \pm SD from a minimum of 3 independent experiments. * $p < 0.05$ compared to siRNA.

The two tangents method helped to determine the number of dendrimer molecules (n) that attach to one molecule of siRNA. Calculated on the basis of the graphs, n is 15 for CBD-1 and Mcl-1, 9 for CBD-2 and Mcl-1, 16 for CBD-1 and Bcl-2 and 11 for CBD-2 and Bcl-2 (Figure 1). Partial deprotonation of tertiary ammonium groups (RNHMe_2) is possible at the assay pH, resulting in a lower cationic density on the surface of CBD-1. This feature could explain the higher number of molecules required to conjugate the siRNA compared to CBD-2.

2.2. Circular Dichroism

Changes in the secondary structure of the siRNAs (Mcl-1 and Bcl-2) under the influence of carboxilane dendrimers were also examined using CD spectroscopy. CD spectra were recorded at a wavelength range of $\lambda = 200\text{--}300$ nm. The spectra for both siRNAs were typical of the A-form, the secondary structure of RNA. They had characteristic peaks at ~ 210 and ~ 265 nm. The changes in the shape of both siRNAs' spectra under the influence of dendrimers were also noted. The signal intensity decreased in all cases for

$\lambda = 210$ nm and $\lambda = 265$ nm. We also found that dendrimers caused a shift toward longer wavelengths of both peaks. Figure 2 gives an example of changes in the spectrum for a system CBD-2/Bcl-2.

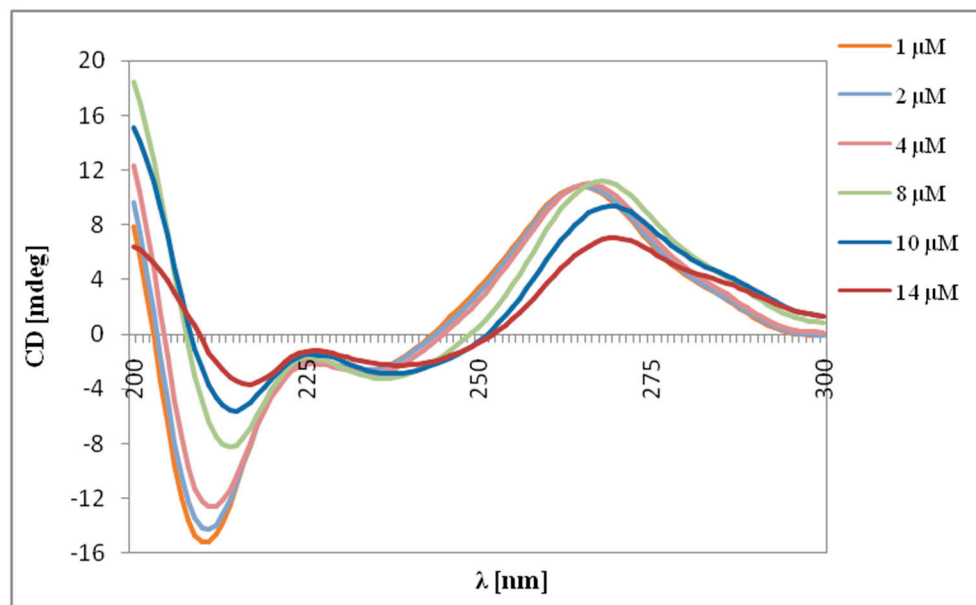


Figure 2. CD spectra of the Bcl-2 (2 μ M) in the presence of CBD-2 dendrimer (1–14 μ M) in 10 mmol/L phosphate buffer.

The ellipticity of complexes decreased with the higher dendrimer/siRNA molar ratio. The changes in θ/θ_0 after addition of dendrimers to siRNAs are shown in Figure 3.

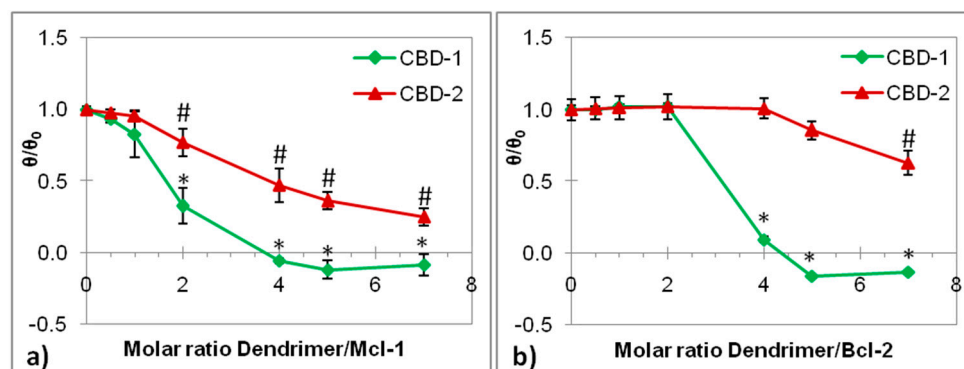


Figure 3. Changes in mean residue ellipticity of Mcl-1 (a) and Bcl-2 (b) at $\lambda = 265$ nm in the presence of the following dendrimers: CBD-1 and CBD-2. siRNA concentration = 2 μ M; wavelength, 200–300 nm; bandwidth, 1.0 nm; response time, 4 s; scanning speed, 50 nm/min; step resolution, 0.5 nm. Naphosphate buffer 10 mmol/L, pH 7.4. Results are presented as mean \pm SD from a minimum of 3 independent experiments. * $p < 0.05$ compared to siRNA (after addition of CBD-1); # $p < 0.05$ compared to siRNA (after addition of CBD-2).

The changes in the siRNA CD spectra depended on the concentration of dendrimers. θ/θ_0 decreased with an increasing concentration of CBD-1, finally reaching a stabilization. This indicates that the CBD-1 molecules gradually bind to both siRNAs until the saturation of the siRNA molecule at a 5:1 molar ratio (CBD-1:siRNA) occurs, whereas for CBD-2 there was decrease in the θ/θ_0 , but stabilization was not visible, probably because the dendrimer concentrations using this method were too low. Higher concentrations of dendrimers could not be used as they would interfere with the siRNA spectrum. Here, the system saturation

was found for dendrimer CBD-1, but not for CBD-2, in contrast with the zeta potential, where CBD-1 needed more molecules to conjugate the siRNA.

2.3. Ethidium Bromide (EtBr) Intercalation Assay

Fluorescence spectra of the EtBr-labeled Bcl-2 in the presence and absence of the CBD-2 dendrimer, as an example, are shown in Figure 4.

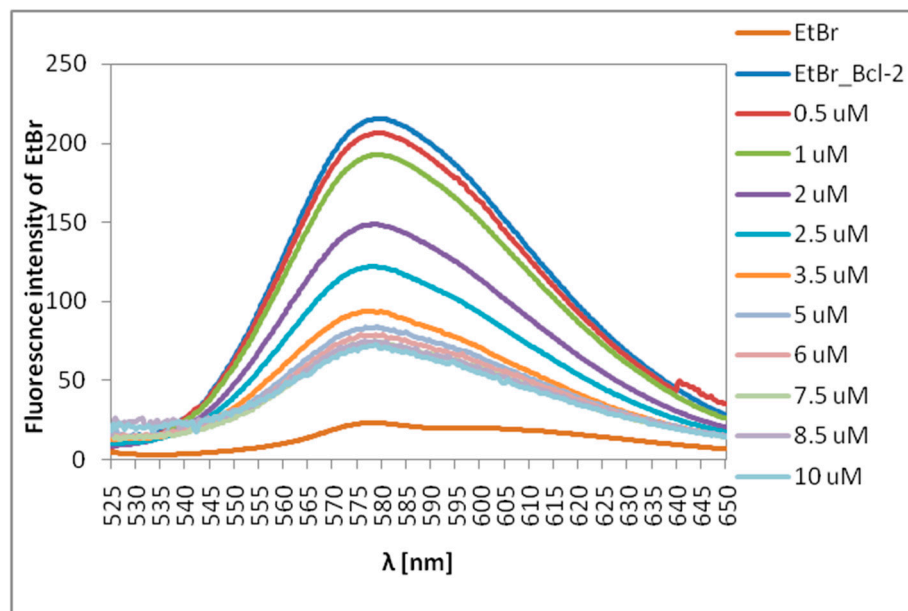


Figure 4. Dependence of the fluorescence intensity of the EtBr-Bcl-2 complex on an increasing concentration of CBD-2.

Dendrimers without siRNA had no effect on the intensity of EtBr fluorescence, due to the lack of any EtBr/dendrimer interaction (data not shown). After the addition of dendrimers, the EtBr fluorescence decreased, which indicates the binding of the dendrimer to the siRNA and displacement of EtBr. Figure 5 shows changes of relative fluorescence intensity (F/F_0) after the addition of dendrimers. The results proved the binding of CBD-1 and CBD-2 to Mcl-1 and Bcl-2. The relative fluorescence intensity (F/F_0) was lower with the increasing dendrimer/siRNA molar ratio. For Bcl-2, the decline in F/F_0 was similar, but differences in the shape of the curves were observed for Mcl-1.

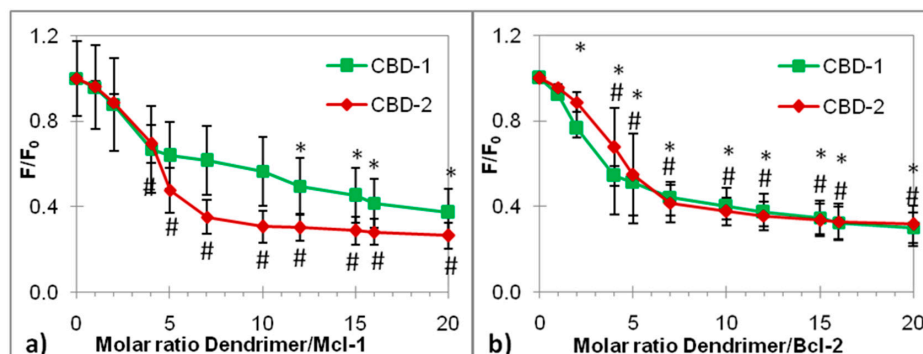


Figure 5. Dependence of the fluorescence intensity of the EtBr-siRNA complex on an increasing concentration of CBD-1 and CBD-2 dendrimers. (a) Mcl-1; (b) Bcl-2. siRNA concentration, 0.5 μ M; EtBr concentration, 5 μ M. Na-phosphate buffer, 10 mmol/L, pH 7.4. λ_{ex} = 480 nm, λ_{em} = 525–650 nm. Results are presented as mean \pm SD obtained from a minimum of 3 independent experiments. * $p < 0.05$ compared to siRNA (after addition of CBD-1); # $p < 0.05$ compared to siRNA (after addition of CBD-2).

2.4. Gel Electrophoresis

Agarose gel electrophoresis helped to evaluate a possible protective effect of dendrimers on siRNA against degradation by RNase. Figure 6 shows photographs of gels after the electrophoresis of complexes of the CBD-2 dendrimer with Mcl-1 and Bcl-2. Naked siRNA was completely digested in the presence of RNase (Figure 6a,b, third lines). Treatment with RNase did not lead to degradation of siRNAs complexed with CBD-2 (Figure 6). Addition of heparin resulted in the release of siRNA from the dendriplexes and its migration through the gel (Figure 6a,b, fifth line).

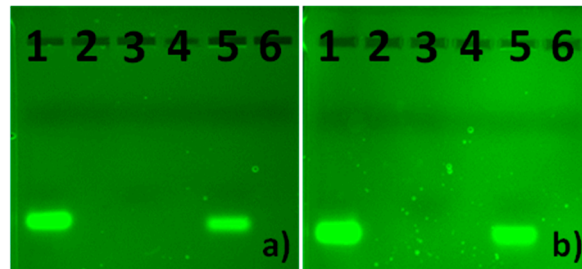


Figure 6. Protective effect of CBD-2 on siRNA in the presence of RNase A/T1 mix. (a) CBD-2 + Mcl-1, (b) CBD-2 + Bcl-2; 1, naked siRNA; 2, CBD-2; 3, siRNA + RNase; 4, siRNA + CBD-2 + RNase; 5, siRNA + CBD-2 + RNase + heparin; 6, siRNA + CBD-2.

2.5. XTT Assay

The MCF-7 cells were exposed to dendrimers and complexes of dendrimer/siRNA at different concentrations for 24 h. An XTT assay was also used for dimethyl sulfoxide (DMSO), the solvent. DMSO had no influence on the viability of the MCF-7 cells at dendrimer concentrations in the range of 0.1–5 μM , but it affected cells at the highest concentration, of 10 μM , decreasing viability to 60.5% vs. a negative control (NC).

Both types of dendrimer decreased the cell viability in a dose-dependent manner (Figure 7). Compared to the control, a small, but statistically significant effect was observed at 2 μM for both the dendrimers and for CBD-2 at 5 μM . Significant cytotoxicity of CBD-1 was noted at 5 μM , with the viability reducing to 29.2%, whereas CBD-2 was cytotoxic at the higher concentration of 10 μM , reducing the viability to 20.0%. However, the toxicity of CBD-1 and CBD-2 might be related to the influence of the solvent at 10 μM .

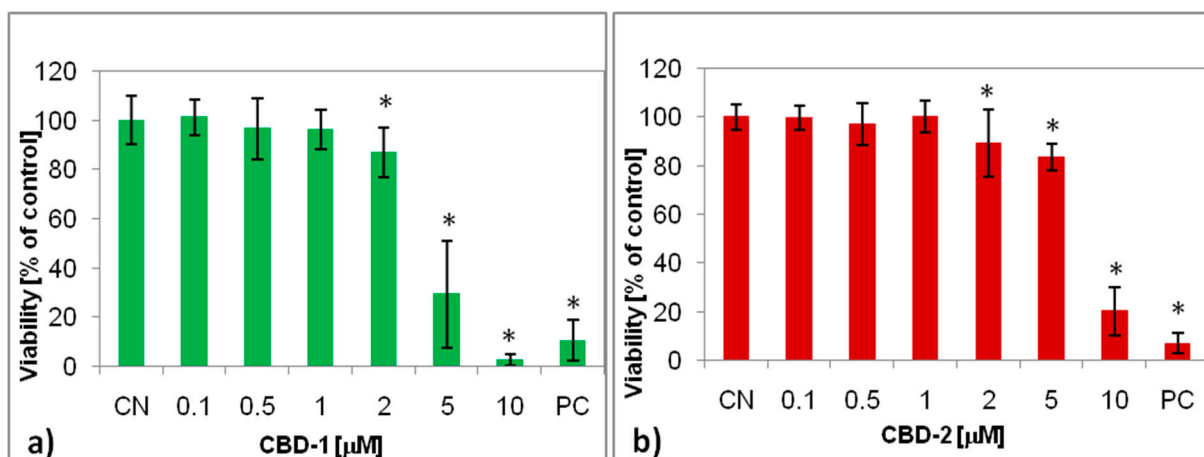


Figure 7. Cont.

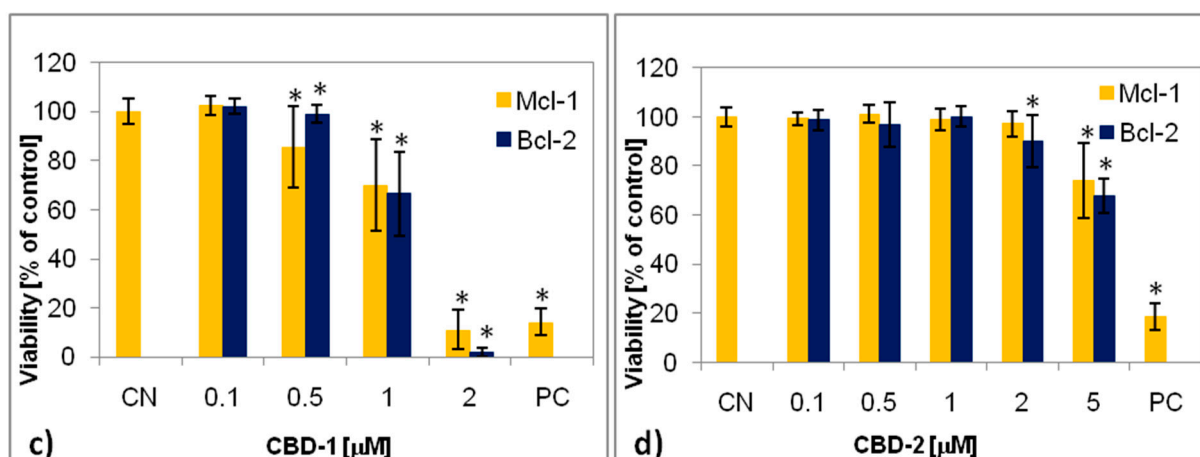


Figure 7. Viability of MCF-7 cells after 24 h exposure to dendrimers: CBD-1 (a) and CBD-2 (b) and dendriplexes (c,d) at different concentrations. The dendrimer/siRNA molar ratio was 20:1; * $p < 0.05$ compared to CN.

The complexes of dendrimer/siRNA significantly decreased the cell viability in the case of CBD-1/siRNA. A cytotoxic effect was obtained at 1 μM , with viability reduced to 69.9 and 66.5% for complexes with Mcl-1 and Bcl-2, respectively. In contrast, the influence of the CBD-2/siRNAs complexes on viability, compared to the CBD-2 alone, was mild. The viability was reduced only at 5 μM to 73.9 and 67.7% for complexes with Mcl-1 and Bcl-2, respectively.

2.6. Cellular Uptake

To analyze the ability of dendriplexes formed by CBD-1 and CBD-2 dendrimers with siRNA to become internalized in MCF-7 cancer cells after a 24-h incubation, confocal microscopy was used. Both the siRNAs (Mcl-1 and Bcl-2) complexed with CBD-1 and CBD-2 dendrimers entered the cells. The CBD/siRNA dendriplexes were visible in the cytoplasm as small green dots (Figure 8).

An automatic microscope INCell Analyzer 2000 aided the quantification of the dendriplexes taken up by the cells. Analysis was carried out using CBD-2, and both examined siRNAs. The data show that $38.8 \pm 5.9\%$ of the cells (Figure 9) had CBD-2/Mcl-1 complexes in their cytoplasm, whereas $55.7 \pm 9.0\%$ of the cells show the presence of CBD-2/Bcl-2 complexes in the cytoplasm. After treatment with naked siRNAs, the fluorescence from the FITC-labeled siRNA was not found in the cells.

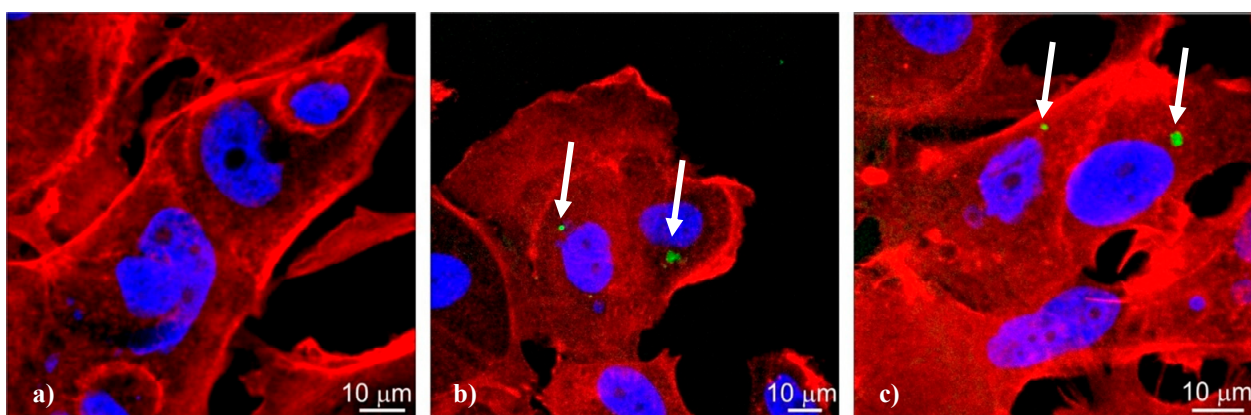


Figure 8. Cont.

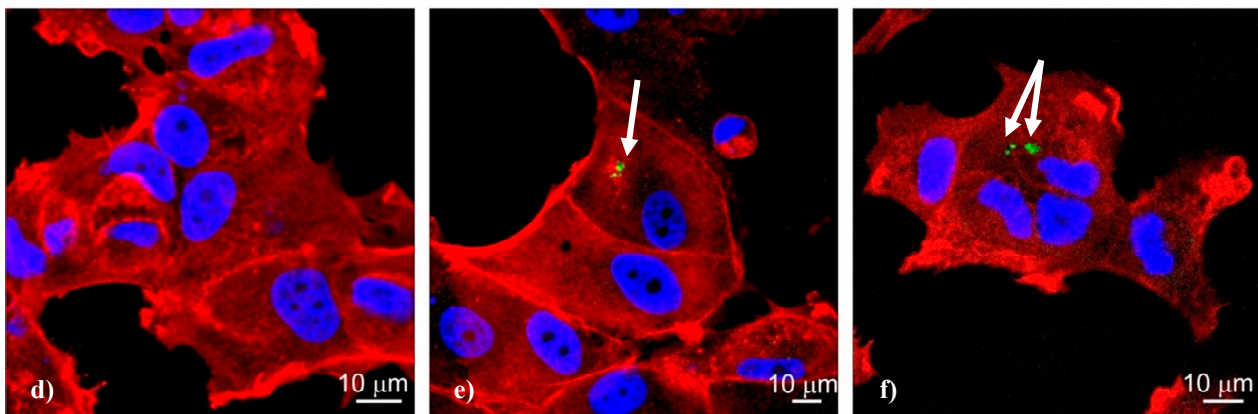


Figure 8. Confocal microscopy images of MCF-7 cells after 24-h incubation with fluorescein labelled siRNA: (a) Bcl-2, (b) CBD-1/Bcl-2, (c) CBD-2/Bcl-2, (d) Mcl-1, (e) CBD-1/Bcl-2, (f) CBD-2/Mcl-1. The concentration of siRNA was 0.1 μ M and the dendrimer/siRNA charge ratio was 20:1. Arrows indicate complexes dendrimer/siRNA.

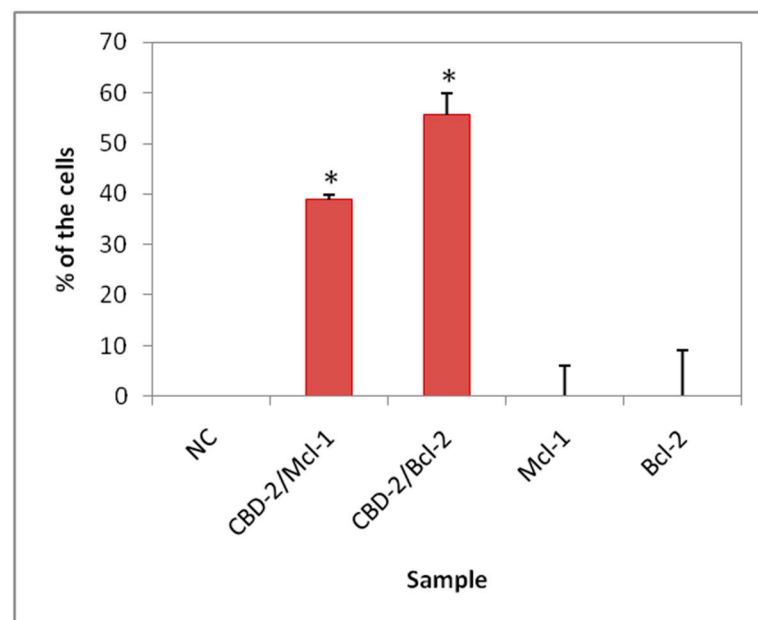


Figure 9. Percentage of cells containing dendrimer/siRNA complexes after 24-h exposure to dendriplexes or naked siRNA; NC, untreated cells. The dendrimer/siRNA charge ratio was 20:1, and the concentration of dendrimer was 2 μ M; * $p < 0.05$.

3. Discussion

RNAi is a promising tool in gene therapy. In this process, the target mRNA is neutralized, and gene expression is inhibited. The following two types of RNA molecules could be used to induce this process: microRNA (miRNA) and siRNA [20,21]. Since nucleic acids are very sensitive to enzymatic degradation, and because their transport through cell membranes is prevented due to being negatively charged, effective delivery systems are needed to overcome these problems [21–24]. Initially, viruses were considered as gene carriers in gene therapy because of their ability to transfect eukaryotic cells and silence gene expression. This system, however, has some disadvantages, which include the high cost of production, generation of certain side effects and induction of immune responses [21,25–27].

Nanomaterials, e.g., dendrimers, are promising as siRNA carriers in gene silencing during gene therapy [5,28–30]. For the first time, carbosilane dendrimers have been characterized as good carriers for siRNA by Weber et al. [31]. These dendrimers silenced

glyceraldehyde 3-phosphate dehydrogenase (GAPDH) expression and reduced HIV replication in PBMC and human leukemia T lymphocytes, remaining at a low cytotoxicity level [16,31]. Posadas et al. [32] demonstrated that the carbosilane dendrimer 2G-NN16 can transport siRNA into neuronal cells and block the synthesis of the HIF1- α protein, and that the efficiency is similar to that achieved with viral vectors [32]. Krasheninina et al. [33] examined the complexation of anti-cancer siRNAs by second (BDEF32) and third (BDEF33) generation cationic carbosilane dendrimers and the influence of those complexes on two types of cancer cells, namely adherent HeLa cells and suspension HL-60 cells. Both types of dendrimers affected cell viability at 2.5, 5 and 10 μ M (HeLa) or 5 and 10 μ M (HL-60 cells). Moreover, dendrimers complexed with pro-apoptotic siRNAs increased cytotoxicity [33]. The methods used for the synthesis of dendrimers also offer wide possibilities in their design. Dendrimers can be modified as needed by changing their size, generation, charge density and the adding functional groups [31]. Therefore, in our experiments using carbosilane dendrimers CBD-1 and CBD-2 as potential anticancer siRNA (Mcl-1 and Bcl-2) carriers, we investigated the formation of complexes of dendrimer/siRNA, characterized them and evaluated their influence on MCF-7 viability and cellular uptake.

The formation of dendrimer/siRNA complexes was confirmed by the zeta potential measurement. This parameter changed significantly from negative to positive values with an increasing dendrimer/siRNA charge ratio. The positive charge of CBD-1 and CBD-2 dendrimers is responsible for penetration of cell membranes, allowing the internalization of the dendriplexes. The internalization of cationic dendrimers is more effective than anionic or neutral dendrimers [34]. It is also proven that positively charged dendrimers are more toxic than their analogs with a negative charge on the surface [35]. Cationic nanoparticles have the ability to damage the integrity of the cell membrane and can lead to the lysis of the cells by increasing their permeability [36]. Zeta potential measurements also helped to estimate the number of CBD molecules bound to one molecule of siRNA. The data show that both Mcl-1 and Bcl-2 can bind more molecules of CBD-1 (15 and 16, respectively) than CBD-2 (9 and 11, respectively). The partial deprotonation of tertiary ammonium groups (RNHMe₂) is possible at the assayed pH, yielding a less cationic density on the surface of CBD-1. This could explain the higher number of molecules required to conjugate with siRNA.

The CD spectrum of the RNA duplexes of A-type is characterized by a positive peak at ~260 nm and a negative peak at ~210 nm [37], which were also seen in our data. The addition of dendrimers and the increase in the dendrimer/siRNA molar ratio reduced ellipticity, which confirmed the formation of complexes. This decrease could be due to a reduction in the absorbance of nucleosides in the dendriplexes [38]. The data show that dendrimers do not significantly affect the structure of siRNAs, because the characteristic A-form pattern is maintained. This corresponds to previous results describing dendrimer/siRNA interactions [39].

Interactions between dendrimers and siRNAs were also confirmed by using EtBr intercalation assay. The addition of dendrimers to siRNAs stained with EtBr strongly quenched its fluorescence intensity ratio F/F_0 , since the dendrimers compete with EtBr and displace it from siRNA. Our results correspond with the results of Ionov et al. [5], Michlewska et al. [38] and Krasheninina et al. [33], who showed the capability of carbosilane dendrimers to form dendriplexes with siRNA.

The gel electrophoresis of CBD-2 complexed with Mcl-1 and Bcl-2, in the presence of RNase A/T1 Mix and heparin, proved the ability of dendrimers to protect siRNA against nucleases. Naked siRNAs were digested, and no stripe was visible. CBD-2 protected siRNAs against degradation, and the addition of heparin allowed for the release and migration of siRNA (Figure 6). The properties of dendrimers to protect siRNA against RNase degradation were also shown in other studies for CBD [5,31].

The chemical and physical properties of dendrimers help them to interact effectively with organelles, biological membranes and proteins. Cationic dendrimers with positively charged groups have an ability to interact with negatively charged biological membranes,

which leads to the internalization of the dendriplexes [5,36]. The analysis of confocal microphotographs showed that both types of dendrimers, CBD-1 and CBD-2, seem to be good carriers of siRNA. The images also show FITC-labeled CBD-1/siRNA and CBD-2/siRNA complexes inside cells. Quantitative analysis also shows that >50% of the cells could be transfected with CBD-2/Bcl-2 complexes.

In contrast to measuring cellular uptake, cytotoxicity assays demonstrated a difference between the tested dendrimers in relation to their ability to reduce the viability of cancer cells. CBD-1 appeared more potently cytotoxic than CBD-2. Both types of dendrimers contain eight surface cationic groups considered responsible for the cytotoxic effects of dendrimers [40]. However, the nature of each peripheral moiety is different. CBD-1 contains pH-dependent tertiary ammonium groups (RNHMe₂Cl), whereas CBD-2 includes pH-stable quaternary ammonium groups (RNMe₃I). Thus, the difference in cytotoxic activity could be ascribed to a different mechanism of action, e.g., the proton sponge effect for endosomal escape from RNHMe₂Cl groups. Interestingly, after the incubation of the cells with dendrimer/siRNA complexes (CBD-1/Mcl-1 and CBD-1/Bcl-2), cytotoxicity was shifted toward the lower concentrations, i.e., 1 μM vs. 5 μM for CBD-1/siRNA and CBD-1 alone, respectively. The viability of the cells treated with complexes of siRNA with the second dendrimer tested, CBD-2, was at a similar level to the viability seen after treatment with the dendrimer alone. Our results are in contrast with some other studies showing that the dendriplex had less toxicity than the dendrimer alone [31,36]. One explanation is that a non-complexed dendrimer exposed all of its cationic groups. However, our results are consistent with the studies of Krasheninina et al. [33] that show the cytotoxicity of dendrimers complexed with pro-apoptotic siRNAs being higher than of dendrimer alone. In the context of anticancer therapy, it would be important to obtain the toxic potential after binding cationic dendrimers with siRNA.

Dendrimers are not the only nanoparticles that can transfer siRNA. Peña-González et al. [41] combined gold nanoparticles (AuNPs) with cationic carbosilane dendrons and examined their ability to transport siRNA against human immunodeficiency virus (HIV). Some advantages of AuNPs as carriers of genetic material are, e.g., biocompatibility, stability and low toxicity. The functionalization of AuNPs with cationic groups, as carbosilane dendrons, enables the compacting of nucleic acid and protects it from degradation. The data confirmed the dependence of this toxicity on the generation, which is characteristic for dendritic systems. Moreover, size determines the toxicity of dendrons [41].

Pędziwiatr-Werbicka et al. [21] used silver nanoparticles (AgNPs) modified with carbosilane dendrons to form complexes with Bcl-XL. The complexes were tested on lymphocytes to evaluate their effect on proliferation and on HeLa cells, and to examine cytotoxic potential. The modified AgNPs formed complexes with tested siRNAs, and protected it against degradation; furthermore, an efficient cellular uptake was observed. However, the binding of siRNA to nanoparticles did not increase their cytotoxicity [21].

4. Materials and Methods

4.1. Carbosilane Dendrimers

The new second generation carbosilane dendrimers, CBD-1 and CBD-2, were synthesized in the Department of Organic and Inorganic Chemistry, University of Alcalá, Madrid, Spain [42]. Carbosilane dendrimer CBD-1 contains 8 surface tertiary ammonium groups (RNHMe₂Cl), Mw = 1997.01 g/mol; C₈₀H₁₈₂Cl₈N₈O₂S₈Si₆. Carbosilane dendrimer CBD-2 contains 8 surface quaternary ammonium groups (RNMe₃I), Mw = 2840.83 g/mol; C₈₈H₁₉₈I₈N₈O₂S₈Si₆. Dendrimers are graphically presented in Figure 10. Dendrimers were dissolved in phosphate buffer (pH = 7.4) with 1% DMSO at 1 mM.

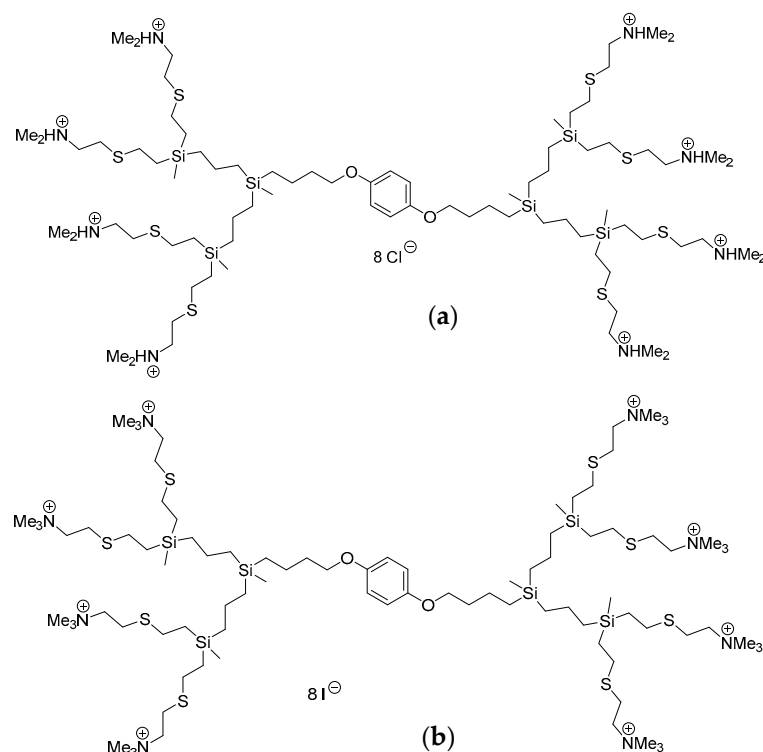


Figure 10. Molecular structure of carbosilane dendrimers: CBD-1 (a) and CBD-2 (b).

4.2. siRNA

Two types of anticancer siRNAs were used in this study: Mcl-1 and Bcl-2.

Mcl-1	
Sense Mcl-1s	5'-GGACUUUUUAUACCUGUUAUdTdT 3'
Antisense Mcl-1a	5'-AUAACAGGUAUAAAAGUCCdTdT 3'
Bcl-2	
Sense E1s	5'-G CUG CAC CUG ACG CCC UUCdTdT 3'
Antisense E1a	5'-GAA GGG CGU CAG GUG CAG CdTdT 3'

The siRNAs were purchased from Dharmacon Inc. (Lafayette, CO, USA).

4.3. Other Reagents

Reagents for cell culture were obtained from Biowest (Riverside, MO, USA). Dimethyl sulfoxide (DMSO), phosphate buffered saline (PBS) tablets, ethidium bromide, formaldehyde, ethylenediaminetetraacetic acid (EDTA) and heparin were obtained from Sigma Aldrich (St. Louis, MO, USA). 2,3-bis-(2-methoxy-4-nitro-5-sulfophenyl)-2H-tetrazolium-5-carboxanilide (XTT) was obtained from Biological Industries (Kibbutz Beit-Haemek, Israel). 4',6-diaminido-2-phenylindole (DAPI), Texas Red-X Phalloidin and RNase A/T1 mix were purchased from Thermo Fisher Scientific (Waltham, MA, USA). Hoechst 33342 was obtained from Santa Cruz Biotechnology Inc. (Dallas, TX, USA). Tris was obtained from GE Healthcare (Chicago, IL, USA). Other basic chemical reagents (sodium dihydrogen phosphate, disodium hydrogen phosphate, acetic acid) were obtained from the local supplier, Chempur (Piekary Śląskie, Poland). Agarose was purchased from the local supplier, Blirt (Gdańsk, Poland). These chemicals were of analytical grade, and solutions were prepared using water purified using the Mili-Q system.

4.4. Dendrimer/siRNA Complexes Formation

Dendrimers and siRNAs were mixed in phosphate buffer (pH = 7.4) at concentrations giving the required molar ratio. Complexes were formed immediately.

4.5. Zeta Potential

The zeta potentials of the complexes were measured using a Malvern Instruments Zetasizer Nano-ZS (Malvern Instruments Ltd., Malvern, UK). Measurement was carried out at 25 °C. From 10 to 15 measurements were collected for each sample and averaged. Increasing concentrations of the dendrimer in the range of 0.5–20 µM were added to siRNA at 0.5 µM and the zeta potential was measured. The zeta potential value was calculated directly from the Helmholtz–Smoluchowski equation using Malvern software [43].

4.6. Circular Dichroism

Structural changes of siRNAs (2 µM) in the presence of dendrimers at increasing concentrations (1–14 µM) were measured using the circular dichroism technique, using Jasco, J-815CD spectrometer (Tokyo, Japan) in 5-millimeter path length quartz cuvettes at 25 °C, with a wavelength step of 1 nm, a response time of 4 s and a scan rate of 50 nm/min. CD spectra were obtained between 300 and 200 nm. Each spectrum was reported as the average of 3 experiments. The dendrimer in phosphate buffer without siRNA was used as a baseline for dendrimer/siRNA complex spectra.

4.7. Ethidium Bromide (EtBr) Intercalation Assay

EtBr is a fluorescent dye that intercalates between nucleic base pairs. Dendrimers can compete with EtBr, bind to siRNA and lead to the displacement of EtBr, resulting in a decrease in its fluorescence [44–46].

Fluorescence of EtBr complexed with siRNA was measured using spectrofluorimetry with a Hitachi F-7000 at 25 °C ($\lambda = 525\text{--}650$ nm). EtBr was used at 5 µM and siRNA at 0.5 µM. Dendrimers were then added with increasing concentrations from 0.5–10 µM.

4.8. Gel Electrophoresis

To study the formation of complexes between dendrimers and siRNAs, and to investigate whether siRNA is protected from the degradation, agarose gel electrophoresis was used. Dendrimers (at 40 µM) were mixed with siRNA (final concentration 2 µM) in 10 mM Na-phosphate buffer, pH 7.4. RNase A/T1 mix (3 µg/mL) was added to evaluate the protective function of dendrimers. Samples were incubated for 30 min at 37 °C and then for 10 min on ice. After incubation on ice, heparin (0.082 mg/mL) was added. The samples were placed on agarose gel (3%) containing ethidium bromide. Electrophoresis was run in Tris-acetate-EDTA (TAE) buffer for 45 min at 90 V, 35 mA. The gel was visualized using ultraviolet (UV).

4.9. MCF-7 Cell Line

The MCF-7 cell line used in this study was purchased from American Type Culture Collection (ATCC[®], cat. No.: HTB-22, Manassas, VA, USA). The cells were cultured in Dulbecco's modified Eagle's medium supplemented with 10% fetal bovine serum (FBS) and antibiotics. Cultures were maintained in an incubator with 5% CO₂, at 37 °C.

4.10. XTT Assay

Cytotoxicity of dendrimers and dendriplexes was evaluated using the XTT assay, based on the ability of living cells to transform negatively charged tetrazolium salt into an orange color when reduced to a soluble formazan dye. Extracellular XTT reduction process is carried out by electron transport across the plasma membrane of living cells. The amount of living cells correlates with the coloration intensity measured spectrophotometrically. Test material is considered cytotoxic when viability is <70% vs. the negative control.

The MCF-7 cells were seeded onto 96-well plate at 5×10^3 cells per well and incubated for 24 h before dendrimers (at 0.1, 0.5, 1, 2, 5 and 10 µM) or dendriplexes (dendrimer concentrations as above) were added. The molar dendrimer/siRNA ratio was 20:1. The cells grown in the supplemented culture medium were used as a negative control (NC). Triton X-100 at 0.01% was used as a positive control (PC). After 24 h, the XTT assay

was performed according to the manufacturer's procedure. Viability was calculated as a percentage of the NC.

4.11. Cellular Uptake

Complexes of dendrimers with FITC labelled siRNA were used to estimate the cellular uptake of dendriplexes. For confocal analysis, cells were seeded on microscopic slides placed at the bottom of 12-well culture plates. After 24 h, dendriplexes were added at the charge ratio dendrimer/siRNA 20:1, and the concentrations of dendrimers and siRNA were 2 and 0.1 μM , respectively. After a 24-h incubation with dendriplexes, the cells were fixed with 3.7% formaldehyde solution for 30 min and washed with PBS. DNA was stained with DAPI for 5 min (0.5 mg/mL) and Texas Red-X Phalloidin for F-actin staining (0.1 $\mu\text{g}/\text{mL}$). Images were taken with confocal laser scanning microscopy platform TCS SP8 (Leica Microsystems, Wetzlar, Germany) with an objective of $63\times/1.40$ (HC PL APO CS2, Leica Microsystems, Wetzlar, Germany) at the following excitation wavelengths: 405 nm (DAPI), 488 nm (FITC) and 565 nm (Texas Red-X Phalloidin).

For quantitative analysis of the uptake of dendriplexes, an automated microscope INCell Analyzer 2000 (GE Healthcare Life Science, Cardiff UK) was used. Cells were seeded onto 96-well plates at 3×10^3 cells per well. Dendriplexes were added as described above. For these analyses, the CBD-2 dendrimer was chosen. Cells were then fixed with 3.7% formaldehyde solution and stained with Hoechst 33342 (1 $\mu\text{g}/\text{mL}$) and Texas Red-X Phalloidin (approximately 1.65 μM), and finally imaged with the INCell Analyzer 2000. The images were submitted to an automated analysis protocol. The number of cells containing dendrimer/FITC-labeled siRNA complexes was measured.

4.12. Statistical Analysis

The results are presented as mean \pm SD. Data were analyzed by a one-way ANOVA test, followed by Tukey's analysis, using Origin software. A value of $p < 0.05$ was accepted as statistically significant.

5. Conclusions

Measurements of the physical properties of dendriplexes (zeta potential, circular dichroism), electrophoresis and ethidium bromide assay have confirmed that both tested dendrimers complex with siRNA. Furthermore, confocal microscopy indicates that both dendrimers can effectively deliver siRNA into target cells. However, the XTT assay showed that cytotoxicity after incubation with tested dendriplexes was significantly higher for complexes with CBD-1. This suggests that, potentially, this dendrimer is more appropriate than CBD-2 as a siRNA carrier in gene therapy.

Author Contributions: Conceptualization, K.B. and K.M.; methodology, K.B. and K.M.; software, K.B. and P.S.; investigation, K.B. and S.M.; resources, K.M. and P.K.; writing—original draft preparation, K.B. and P.S.; writing—review and editing, K.B., K.M., S.M., P.S., P.K., T.L.-C., R.G.-R., F.J.d.l.M. and M.B.; supervision, K.M. and P.K.; funding acquisition, K.M. All authors have read and agreed to the published version of the manuscript.

Funding: This research received no external funding.

Institutional Review Board Statement: Not applicable.

Informed Consent Statement: Not applicable.

Acknowledgments: This work was prepared as a part of the first edition of the Ministry of Science and Higher Education program called "Doktorat wdrożeniowy". This work was supported by PIE14/00061 (CIBER), CTQ2017-86224-P (MINECO), Consortium IMMUNOTHERCAN-CM B2017/BMD-3733 (CAM), NANODENDMED II-CM ref B2017/BMD-3703 and project SBPLY/17/180501/000358 JCCM. CIBER-BBN is an initiative funded by the VI National R&D&i Plan 2008–2011, Iniciativa Ingenio 2010, Consolider Program, CIBER Actions and financed by the Instituto de Salud Carlos III with assistance from the European Regional Development Fund. This work has been supported partially by a EUROPARTNER: Strengthening and spreading international

partnership activities of the Faculty of Biology and Environmental Protection for interdisciplinary research and innovation of the University of Lodz Programme: NAWA International Academic Partnership Programme.

Conflicts of Interest: The authors declare no conflict of interest.

References

1. Vankayala, R.; Hwang, K.C. Near-infrared-light-activatable nanomaterial-mediated phototheranostic nanomedicines: An emerging paradigm for cancer treatment. *Adv. Mater.* **2018**, *30*, 1706320. [[CrossRef](#)] [[PubMed](#)]
2. Michlewska, S.; Kubczak, M.; Maroto-Diaz, M.; Sanz del Olmo, N.; Ortega, P.; Shcharbin, D.; Gomez-Ramirez, R.; de la Mata, F.J.; Ionov, M.; Bryszewska, M. Synthesis and characterization of FITC labelled ruthenium dendrimer as a prospective anticancer drug. *Biomolecules* **2019**, *9*, 411. [[CrossRef](#)]
3. Ola, M.S.; Nawaz, M.; Ahsan, H. Role of Bcl-2 family proteins and caspases in the regulation of apoptosis. *Mol. Cell. Biochem.* **2011**, *351*, 41–58. [[CrossRef](#)] [[PubMed](#)]
4. Burlacu, A. Regulation of apoptosis by Bcl-2 family proteins. *J. Cell. Mol. Med.* **2003**, *7*, 249–257. [[CrossRef](#)]
5. Ionov, M.; Lazniewska, J.; Dzitruk, V.; Halets, I.; Loznikova, S.; Novopashina, D.; Apartsin, E.; Krasheninina, O.; Venyaminova, A.; Milowska, K.; et al. Anticancer siRNA cocktails as a novel tool to treat cancer cells. Part (A). Mechanisms of interaction. *Int. J. Pharm.* **2015**, *485*, 261–269. [[CrossRef](#)] [[PubMed](#)]
6. Ambesajir, A.; Kaushik, A.; Kaushik, J.J.; Petros, S.T. RNA interference: A futuristic tool and its therapeutic applications. *Saudi J. Biol. Sci.* **2012**, *19*, 395–403. [[CrossRef](#)] [[PubMed](#)]
7. Angart, P.; Vocelle, D.; Chan, C.; Walton, S.P. Design of siRNA therapeutics from the molecular scale. *Pharmaceuticals* **2013**, *6*, 440–468. [[CrossRef](#)]
8. Dzitruk, V.; Szulc, A.; Shcharbin, D.; Janaszewska, A.; Shcharbina, N.; Lazniewska, J.; Novopashina, D.; Buyanova, M.; Ionov, M.; Klajnert-Maculewicz, B.; et al. Anticancer siRNA cocktails as a novel tool to treat cancer cells. Part (B). Efficiency of pharmacological action. *Int. J. Pharm.* **2015**, *485*, 288–294. [[CrossRef](#)]
9. Chang, P.K.C.; Prestidge, C.A.; Bremmell, K.E. Interfacial analysis of siRNA complexes with poly-ethylenimine (PEI) or PAMAM dendrimers in gene delivery. *Colloids Surf. B Biointerfaces* **2017**, *158*, 370–378. [[CrossRef](#)]
10. Tokatlian, T.; Segura, T. siRNA applications in nanomedicine. *Wiley Interdiscip. Rev. Nanomed. Nanobiotechnol.* **2010**, *2*, 305–315. [[CrossRef](#)]
11. Song, E.W.; Zhu, P.C.; Lee, S.K.; Chowdhury, D.; Kussman, S.; Dykxhoorn, D.M.; Feng, Y.; Palliser, D.; Weiner, D.B.; Shankar, P.; et al. Antibody mediated in vivo delivery of small interfering RNAs via cell-surface receptors. *Nat. Biotechnol.* **2005**, *23*, 709–717. [[CrossRef](#)]
12. Zhou, J.; Wu, J.; Hafdi, N.; Behr, J.P.; Erbacher, P.; Peng, L. PAMAM dendrimers for efficient siRNA delivery and potent gene silencing. *Chem. Commun.* **2006**, *22*, 2362–2364. [[CrossRef](#)] [[PubMed](#)]
13. Tomalia, D.A.; Uppuluri, S.; Swanson, D.R.; Li, J. Dendrimers as reactive modules for the synthesis of new structure-controlled, higher-complexity megamers. *Pure Appl. Chem.* **2000**, *72*, 2343–2358. [[CrossRef](#)]
14. Tomalia, D.A. Architecturally driven properties based on the dendritic state. *High Perform. Polym.* **2001**, *13*, S1–S10. [[CrossRef](#)]
15. Sękowski, S.; Miłowska, K.; Gabryelak, T. Dendrymery w naukach biomedycznych i nanotechnologii. *Postep. Hig. Med. Dosw.* **2008**, *62*, 725–733.
16. Wu, J.; Huang, W.; He, Z. Dendrimers as carriers for siRNA delivery and gene silencing: A review. *Sci. World J.* **2013**, *2013*, 630654. [[CrossRef](#)]
17. Wang, J.; Lu, Z.; Wientjes, M.G.; Au, J.L.S. Delivery of siRNA therapeutics: Barriers and carriers. *AAPS J.* **2010**, *12*, 492–503. [[CrossRef](#)]
18. Solassol, J.; Crozet, C.; Perrier, V.; Leclaire, J.; Beranger, F.; Caminade, A.M.; Meunier, B.; Dormont, D.; Majoral, J.P.; Lehmann, S. Cationic phosphorus-containing dendrimers reduce prion replication both in cell culture and in mice infected with scrapie. *J. Gen. Virol.* **2004**, *85*, 1791–1799. [[CrossRef](#)]
19. Caminade, A.M.; Majoral, J.P. Water-soluble phosphorus-containing dendrimers. *Prog. Polym. Sci.* **2005**, *30*, 491–505. [[CrossRef](#)]
20. Hannon, G.J. RNA interference. *Nature* **2002**, *418*, 244–251. [[CrossRef](#)]
21. Pedziwiatr-Werbicka, E.; Gorzkiewicz, M.; Horodecka, K.; Abashkin, V.; Klajnert-Maculewicz, B.; Pena-Gonzalez, C.E.; Sanchez-Nieves, J.; Gomez, R.; de la Mata, F.J.; Bryszewska, M. Silver nanoparticles surface-modified with carbosilane dendrons as carriers of anticancer siRNA. *Int. J. Mol. Sci.* **2020**, *21*, 4647. [[CrossRef](#)]
22. Kaneda, Y. Gene therapy: A battle against biological barriers. *Curr. Mol. Med.* **2001**, *1*, 493–499. [[CrossRef](#)] [[PubMed](#)]
23. Hickerson, R.P.; Vlassov, A.V.; Wang, Q.; Leake, D.; Ilves, H.; Gonzalez-Gonzalez, E.; Contag, C.H.; Johnston, B.H.; Kaspar, R.L. Stability study of unmodified siRNA and relevance to clinical use. *Oligonucleotides* **2008**, *18*, 345–354. [[CrossRef](#)] [[PubMed](#)]
24. Whitehead, K.A.; Langer, R.; Anderson, D.G. Knocking down barriers: Advances in siRNA delivery. *Nat. Rev. Drug Discov.* **2009**, *8*, 129–138. [[CrossRef](#)] [[PubMed](#)]
25. Thomas, C.E.; Ehrhardt, A.; Kay, M.A. Progress and problems with the use of viral vectors for gene therapy. *Nat. Rev. Genet.* **2003**, *4*, 346–358. [[CrossRef](#)] [[PubMed](#)]
26. Giacca, M.; Zacchigna, S. Virus-mediated gene delivery for human gene therapy. *J. Control. Release* **2012**, *161*, 377–388. [[CrossRef](#)] [[PubMed](#)]

27. Xin, Y.; Huang, M.; Guo, W.W.; Huang, Q.; Zhang, L.Z.; Jiang, G. Nano-based delivery of RNAi in cancer therapy. *Mol. Cancer* **2017**, *16*, 134. [[CrossRef](#)] [[PubMed](#)]
28. Gardikis, K.; Fessas, D.; Signorelli, M.; Dimas, K.; Tsimplouli, C.; Ionov, M.; Demetzos, C. A new chimeric drug delivery nano system (chi-aDDnS) composed of PAMAM G 3. 5 dendrimer and liposomes as doxorubicin's carrier, in vitro pharmacological studies. *J. Nanosci. Nanotechnol.* **2011**, *11*, 3764–3772. [[CrossRef](#)] [[PubMed](#)]
29. Shcharbin, D.; Janaszewska, A.; Klajnert-Maculewicz, B.; Ziembra, B.; Dzmitruk, V.; Halets, I.; Loznikova, S.; Shcharbina, N.; Milowska, K.; Ionov, M.; et al. How to study dendrimers and dendriplexes III. Biodistribution: Pharmacokinetics and toxicity in vivo. *J. Control. Release* **2014**, *181*, 40–52. [[CrossRef](#)]
30. Białkowska, K.; Komorowski, P.; Bryszewska, M.; Miłowska, K. Spheroids as a type of three-dimensional cell cultures—Examples of methods of preparation and the most important application. *Int. J. Mol. Sci.* **2020**, *21*, 6225. [[CrossRef](#)]
31. Weber, N.; Ortega, P.; Clemente, M.I.; Shcharbin, D.; Bryszewska, M.; de la Mata, F.J.; Gomez, R.; Munoz-Fernandez, M.A. Characterization of carbosilane dendrimers as effective carriers of siRNA to HIV-infected lymphocytes. *J. Control. Release* **2008**, *132*, 55–64. [[CrossRef](#)]
32. Posadas, I.; Lopez-Hernandez, B.; Clemente, M.I.; Jimenez, J.L.; Ortega, P.; de la Mata, J.; Gomez, R.; Munoz-Fernandez, M.A.; Cena, V. Highly efficient transfection of rat cortical neurons using carbosilane dendrimers unveils a neuroprotective role for HIF-1 alpha in early chemical hypoxia-mediated neurotoxicity. *Pharm. Res.* **2009**, *26*, 1181–1191. [[CrossRef](#)]
33. Krasheninina, O.A.; Apartsin, E.K.; Fuentes, E.; Szulc, A.; Ionov, M.; Venyaminova, A.G.; Shcharbin, D.; de la Mata, F.J.; Bryszewska, M.; Gomez, R. Complexes of pro-apoptotic siRNAs and carbosilane dendrimers: Formation and effect on cancer cells. *Pharmaceutics* **2019**, *11*, 25. [[CrossRef](#)] [[PubMed](#)]
34. Albertazzi, L.; Mickler, F.M.; Pavan, G.M.; Salomone, F.; Bardi, G.; Panniello, M.; Amir, E.; Kang, T.; Killops, K.L.; Brauchle, C.; et al. Enhanced bioactivity of internally functionalized cationic dendrimers with PEG cores. *Biomacromolecules* **2012**, *13*, 4089–4097. [[CrossRef](#)]
35. Aisina, R.; Mukhametova, L.; Ivanova, E. Influence cationic and anionic PAMAM dendrimers of low generation on selected hemostatic parameters in vitro. *Mater. Sci. Eng. C Mater. Biol. Appl.* **2020**, *109*, 110605. [[CrossRef](#)]
36. Wrobel, D.; Kolanowska, K.; Gajek, A.; Gomez-Ramirez, R.; de la Mata, J.; Pedziwiatr-Werbicka, E.; Klajnert, B.; Waczulikova, I.; Bryszewska, M. Interaction of cationic carbosilane dendrimers and their complexes with siRNA with erythrocytes and red blood cell ghosts. *Biochim. Biophys. Acta* **2014**, *1838*, 882–889. [[CrossRef](#)]
37. Kyrp, J.; Kejnovska, I.; Renciuik, D.; Vorlickova, M. Circular dichroism and conformational polymorphism of DNA. *Nucleic Acids Res.* **2009**, *37*, 1713–1725. [[CrossRef](#)] [[PubMed](#)]
38. Michlewska, S.; Ionov, M.; Maroto-Diaz, M.; Szwed, A.; Ihnatsyey-Kachan, A.; Loznikova, S.; Shcharbin, D.; Maly, M.; Ramirez, R.G.; de la Mata, F.J.; et al. Ruthenium dendrimers as carriers for anticancer siRNA. *J. Inorg. Biochem.* **2018**, *181*, 18–27. [[CrossRef](#)] [[PubMed](#)]
39. Reyes-Reveles, J.; Sedaghat-Herati, R.; Gilley, D.R.; Schaeffer, A.M.; Ghosh, K.C.; Greene, T.D.; Gann, H.E.; Dowler, W.A.; Kramer, S.; Dean, J.M.; et al. mPEG-PAMAM-G4 nucleic acid nanocomplexes: Enhanced stability, RNase protection, and activity of splice switching oligomer and Poly I:C RNA. *Biomacromolecules* **2013**, *14*, 4108–4115. [[CrossRef](#)] [[PubMed](#)]
40. Jevprasesphant, R.; Penny, J.; Jalal, R.; Attwood, D.; McKeown, N.B.; D'Emanuele, A. The influence of surface modification on the cytotoxicity of PAMAM dendrimers. *Int. J. Pharm.* **2003**, *252*, 263–266. [[CrossRef](#)]
41. Peña-González, C.E.; Pedziwiatr-Werbicka, E.; Shcharbin, D.; Guerrero-Beltran, C.; Abashkin, V.; Loznikova, S.; Jimenez, J.L.; Munoz-Fernandez, M.A.; Bryszewska, M.; Gomez, R.; et al. Gold nanoparticles stabilized by cationic carbosilane dendrons: Synthesis and biological properties. *Dalton Trans.* **2017**, *46*, 8736–8745. [[CrossRef](#)] [[PubMed](#)]
42. Lozano-Cruz, T.; Alcarraz-Vizan, G.; de la Mata, F.J.; de Pablo, S.; Ortega, P.; Duarte, Y.; Bravo-Moraga, F.; Gonzalez-Nilo, F.D.; Novials, A.; Gomez, R. Cationic carbosilane dendritic systems as promising anti-amyloid agents in type 2 diabetes. *Chem. Eur. J.* **2020**, *26*, 7609–7621. [[CrossRef](#)]
43. Sze, A.; Erickson, D.; Ren, L.; Li, D. Zeta-potential measurement using the Smoluchowski equation and the slope of the current-time relationship in electroosmotic flow. *J. Colloid Interface Sci.* **2003**, *261*, 402–410. [[CrossRef](#)]
44. Olmsted, J.; Kearns, D.R. Mechanism of ethidium-bromide fluorescence enhancement on binding to nucleic-acids. *Biochemistry* **1977**, *16*, 3647–3654. [[CrossRef](#)] [[PubMed](#)]
45. Boger, D.L.; Fink, B.E.; Brunette, S.R.; Tse, W.C.; Hedrick, M.P. A simple, high-resolution method for establishing DNA binding affinity and sequence selectivity. *J. Am. Chem. Soc.* **2001**, *123*, 5878–5891. [[CrossRef](#)] [[PubMed](#)]
46. Fischer, W.; Calderón, M.; Schulz, A.; Andreou, I.; Weber, M.; Haag, R. Dendritic polyglycerols with oligoamine shells show low toxicity and high siRNA transfection efficiency in vitro. *Bioconj. Chem.* **2010**, *21*, 1744–1752. [[CrossRef](#)]

Article

Interaction of Cationic Carbosilane Dendrimers and Their siRNA Complexes with MCF-7 Cells Cultured in 3D Spheroids

Kamila Białkowska ^{1,2,*} , Piotr Komorowski ^{2,3} , Rafael Gomez-Ramirez ^{4,5,6} ,
Francisco Javier de la Mata ^{4,5,6} , Maria Bryszewska ¹  and Katarzyna Miłowska ¹ 

- ¹ Department of General Biophysics, Faculty of Biology and Environmental Protection, University of Lodz, 141/143 Pomorska St., 90-236 Lodz, Poland; maria.bryszewska@biol.uni.lodz.pl (M.B.); katarzyna.milowska@biol.uni.lodz.pl (K.M.)
- ² Molecular and Nanostructural Biophysics Laboratory, “Bionanopark” Ltd., 114/116 Dubois St., 93-465 Lodz, Poland; p.komorowski@bionanopark.pl
- ³ Department of Biophysics, Institute of Materials Science, Lodz University of Technology, 1/15 Stefanowskiego St., 90-924 Lodz, Poland
- ⁴ Department of Organic and Inorganic Chemistry, IQAR, University of Alcalá, 28805 Madrid, Spain; rafael.gomez@uah.es (R.G.-R.); javier.delamata@uah.es (F.J.d.I.M.)
- ⁵ Networking Research Center on Bioengineering, Biomaterials and Nanomedicine (CIBER-BBN), 28029 Madrid, Spain
- ⁶ Ramón y Cajal Health Research Institute (IRYCIS), 28034 Madrid, Spain
- * Correspondence: kamila.bialkowska@edu.uni.lodz.pl

Abstract: Cationic dendrimers are effective carriers for the delivery of siRNA into cells; they can penetrate cell membranes and protect nucleic acids against RNase degradation. Two types of dendrimers (CBD-1 and CBD-2) and their complexes with pro-apoptotic siRNA (Mcl-1 and Bcl-2) were tested on MCF-7 cells cultured as spheroids. Cytotoxicity of dendrimers and dendriplexes was measured using the live–dead test and Annexin V-FITC Apoptosis Detection Kit (flow cytometry). Uptake of dendriplexes was examined using flow cytometry and confocal microscopy. The live–dead test showed that for cells in 3D, CBD-2 is more toxic than CBD-1, contrasting with the data for 2D cultures. Attaching siRNA to a dendrimer molecule did not lead to increased cytotoxic effect in cells, either after 24 or 48 h. Measurements of apoptosis did not show a high increase in the level of the apoptosis marker after 24 h exposure of spheroids to CBD-2 and its dendriplexes. Measurements of the internalization of dendriplexes and microscopy images confirmed that the dendriplexes were transported into cells of the spheroids. Flow cytometry analysis of internalization indicated that CBD-2 transported siRNAs more effectively than CBD-1. Cytotoxic effects were visible after incubation with 3 doses of complexes for CBD-1 and both siRNAs.

Keywords: siRNA; carbosilane dendrimers; dendriplexes; nanocarriers; 3D cell culture; spheroids



Citation: Białkowska, K.; Komorowski, P.; Gomez-Ramirez, R.; de la Mata, F.J.; Bryszewska, M.; Miłowska, K. Interaction of Cationic Carbosilane Dendrimers and Their siRNA Complexes with MCF-7 Cells Cultured in 3D Spheroids. *Cells* **2022**, *11*, 1697. <https://doi.org/10.3390/cells11101697>

Academic Editor: Joni H. Ylostalo

Received: 27 April 2022

Accepted: 19 May 2022

Published: 19 May 2022

Publisher’s Note: MDPI stays neutral with regard to jurisdictional claims in published maps and institutional affiliations.



Copyright: © 2022 by the authors. Licensee MDPI, Basel, Switzerland. This article is an open access article distributed under the terms and conditions of the Creative Commons Attribution (CC BY) license (<https://creativecommons.org/licenses/by/4.0/>).

1. Introduction

Gene therapy is one of the most promising and effective ways of treating cancers, this disease being a major cause of death in the world [1–6]. Gene therapy is the ability to make genetic improvements by correction of mutated genes or site-specific modifications for therapeutic purposes [7], and it results in the regulation or replacement of altered genes when therapeutic genes are transported into the chromosomes of target tissues or cells [8], with genes being used as medicines [9]. Correction of defective genes is performed in several ways: (1) The nonfunctional gene can be replaced by a normal gene, inserted within the genome into a nonspecific location; (2) A mutated gene can be exchanged for a recombined homologous or normal gene; (3) A mutated gene can be repaired by using selective reverse mutation; (4) The degree to which a gene is turned on or off can be altered [9]. Target diseases for gene therapy include those caused by recessive gene disorders, e.g., hemophilia, cystic fibrosis, sickle-cell anemia and muscular dystrophy, and

those that are acquired, e.g., cancers. Target diseases also include some viral infections such as AIDS [7].

A cell membrane is a strong barrier against genes in the form of large and anionic nucleic acids, DNA or RNA [3]. For this reason, effective application of gene therapy is dependent on technologies that allow delivery of genes into cells, tissues and organs [10]. It means that the most important factor determining the implementation of gene therapy is the development of effective vectors that are also safe for healthy organs [10,11]. Two types of vectors are currently available as gene carriers: viral or non-viral [11]. With viral vectors, most of the viral genome is replaced by the therapeutic nucleic acids. Transport into the cells is possible due to viral proteins that mediate internalization and prevent degradation of the vector in the extracellular environment [3]. Viral vectors provide a possibility of efficient transfection and long-term silencing of gene expression. However, there are some problems with using viral vectors as gene carriers, e.g., high cost of production and more importantly, the generation of various side effects and induction of immune responses that lead to a reduction of the therapeutic effect. For these reasons, attention has been concentrated on new non-viral carriers [5,12].

The most commonly tested non-viral vectors include nanoparticles, e.g., liposomes, carbon nanotubes and dendrimers [5]. Dendrimers, which are synthetic polymers, are promising because of their size and water solubility [13]. Cationic dendrimers can bind with nucleic acids and pass through the cell membrane due to their positive charge [4,14]. Other advantages of dendrimers include a large number of functional groups for nucleic-acid binding and their stability [13–15]. Therefore, we examined two types of cationic, carbosilane dendrimers: CBD-1 and CBD-2 (see Figure 1 in Section 2), described previously [14] as carriers for two types of small interfering RNAs (siRNAs): Mcl-1 and Bcl-2.

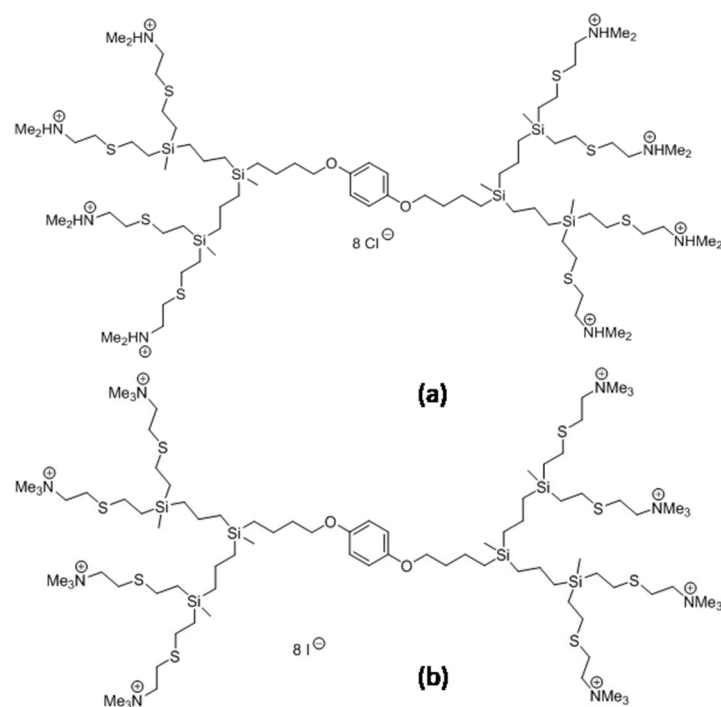


Figure 1. Molecular structure of carbosilane dendrimers: CBD-1 (a) and CBD-2 (b).

siRNA is a small, double-stranded nucleic acid [16], which can promote messenger RNA (mRNA) degradation [17,18]. This process is called RNA interference (RNAi) and results in silencing of target genes [17,18]. The RNAi process with the use of Mcl-1 and Bcl-2 can be applied in anticancer therapy, since the proteins encoded by these siRNAs are involved in regulation of apoptosis [19,20]. Application of pro-apoptotic Mcl-1 and Bcl-2 can lead to neutralization of mRNA encoding anti-apoptotic proteins and this, finally, can lead to induction of apoptosis in cancer cells [14,17,18,21].

Dendriplexes formed by CBD-1 and CBD-2 with both siRNAs were characterized in our previous work [14]. We also carried out preliminary research with MCF-7 cells, testing cytotoxicity of dendrimers and dendriplexes. However, those experiments used 2D cell culture. 2D models limit cell–cell and cell–matrix interactions and significantly reduce cellular responses, and there is no normal physiological process such as transport of nanoparticles through cell layers [22,23]. Naturally, cells reside in the 3D environment, which is crucial for their growth and metabolism. The functions and the phenotype of each cell depend on complex interactions with extracellular matrix (ECM) proteins and neighboring cells [6,22]. Therefore, we investigated dendrimers and dendriplexes with MCF-7 cells cultured as 3D spheroids and examined cytotoxicity of the tested materials and their uptake by cells. Articles presenting the influence of dendrimers as siRNA carriers on cells cultured in 2D are common, but it is harder to find articles presenting the impact of these systems on cells cultured in 3D.

The data show that both dendrimers are taken up by the cells and there is a difference between cytotoxicity of CBD-1 and CBD-2. After 24 h of treatment with CBD/siRNA, the viability of cells did not decrease when compared to viability after 24 h of treatment with dendrimer alone. However, analysis of cytotoxicity after incubation with 3 doses of dendriplexes revealed the toxic potential of CBD-1 complexed with both siRNAs.

2. Materials and Methods

2.1. Carbosilane Dendrimers

The second generation carbosilane dendrimers, CBD-1 and CBD-2, were synthesized and characterized as described previously [14,24]. The molecular structure of investigated dendrimers is shown in Figure 1.

2.2. siRNA

Two types of anticancer siRNAs used in this study (Mcl-1 and Bcl-2) were described previously [14].

Mcl-1,

Sense Mcl-1s:5'-GGACUUUUAUA-CCUGUUAUdTdT-3'

Antisense Mcl-1a:5'-AUAACAG-GUAUAAAAGUCCdTdT-3'

Bcl-2,

Sense E1s:5'-G CUG CAC CUG ACG CCC UUCdTdT-3'

Antisense E1a:5'-GAA GGG CGU CAG GUG CAG CdTdT-3'

siRNAs and siRNAs-FITC were obtained from Dharmacon Inc. (Lafayette, CO, USA).

2.3. Other Reagents

Reagents for cell culture were provided by Biowest (Riverside, MO, USA). TrypLE for cell detachment was from Gibco (Amarillo, TX, USA). Dimethyl sulfoxide (DMSO), phosphate buffered saline (PBS) tablets, 4-(2-hydroxyethyl)-1-piperazineethanesulfonic acid (HEPES) and formaldehyde were purchased from Sigma-Aldrich (St. Louis, MO, USA). Hoechst 33342 was obtained from Santa Cruz Biotechnology, Inc. (Dallas, TX, USA). Calcein AM and propidium iodide (PI) were from Biotium (San Francisco, CA, USA). Annexin V-FITC Apoptosis Detection Kit was from BD Pharmingen (Franklin Lakes, NJ, USA). Tris was obtained from GE Healthcare (Chicago, IL, USA). Other basic chemical reagents (sodium dihydrogen phosphate, disodium hydrogen phosphate, acetic acid, sodium chloride, glucose, potassium chloride, sodium bicarbonate, disodium hydrogen phosphate, potassium dihydrogen phosphate, magnesium chloride 6 hydrate, magnesium sulfate 7 hydrate) were obtained from the local supplier, Chempur, (Piekary Śląskie, Poland). Agarose was purchased from the local supplier, Blirt (Gdańsk, Poland). These chemicals were of analytical grade, and solutions were prepared using water purified using the Mili-Q system.

2.4. Dendrimer/siRNA Complexes Formation

Dendrimers and siRNAs were mixed in phosphate buffer (pH = 7.4) at concentrations with molar ratio 20:1 where complexes formed immediately. The complexes were characterized previously [14].

2.5. MCF-7 Cell Line

The MCF-7 cell line used in this study was purchased from American Type Culture Collection (ATCC[®], cat. No: HTB-22, Manassas, VA, USA). The cells were cultured in Dulbecco's modified Eagle's medium (DMEM) supplemented with 10% fetal bovine serum (FBS) and antibiotics. Cultures were maintained in an incubator with 5% CO₂, at 37 °C.

In 2D cell cultures, the cells were seeded onto 12-well plates at the density of 6×10^5 cells per well. Dendrimers or dendriplexes were added after 24 h.

For preparing 3D cell culture, the agarose gels produced using 3D Petri Dish[®] for small spheroids from MicroTissues Inc. were used (Providence RI, USA). Hydrogel was prepared according to the manufacturer's instruction using 12-well plates. 2% agarose in PBS was placed in micro-mold and allowed to dry, then the gels were transferred into 12-well plates and the cells were seeded at a density of 1×10^5 per agarose gel and cultured for 7 days in conditions described above. Microscopy image of spheroid after 7 days of culture is shown on Figure 2. After 7 days dendrimers or dendriplexes were added. The diameter of spheroids on the measurement day was <350 nm.

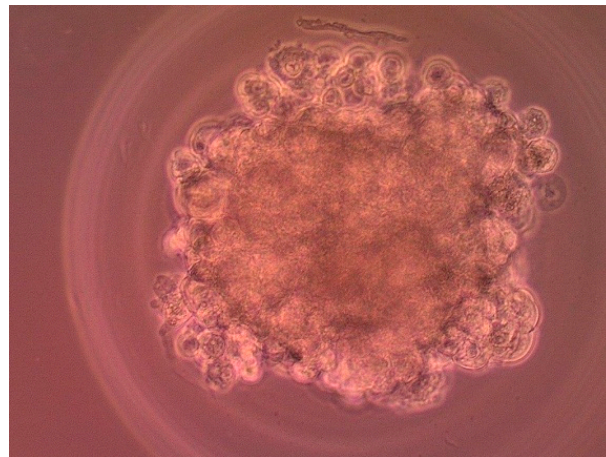


Figure 2. Microscopy image of 3D cultured MCF-7 cells after 7 days after seeding.

2.6. Flow Cytometry Assays

For cytometry analysis of the cells cultured in 2D, the media from each well were transferred into centrifuge tubes and centrifuged for 5 min. at $300 \times g$ to recover dead cells, after centrifugation the supernatant was discarded. The cells on the plates were washed with PBS and then detached with TrypLE for approx. 5 min. in the incubator with 5% CO₂, at 37 °C. Hanks' balanced salt solution (HBSS) with 10% FBS was added. The cells from the plates were transferred to the dead cells in the tubes and mixed. All cells were transferred to the cytometry tubes through cytometry filters and stained with fluorescent dyes. 10,000 events were collected from each sample.

For analysis, the 3D cell cultures after incubation with dendrimers or dendriplexes, were washed with PBS and the cells were removed from gels according to manufacturer's protocol. TrypLE was added (0.5 mL) onto the new 12-well plate, the gels were transferred to this plate and inverted upside down without any bubbles. The plates were centrifuged for 5 min., at 500 rpm, gels were removed and the cells were incubated for 10 min. in the incubator with 5% CO₂, at 37 °C. After incubation, 0.25 mL of the HBSS with 10% FBS were added, the cells were gently mixed with automatic pipette, transferred into the cytometry tubes through cytometry filters and stained with fluorescent dyes. 10,000 events were collected from each sample.

2.6.1. Live–Dead Assay

Cytotoxicity effect of dendrimers and dendriplexes was evaluated using the live–dead test. The cells in 2D cell culture were incubated with dendrimers (at 0.5, 1 and 2 μM). The cells in 3D cell culture were incubated with dendrimers (at 5, 10, 20, 30 and 50 μM) or dendriplexes (dendrimer concentration of 5 and 10 μM ; dendrimer/siRNA molar ratio 20:1) for 24 or 48 h. Untreated cells were used as a negative control (NC), and the cells treated with 1 mM (2D) or 3 mM H_2O_2 (3D) were used as a positive control (PC). After incubation, the cells, prepared as described above, were stained with calcein AM (labeling of live cells) and with PI (labeling of dead cells) and analyzed using flow cytometer LSR[®] II (Becton Dickinson, Erembodegem, Belgium).

The live–dead assay was also performed after treatment with 3 doses of dendrimers and dendriplexes with cells being cultured as described above. After 7 days of culture the first dose of dendrimers or dendriplexes was added. The second dose was added after 48 h and third dose was added after the next 48 h. After treatment the cells were prepared as described above and analyzed using flow cytometer LSR[®] II (Becton Dickinson, Erembodegem, Belgium).

2.6.2. Apoptosis Detection by Flow Cytometry (Annexin V-FITC Apoptosis Detection Test)

After 24 h incubation with dendrimers or dendriplexes, the cells cultured in 3D were stained using the Annexin V-FITC Apoptosis Detection Kit. The cells were washed 3 times with PBS, then the cell suspension was prepared as described above. The suspension was centrifuged at $130\times g$ for 5 min., resuspended in the binding buffer and stained with the Annexin V-FITC Apoptosis Detection Kit according to manufacturer's instructions. Finally, the cells were analyzed using the flow cytometer LSR[®] II (Becton Dickinson, Erembodegem, Belgium).

2.6.3. Cellular Uptake

To estimate the cellular uptake of dendriplexes, complexes of dendrimers with fluorescein (FITC) labeled siRNA were used. The cells were treated with dendriplexes for 24 h (dendrimers at 10 μM ; dendrimer/siRNA molar ratio 20:1). For cytometry analysis the cells were prepared as described above and analyzed using flow cytometer LSR[®] II (Becton Dickinson, Erembodegem, Belgium).

2.7. Confocal Analysis of Cellular Uptake

Cells cultured in 3D were used for confocal analysis. After incubation with dendrimer/FITC-labeled siRNA complexes (dendrimer at 10 μM ; molar ratio 20:1), the cells were washed with PBS and fixed with 3.7% formaldehyde solution for 1 h. Then the cells were washed 3 times with PBS for 20 min. Hoechst 33342 was utilized to stain DNA (2 h, 1 mg/mL), and F-actin was stained with Texas Red-X Phalloidin (2 h, 0.1 $\mu\text{g}/\text{mL}$). The cells were observed with confocal laser scanning microscopy platform TCS SP8 (Leica Microsystems, Wetzlar, Germany) with an objective of $63\times/1.40$ (HC PL APO CS2, Leica Microsystems, Wetzlar, Germany) at excitation wavelengths: 405 nm (Hoechst 33342), 488 nm (FITC) and 565 nm (Texas Red-X Phalloidin).

2.8. Statistical Analysis

The results are presented as mean \pm SD. Data were analyzed by the one-way ANOVA test, followed by Tuckey's analysis using Origin software; $p < 0.05$ was accepted as statistically significant. All experiments were performed in at least 3 independent replications.

3. Results

3.1. Live–Dead Test Using Flow Cytometry

For the live–dead test, the MCF-7 cells were exposed to dendrimers or dendrimer/siRNA complexes at different concentrations for 24 h or 48 h and stained with calcein AM (Calc) and propidium iodide (PI). Three main populations can be distinguished after measurements:

calcein positive/PI negative (Calc+/PI−), considered live cells, calcein positive/PI positive (Calc+/PI+), considered the cells with disturbed cell membranes (apoptotic cells) and calcein negative/PI positive (Calc−/PI+) cells, considered death cells. The data show that CBD-1 and CBD-2 influenced cell viability in a dose-dependent manner, the higher concentrations of dendrimer caused the number of Calc+/PI− cells to decrease, while the number of Calc+/PI+ and Calc−/PI+ cells increased (Figures 3 and 4).

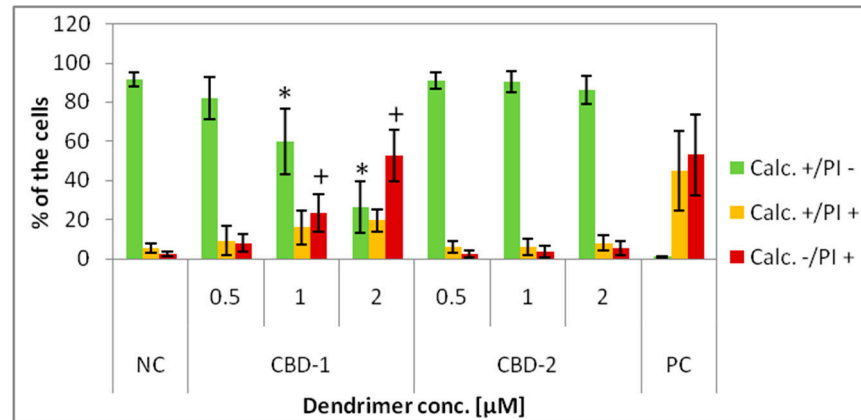


Figure 3. Percentage of 2D cultured cells Calc+/PI−, Calc+/PI+ and Calc−/PI+ after 24 h exposure to dendrimers: CBD-1 and CBD-2 at different concentrations. * $p < 0.05$ vs. NC for group Calc+/PI−; + $p < 0.05$ vs. NC for group Calc−/PI+. $n = 6$.

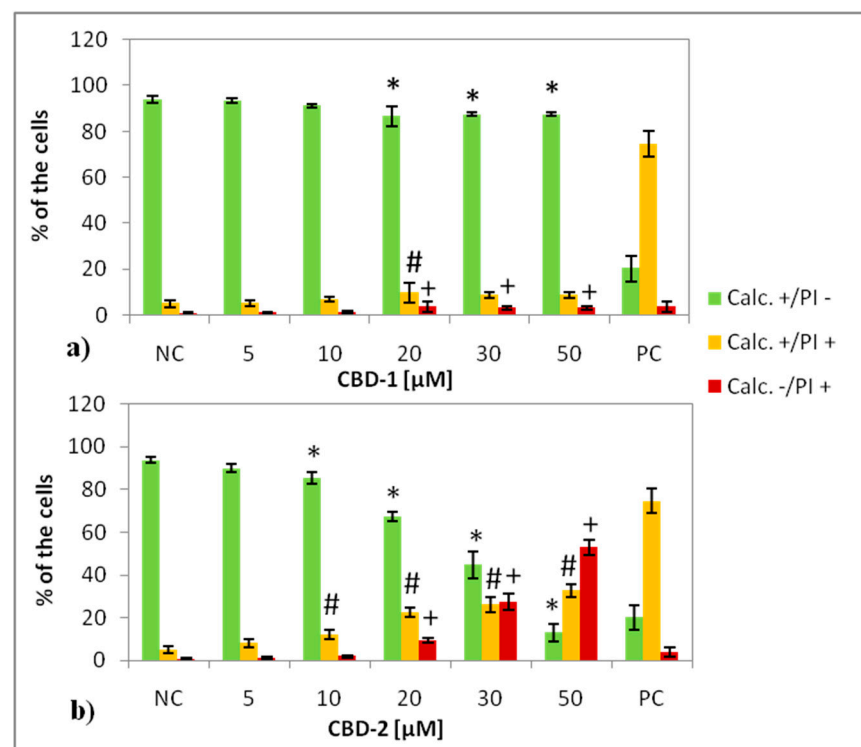


Figure 4. Percentage of 3D cultured cells Calc+/PI−, Calc+/PI+ and Calc−/PI+ after 24 h exposure to dendrimers: CBD-1 (a) and CBD-2 (b) at different concentrations. * $p < 0.05$ vs. NC for group Calc+/PI−; # $p < 0.05$ vs. NC for group Calc+/PI+; + $p < 0.05$ vs. NC for group Calc−/PI+. $n = 6$.

For cells cultured in 2D exposed to dendrimers for 24 h, a statistically significant decrease of the number of Calc+/PI− cells was observed at 1 μM and 2 μM for CBD-1

(Figure 3). CBD-2 did not lead to any significant decrease of the number of Calc+/PI− cells. This means that CBD-1 seems to be more cytotoxic to the cells cultured in 2D than CBD-2.

In the case of the cells cultured in 3D after 24 h of the treatment, with CBD-1, statistically significant effects for Calc+/PI− cells were visible for dendrimer at 20, 30 and 50 μM and the number of the Calc+/PI− cells was reduced to 86.63 ± 4.41%, 87.43 ± 0.86% and 79.67 ± 4.50%, respectively (Figure 4). For CBD-2, statistically significant effects on Calc+/PI− cells appeared with the dendrimer at 10, 20, 30 and 50 μM, causing a decrease in the number of Calc+/PI− cells to 85.50 ± 2.65%, 67.20 ± 2.26%, 44.78 ± 6.33% and 13.08 ± 4.00%, respectively (Figure 4). This dendrimer was more toxic than CBD-1. Along with the decrease of the number of the Calc+/PI− cells, an increase of the number of Calc+/PI+ cells and Calc−/PI+ cells was noted (Figure 4).

For experiments with dendriplexes, dendrimers at 5 and 10 μM were used, the concentrations at which dendrimers (siRNA carriers) were not toxic to cells. The dendrimer/siRNA molar ratio was 20:1. Statistically significant decreases of the percentage of Calc+/PI− cells compared to NC was visible for complexes CBD-1/Bcl-2, CBD-2/Mcl-1 and CBD-2/Bcl-2, at concentrations of dendrimer at 10 μM (Figure 5). The number of Calc+/PI− cells decreased to approx. 90%. For all complexes with both dendrimers at 5 μM and for CBD-1/Mcl-1 at 10 μM there was no significant effect (Figure 5).

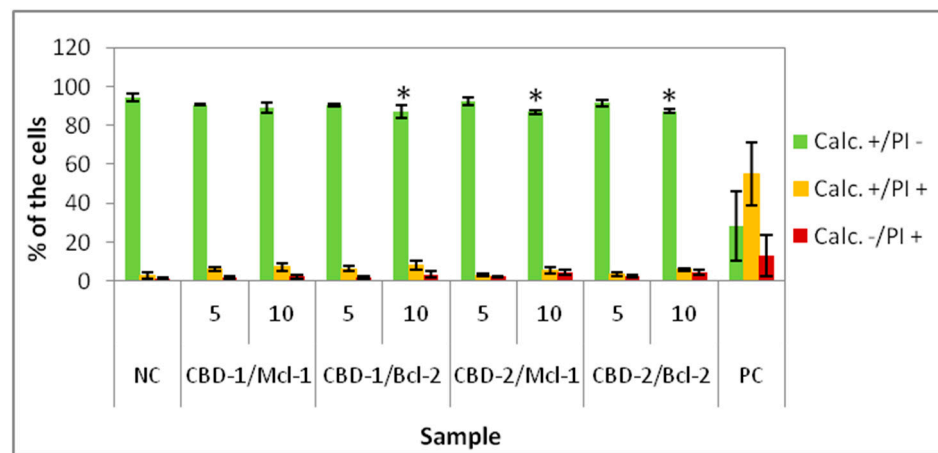


Figure 5. Percentage of 3D cultured cells Calc+/PI−, Calc+/PI+ and Calc−/PI+ after 24 h exposure to dendriplexes. Dendrimers concentrations: 5 and 10 μM; CBD/siRNA molar ratio 20:1. * *p* < 0.05 vs. NC for group Calc+/PI−. *n* = 6.

Comparing the decrease in the number of Calc+/PI− cells after incubation with dendriplexes to the number of Calc+/PI− cells after incubation with the dendrimer alone, statistically significant effects were found for CBD-1/Mcl-1 (CBD-1 at 5 μM) vs. CBD-1 (5 μM), for CBD-1/Bcl-2 (CBD-1 at 5 μM) vs. CBD-1 (5 μM) and for CBD-1/Bcl-2 (CBD-1 at 10 μM) (Table 1).

Table 1. Statistical significance for % of the Calc+/PI− 3D cultured cells after treatment with dendriplexes vs. % of the Calc+/PI− cells after treatment with dendrimer alone. * *p* < 0.05, -no significance.

CBD 5 μM		CBD 10 μM	
CBD-1/Mcl-1 vs. CBD-1 *	CBD-1/Bcl-2 vs. CBD-1 *	CBD-1/Mcl-1 vs. CBD-1 -	CBD-1/Bcl-2 vs. CBD-1 *
CBD-2/Mcl-1 vs. CBD-2 -	CBD-2/Bcl-2 vs. CBD-2 -	CBD-2/Mcl-1 vs. CBD-2 -	CBD-2/Bcl-2 vs. CBD-2 -

The effect of dendrimers and dendriplexes on the MCF-7 cells cultured in 3D was also measured after 48 h of incubation with dendrimers alone and their complexes with siRNAs. The dendrimer concentration was 10 μM and dendrimer/siRNA molar ratio was

20:1. A statistically significant decrease of the percentage of Calc⁺/PI⁻ cells compared to NC was recorded for dendrimer CBD-2 and CBD-2/siRNAs (Figure 6), but the number of live cells was still ~90%. No statistically significant effect was apparent for dendriplexes vs. dendrimer for Calc⁺/PI⁻ cells (for both dendrimers).

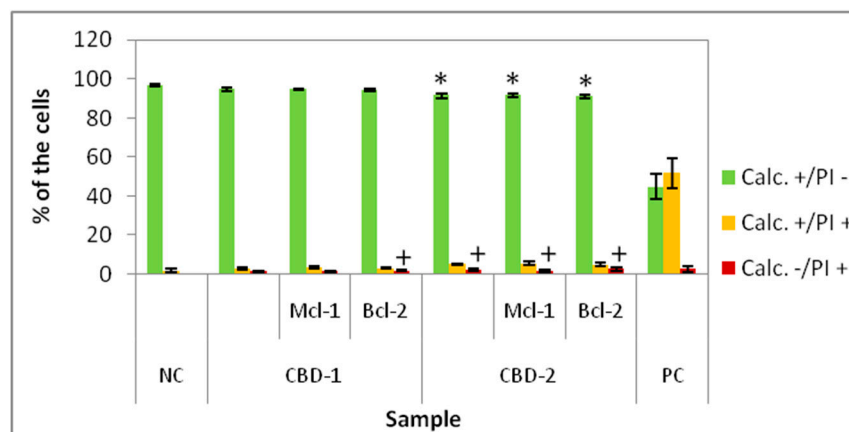


Figure 6. Percentage of 3D cultured cells Calc⁺/PI⁻, Calc⁺/PI⁺ and Calc⁻/PI⁺ after 48 h exposure to dendrimers and dendriplexes. Dendrimers concentration: 10 μ M; CBD/siRNA molar ratio 20:1. * $p < 0.05$ vs. NC for group Calc⁺/PI⁻; + $p < 0.05$ vs. NC for group Calc⁻/PI⁺. $n = 6$.

3.2. Apoptosis Detection by Flow Cytometry (Annexin V-FITC Apoptosis Detection Test)

For apoptosis detection, MCF-7 cells in 3D cultures were exposed to CBD-2 dendrimer or CBD-2/siRNA complexes for 24 h and the Annexin V-FITC Apoptosis Detection Test was performed. Three populations could be distinguished after measurements: FITC⁺/PI⁻, apoptotic cells with the changes in phosphatidylserine location in the plasma membrane, FITC⁺/PI⁺, apoptotic cells with the changes in phosphatidylserine location in the plasma membrane and simultaneously with the disturbances in the continuity of the plasma membrane, and FITC⁻/PI⁺, related to the dead cells.

There was no significant increase in the percentage of FITC⁺/PI⁻ cells compared to untreated cells. A statistically significant increase in the percentage of FITC⁺/PI⁺ was visible for CBD-2/Bcl-2. There was no significant increase in the percentage of FITC⁻/PI⁺ cells (Figure 7) and no statistically significant effects for dendriplexes vs. dendrimer alone for FITC⁺/PI⁻ cells.

3.3. Cellular Uptake by Flow Cytometry and Confocal Microscopy

Flow cytometry analysis was used for quantification of dendriplexes taken up by the cells. Analysis was performed using both dendrimers and both siRNAs labeled with FITC. The data (Figure 8) show that in $3.83 \pm 0.63\%$ of the cells and in $5.85 \pm 0.93\%$ of the cells, complexes with CBD-1 were detected (CBD-1/Mcl-1 and CBD-1/Bcl-2, respectively), whereas for CBD-2, complexes were detected in $6.95 \pm 0.93\%$ and in $7.35 \pm 1.59\%$ of the cells (for CBD-2/Mcl-1 and CBD-2/Bcl-2, respectively).

Confocal microscopy was used for visualization of internalized complexes inside the MCF-7 cells. Both, Mcl-1 and Bcl-2, complexed with CBD-1 and CBD-2 were visible in the cytoplasm as small green dots (Figure 9).

3.4. Live–Dead Test after Treatment with Three Doses of Dendrimers or Dendriplexes Using Flow Cytometry

Since 24 and 48 h of treatment did not cause significant changes in the number of live cells, we performed an experiment in which three doses of dendrimers and dendriplexes were added to the 3D cell culture. Statistically significant effects in reduction in the number of Calc⁺/PI⁻ cells were visible for all tested groups (CBD-1 and CBD-2 alone and with both tested siRNAs). However, the most visible effect was seen with CBD-1/Mcl-1 and

CBD-1/Bcl-2. The number of live cells was reduced to $15.00 \pm 9.88\%$ and $8.63 \pm 4.92\%$, respectively. Simultaneously, the number of Calc⁻/PI⁺ cells increased to $63.00 \pm 9.60\%$ and $71.33 \pm 5.71\%$, respectively (Figure 10).

Comparing the decrease in the number of Calc⁺/PI⁻ cells after incubation with 3 doses of dendriplexes to the number of Calc⁺/PI⁻ cells after incubation with 3 doses of dendrimer alone, a statistically significant effect is visible for CBD-1/Mcl-1 vs. CBD-1 and for CBD-1/Bcl-2 vs. CBD-1 (Table 2).

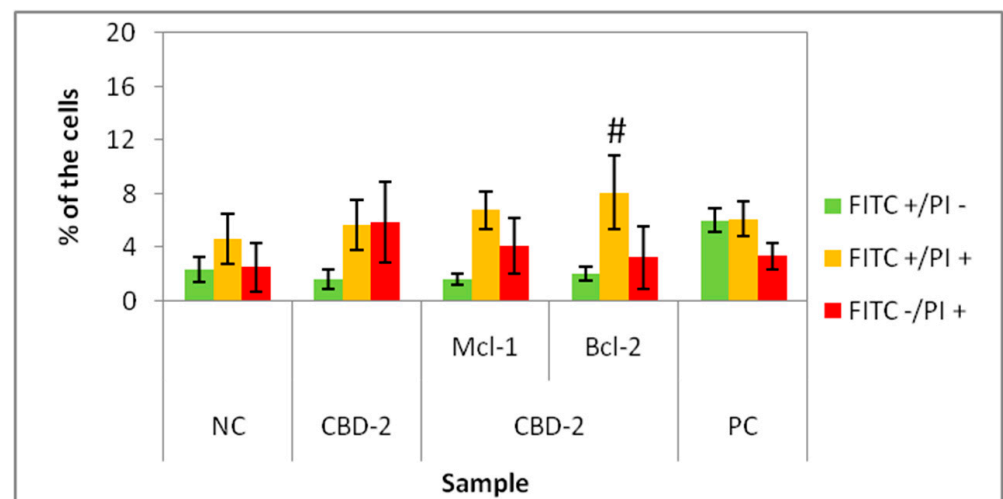


Figure 7. Percentage of 3D cultured cells FITC⁺/PI⁻, FITC⁺/PI⁺ and FITC⁻/PI⁺ after 24 h exposure to CBD-2 and CBD-2/siRNA complexes. Dendrimer concentration: 10 μ M; CBD/siRNA molar ratio 20:1. # $p < 0.05$ vs. NC for group FITC⁺/PI⁺. $n = 6$.

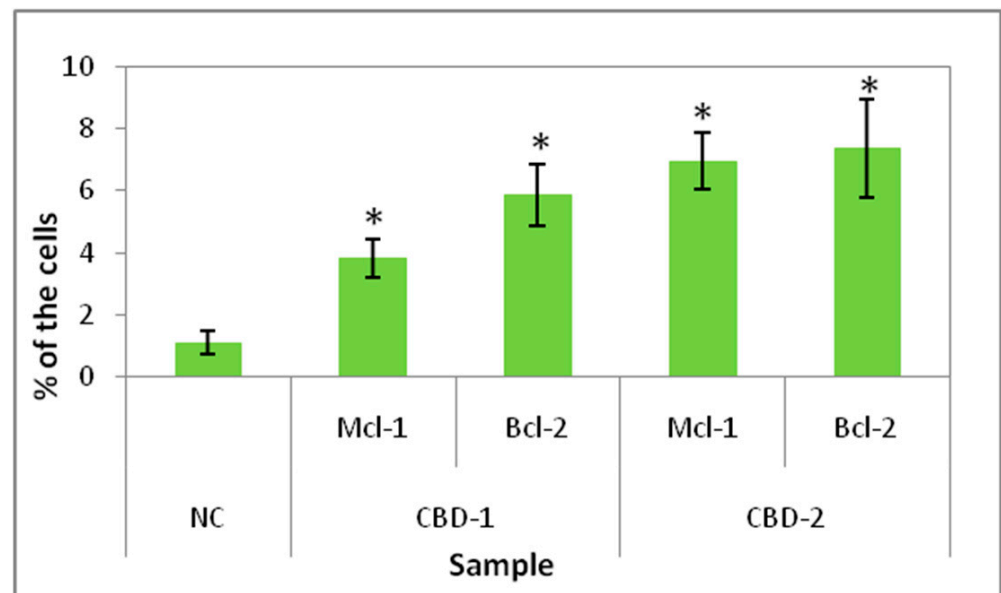


Figure 8. Percentage of 3D cultured cells with complexes of CBD/siRNA-FITC in their cytoplasm after 24 h exposure to dendrimers and dendriplexes. Dendrimer concentration: 10 μ M; CBD/siRNA molar ratio 20:1. * $p < 0.05$ vs. NC. $n = 4$.

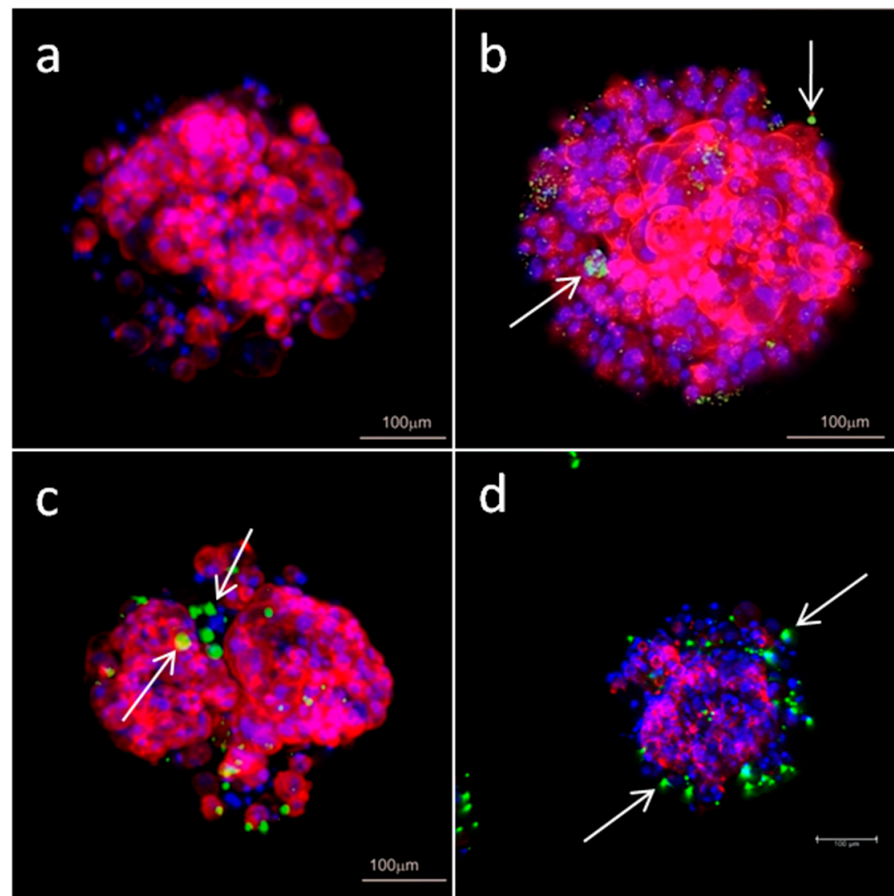


Figure 9. Confocal microscopy images of 3D cultured MCF-7 cells after 24 h incubation with FITC labeled siRNA: (a) Mcl-1, (b) CBD-1/Mcl-1, (c) CBD-2/Mcl-1, (d) CBD-2/Bcl-2. The concentration of siRNA was 0.5 μ M and the dendrimer/siRNA molar ratio was 20:1. Arrows indicate complexes dendrimer/siRNA.

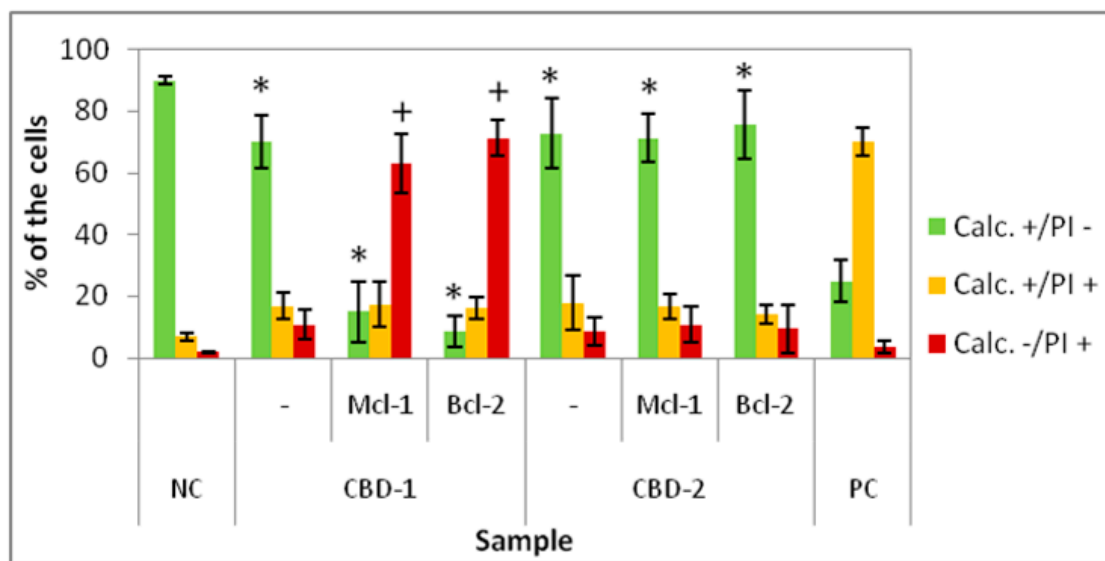


Figure 10. Percentage of 3D cultured cells Calc+/PI-, Calc+/PI+ and Calc-/PI+ after exposure to three doses of dendrimers and dendriplexes. Dendrimers concentration: 10 μ M; CBD/siRNA molar ratio 20:1. * $p < 0.05$ vs. NC for group Calc+/PI-; + $p < 0.05$ vs. NC for group Calc-/PI+. $n = 6$.

Table 2. Statistical significance for % of the Calc+/PI− 3D cultured cells after treatment with 3 doses of dendriplexes vs. % of the Calc+/PI− cells after treatment with 3 doses of dendrimer alone. * $p < 0.05$, -no significance.

CBD 10 μ M	
CBD-1/Mcl-1 vs. CBD-1 *	CBD-1/Bcl-2 vs. CBD-1 *
CBD-2/Mcl-1 vs. CBD-2 -	CBD-2/Bcl-2 vs. CBD-2 -

4. Discussion

Initially, gene therapy was a therapeutic process in which missing cellular functions were reintroduced by providing a normal copy of a mutated gene into target cells. Currently, protein-coding cDNAs are used in gene therapy to influence cell behavior. These applications include the influence on cell cycle regulatory proteins to block cancer cell proliferation, immune cell activation by transferring gene coding for co-stimulatory proteins into cancer cells, the secretion of cytokines and growth factors coding for neurotrophic factors in Alzheimer's or Parkinson's diseases, and the production of angiogenic factors in cardiac or peripheral ischemia. Small nucleic acids, DNAs or RNAs with regulatory functions as well as protein-coding nucleic acids can be used [3]. For example, siRNA can silence target genes by the degradation of complementary mRNA in the cytoplasm [15]. However, siRNA must be transported by carriers, since siRNA alone is repelled from the anionic cell membrane because of its anionic charge and it is not resistant to cellular enzymes [16,25]. Dendrimers are among nanomaterials considered siRNA carriers. They are synthetic polymers, characterized by a branched structure and a large number of terminal groups for interaction with a range of compounds, including siRNA [26–30]. Using dendrimers as nucleic acid carriers is advantageous due to the possibility to control their structure and size, high density of ligand and functionality, and high structural and chemical homogeneity [26].

Transport of siRNA into cells by dendrimers has been investigated by other researchers. For example, Dzmitruk et al. [21], tested three groups of cationic dendrimers: phosphorous based dendrimers, poly(amidoamine) (PAMAM) dendrimers and carbosilane dendrimers, as carriers for anticancer siRNAs (Bcl-x1, Bcl-2, Mcl-1 and a scrambled sequence siRNA). They showed that tested dendrimers complexed with siRNAs could be transported into HeLa and HL-60 cells effectively. Michlewska et al. [13] and Krasheninina et al. [31] proved that various cationic dendrimers could transport siRNA and transfect HeLa and HL-60 cells. Weber et al. [32] proposed amino-terminated carbosilane dendrimers (CBS) as carriers for the siRNA used to reduce HIV replication in peripheral blood mononuclear cells (PBMC) and the lymphocytic cell line SupT1. However, these experiments were conducted using 2D or suspension cell cultures. The physiological environment for cells is 3D and this is crucial for their growth and metabolism [6,22]. For this reason, 3D spheroids are a better model for testing substances (e.g., drugs and nanoparticles), since the results reflect more accurately in vivo cellular responses [6,23]. 2D cultures are deprived of any process of transporting nanoparticles through cell layers and this could affect toxicity results [22]. In addition, some ECM compounds are expressed in spheroids at high levels; thus, spheroids imitate barriers seen in vivo more adequately [33].

The MCF-7 cell line, cultured as spheroids, was chosen for our experiments. We tested two types of cationic carbosilane dendrimers (CBD-1 and CBD-2) in complexes with pro-apoptotic siRNAs (Mcl-1 and Bcl-2), and investigated their influence on MCF-7 cells cultured in 3D. Dendrimers and their complexes with siRNA were characterized and reported previously [14,24].

Firstly, flow cytometry analysis of the cells cultured in 2D, after 24 h incubation with dendrimers was prepared. Those experiments confirmed our previous results [14], that CBD-1 is more toxic for cells in 2D than CBD-2 (Figure 3). Statistically significant decreases of the number of live (Calc+/PI−) cells was visible for CBD-1 at 1 μ M. Since the toxic effect on cells is reduced in the spheroid compared to 2D models [22], experiments on 3D

cell culture used higher concentrations of dendrimers. Interestingly, the cells cultured as spheroids had a decrease in the number of Calc⁺/PI[−] cells higher with CBD-2. Small but statistically significant effects were visible for CBD-2 at 10 μ M. Reduction in the numbers of Calc⁺/PI[−] was higher with the increasing concentration of CBD-2. For CBD-1, statistically significant decreases in numbers were visible for dendrimers at 20, 30 and 50 μ M, but the number of live cells was still above 86%. Therefore, an opposite toxicity behavior was observed between 2D and 3D cultures. For experiments with siRNAs, we chose dendrimers at concentrations that were non-toxic for cells: 5 and 10 μ M. Delivery of siRNA using tested dendrimers did not increase the cytotoxic effect in cells either after 24 or 48 h. Measurements of apoptosis did not show an increased level of apoptosis marker after 24 h exposure of spheroids to CBD-2 and its complexes with Mcl-1, but a significant effect was visible for apoptotic cells with a damaged cell membrane after incubation with CBD-2/Bcl-2 (Figure 7).

Measurements of internalization of dendriplexes and microscopy images confirmed that dendriplexes were transported into the cells growing as spheroids. Flow cytometry analysis of internalization indicated that CBD-2 transports siRNAs more effectively than CBD-1, after 24 h of treatment, which could account for the higher cytotoxic effect of CBD-2 on cells in 3D.

Since 24 or 48 h treatments did not lead to changes in viability of the cells, experiments were designed with longer times of exposition to dendrimers and dendriplexes. We added 3 doses of dendrimers or dendriplexes to the cells at 48 h intervals. The results showed a decrease in cell viability, with the greatest effect being visible for CBD-1 complexed with siRNAs. Both dendrimers contain 8 surface cationic groups, which are considered a reason for the cytotoxic action of dendrimers [34]. However, the nature of these moieties is different. CBD-1 contains tertiary ammonium groups (RNHMe₂Cl), which are dependent on pH, whereas in the CBD-2 structure pH-stable quaternary ammonium groups (RNMe₃I) are observed. Another subtle difference is associated with hydrophobicity—the (RNMe₃I)-terminated dendrimer is slightly more hydrophobic. Thus, the difference in cytotoxic activity can be explained by different mechanisms of action [14]. However, differences in action are not the only explanation. The differences in cytotoxicity for CBD-1 and CBD-2 and their complexes with siRNAs may result from differences in distribution of nanoparticles within spheroids. It is possible that CBD-2 can penetrate only to the external layers of spheroids. Complexity of the tissue can affect delivery of nanoparticles into the cells. Moreover, the ECM, which is a mixture of proteins and compounds, forms a negatively charged and viscous barrier [33]. The ability of nanoparticles to penetrate through the ECM is affected by their size, charge and surface chemistry. Tchoryk et al. [33] proved that larger particles penetrate less into the core of the spheroid. They investigated poly(styrene) particles of size 30, 50 and 100 nm, observing that within the first 2 h of incubation, over 70% and 80% of the cells in the spheroid internalized particles of 30 and 50 nm size, respectively, and less than 10% of the cells had particles of 100 nm size [33]. Tang et al. [35] showed that camptothecin-silica nanoparticle conjugates of 50 nm were more effectively taken up by mouse-tumor models in vivo and ex vivo than particles of 200 nm. In our studies, confocal images of spheroids suggest that complexes CBD-2/siRNA may aggregate into larger particles and this could be the reason for lower penetration of CBD-2/siRNA complexes and consequently lower toxicity.

Our results suggest that CBD-1 is better as an siRNA carrier as it transports siRNA into the cells and is not cytotoxic for MCF-7 cells cultured as 3D spheroids. Finally, siRNA leads to apoptosis in cancer cells.

Recent research has shown other technologies with potential to correct gene mutations. In 2014, the CRISPR-Cas system was prepared to be used in various organisms to change or silence gene sequences [36]. The CRISPR (Clustered Regularly Interspaced Short Palindromic Repeats) is a region in the prokaryotic genome, consisting of palindromic sequence inserts [36,37]. In this region, Cas protein preserves genetic information. The CRISPR-Cas complex detects foreign genetic information, then stores it and finally destroys it. It works

as a antiviral unit in prokaryotic cells [36]. Studies with the use of bacteria and mammalian cells revealed that biologically engineered CRISPR-Cas technology is promising for repairing gene mutations. However, the application of this system has some limitations because of unpredictable side effects and consequences for the next generations [36]. Currently, the CRISPR-Cas system is used in diagnostics to detect RNA and DNA [37].

Besides systems for correction of mutated genes, other anti-tumor approaches are under investigation. Semi-interpenetrating polymer network (semi-IPN) hydrogels containing extracellular polysaccharide Salcan were examined as containers for an anticancer drug doxorubicin (DOX). Hydrogels without a drug were not toxic for HepG2 and A549 cells, while hydrogels with a DOX released a drug into cells, leading to cell death [38].

5. Conclusions

Analysis of the internalization of dendriplexes (confocal microscopy and flow cytometry) proved that CBD-1 and CBD-2 complexed with both tested siRNAs (Mcl-1 and Bcl-2) can penetrate into spheroids. Flow cytometry analysis of cytotoxicity of dendrimers alone showed differences in relation to their ability to reduce the viability of MCF-7 cells cultured as spheroids, and CBD-2 seems to be more toxic. The connection of siRNAs to tested dendrimers did not decrease viability of cells when compared to viability after treatment with dendrimers alone in 24 h treatments. However, analysis of cytotoxicity after incubation with 3 doses of dendriplexes revealed the toxic potential of CBD-1 complexed with both siRNAs. This indicates that the effect of dendriplexes on MCF-7 cells cultured as spheroids depends on a variety of factors as a mechanism of action resulting from the structure of the molecule, and also depends on the size of the complex and doses of dendriplexes added at specified time intervals.

Our results on the MCF-7 cells cultured as 3D spheroids suggest that CBD-1 is the better siRNA carrier as it is not cytotoxic and transports siRNA into the cells. Finally, siRNA leads to apoptosis in cancer cells.

It is worth testing other dendrimers at different concentrations, adding doses of dendrimers in different time intervals to choose the best variant.

It is important to test anticancer drugs or materials used in gene therapy on 3D cell cultures, as 3D spheroids mimic tumor structure more properly than monolayers.

Author Contributions: Conceptualization, K.B. and K.M.; methodology, K.B. and K.M.; software, K.B.; investigation, K.B.; synthesis of dendrimers, R.G.-R. and F.J.d.l.M.; resources, K.M. and P.K.; writing—original draft preparation, K.B.; writing—review and editing, K.B., K.M., P.K., R.G.-R., F.J.d.l.M. and M.B.; supervision, K.M. and P.K.; funding acquisition, K.M. All authors have read and agreed to the published version of the manuscript.

Funding: This research received no external funding.

Institutional Review Board Statement: Not applicable.

Informed Consent Statement: Not applicable.

Data Availability Statement: Not applicable.

Acknowledgments: This work was prepared as a part of the first edition of the Ministry of Science and Higher Education program called “Doktorat wdrożeniowy”. This work was supported by PIE14/00061 (CIBER), PID2020-112924RB (MINECO), Consortium IMMUNOTHERCAN-CM B2017/BMD-3733 (CAM), NANODENDMED II-CM ref B2017/BMD-3703. CIBER-BBN is an initiative funded by the VI National R&D&i Plan 2008–2011, Iniciativa Ingenio 2010, Consolider Program, CIBER Actions and financed by the Instituto de Salud Carlos III with assistance from the European Regional Development Fund. This work has been supported partially by a EUROPARTNER: Strengthening and spreading international partnership activities of the Faculty of Biology and Environmental Protection for interdisciplinary research and innovation of the University of Lodz Programme: NAWA International Academic Partnership Programme. We would like to thank the Laboratory of Microscopic Imaging and Specialized Biological Techniques, Faculty of Biology and Environmental Protection, University of Lodz, especially Sylwia Michlewska.

Conflicts of Interest: The authors declare no conflict of interest.

References

1. Mulligan, R.C. The Basic Science of Gene Therapy. *Science* **1993**, *260*, 926–932. [[CrossRef](#)] [[PubMed](#)]
2. Dubé, I.D.; Cournoyer, D. Gene Therapy: Here to Stay. *Can. Med. Assoc. J.* **1995**, *152*, 10.
3. Giacca, M.; Zacchigna, S. Virus-Mediated Gene Delivery for Human Gene Therapy. *J. Control. Release* **2012**, *161*, 377–388. [[CrossRef](#)] [[PubMed](#)]
4. Ionov, M.; Łaźniewska, J.; Dźmitruk, V.; Halets, I.; Loznikova, S.; Novopashina, D.; Apartsin, E.; Krasheninina, O.; Venyaminova, A.; Miłowska, K.; et al. Anticancer siRNA Cocktails as a Novel Tool to Treat Cancer Cells. Part (A). Mechanisms of Interaction. *Int. J. Pharm.* **2015**, *485*, 261–269. [[CrossRef](#)]
5. Pędziwiatr-Werbicka, E.; Gorzkiewicz, M.; Horodecka, K.; Abashkin, V.; Klajnert-Maculewicz, B.; Peña-González, C.E.; Sánchez-Nieves, J.; Gomez-Ramirez, R.; de la Mata, F.J.; Bryszewska, M. Silver Nanoparticles Surface-Modified with Carbosilane Dendrons as Carriers of Anticancer siRNA. *Int. J. Mol. Sci.* **2020**, *21*, 4647. [[CrossRef](#)]
6. Białkowska, K.; Komorowski, P.; Bryszewska, M.; Miłowska, K. Spheroids as a Type of Three-Dimensional Cell Cultures—Examples of Methods of Preparation and the Most Important Application. *Int. J. Mol. Sci.* **2020**, *21*, 6225. [[CrossRef](#)]
7. Gonçalves, G.A.R.; Paiva, R.M.A. Gene Therapy: Advances, Challenges and Perspectives. *Einstein* **2017**, *15*, 369–375. [[CrossRef](#)]
8. Shi, B.; Zheng, M.; Tao, W.; Chung, R.; Jin, D.; Ghaffari, D.; Farokhzad, O.C. Challenges in DNA Delivery and Recent Advances in Multifunctional Polymeric DNA Delivery Systems. *Biomacromolecules* **2017**, *18*, 2231–2246. [[CrossRef](#)]
9. Misra, S. Human Gene Therapy: A Brief Overview of the Genetic Revolution. *J. Assoc. Phys. India* **2012**, *61*, 127–133.
10. Verma, I.M.; Weitzman, M.D. Gene Therapy: Twenty-First Century Medicine. *Annu. Rev. Biochem.* **2005**, *74*, 711–738. [[CrossRef](#)]
11. Matthews, Q.L.; Curriel, D.T. Gene Therapy: Human Germline Genetic Modifications—Assessing the Scientific, Socioethical, and Religious Issues. *South. Med. J.* **2007**, *100*, 98–100. [[CrossRef](#)]
12. Xin, Y.; Huang, M.; Guo, W.W.; Huang, Q.; Zhang, L.Z.; Jiang, G. Nano-Based Delivery of RNAi in Cancer Therapy. *Mol. Cancer* **2017**, *16*, 134. [[CrossRef](#)]
13. Michlewska, S.; Ionov, M.; Maroto-Díaz, M.; Szwed, A.; Ihnatsyeu-Kachan, A.; Loznikova, S.; Shcharbin, D.; Maly, M.; Gomez-Ramirez, R.; de la Mata, F.J.; et al. Ruthenium Dendrimers as Carriers for Anticancer siRNA. *J. Inorg. Biochem.* **2018**, *181*, 18–27. [[CrossRef](#)]
14. Białkowska, K.; Miłowska, K.; Michlewska, S.; Sokołowska, P.; Komorowski, P.; Lozano-Cruz, T.; Gomez-Ramirez, R.; de la Mata, F.J.; Bryszewska, M. Interaction of Cationic Carbosilane Dendrimers and Their siRNA Complexes with MCF-7 Cells. *Int. J. Mol. Sci.* **2021**, *22*, 7097. [[CrossRef](#)]
15. Wang, J.; Lu, Z.; Wientjes, M.G.; Au, J.L.-S. Delivery of siRNA Therapeutics: Barriers and Carriers. *AAPS J.* **2010**, *12*, 4. [[CrossRef](#)]
16. Tokatlian, T.; Segura, T. siRNA Applications in Nanomedicine. *Wiley Interdiscip. Rev. Nanomed. Nanobiotechnol.* **2010**, *2*, 305–315. [[CrossRef](#)]
17. Ambesajir, A.; Kaushik, A.; Kaushik, J.J.; Petros, S.T. RNA Interference: A Futuristic Tool and Its Therapeutic Applications. *Saudi J. Biol. Sci.* **2012**, *19*, 395–403. [[CrossRef](#)]
18. Angart, P.; Vocelle, D.; Chan, C.; Walton, S.P. Design of siRNA Therapeutics from the Molecular Scale. *Pharmaceuticals* **2013**, *6*, 440–468. [[CrossRef](#)]
19. Burlacu, A. Regulation of Apoptosis by Bcl-2 Family Proteins. *J. Cell. Mol. Med.* **2003**, *7*, 249–257. [[CrossRef](#)]
20. Ola, M.S.; Nawaz, M.; Ahsan, H. Role of Bcl-2 Family Proteins and Caspases in the Regulation of Apoptosis. *Mol. Cell. Biochem.* **2011**, *351*, 41–58. [[CrossRef](#)]
21. Dźmitruk, V.; Szulc, A.; Shcharbin, D.; Janaszewska, A.; Shcharbina, N.; Łaźniewska, J.; Novopashina, D.; Buyanova, M.; Ionov, M.; Klajnert-Maculewicz, B.; et al. Anticancer siRNA Cocktails as a Novel Tool to Treat Cancer Cells. Part (B). Efficiency of Pharmacological Action. *Int. J. Pharm.* **2015**, *485*, 288–294. [[CrossRef](#)]
22. Lee, J.; Lilly, G.D.; Doty, R.C.; Podsiadlo, P.; Kotov, N.A. In Vitro Toxicity Testing of Nanoparticles in 3D Cell Culture. *Small* **2009**, *5*, 1213–1221. [[CrossRef](#)]
23. Edmondson, R.; Broglie, J.J.; Adcock, A.F.; Yang, L. Three-Dimensional Cell Culture Systems and Their Applications in Drug Discovery and Cell-Based Biosensors. *Assay Drug Dev. Technol.* **2014**, *12*, 207–218. [[CrossRef](#)]
24. Lozano-Cruz, T.; Alcarraz-Vizán, G.; de la Mata, F.J.; de Pablo, S.; Ortega, P.; Duarte, Y.; Bravo-Moraga, F.; González-Nilo, F.D.; Novials, A.; Gomez, R. Cationic Carbosilane Dendritic Systems as Promising Anti-Amyloid Agents in Type 2 Diabetes. *Chem. Eur. J.* **2020**, *26*, 7609–7621. [[CrossRef](#)]
25. Song, E.; Zhu, P.; Lee, S.-K.; Chowdhury, D.; Kussman, S.; Dykxhoorn, D.M.; Feng, Y.; Palliser, D.; Weiner, D.B.; Shankar, P.; et al. Antibody Mediated In Vivo Delivery of Small Interfering RNAs via Cell-Surface Receptors. *Nat. Biotechnol.* **2005**, *23*, 6. [[CrossRef](#)]
26. Zhou, J.; Wu, J.; Hafdi, N.; Behr, J.-P.; Erbacher, P.; Peng, L. PAMAM Dendrimers for Efficient siRNA Delivery and Potent Gene Silencing. *Chem. Commun.* **2006**, *22*, 2362–2364. [[CrossRef](#)]
27. Tomalia, D.A.; Uppuluri, S.; Swanson, D.R.; Li, J. Dendrimers as Reactive Modules for the Synthesis of New Structure-Controlled, Higher-Complexity Megamers. *Pure Appl. Chem.* **2000**, *72*, 2343–2358. [[CrossRef](#)]
28. Tomalia, D.A. Architecturally Driven Properties Based on the Dendritic State. *High Perform. Polym.* **2001**, *13*, S1–S10. [[CrossRef](#)]
29. Sękowski, S.; Miłowska, K.; Gabryelak, T. Dendrymery w Naukach Biomedycznych i Nanotechnologii. *Postep. Hig. Med. Dosw.* **2008**, *62*, 725–733.

30. Wu, J.; Huang, W.; He, Z. Dendrimers as Carriers for siRNA Delivery and Gene Silencing: A Review. *Sci. World J.* **2013**, *2013*, 630654. [[CrossRef](#)]
31. Krasheninina, O.A.; Apartsin, E.K.; Fuentes, E.; Szulc, A.; Ionov, M.; Venyaminova, A.G.; Shcharbin, D.; de la Mata, F.J.; Bryszewska, M.; Gomez, R. Complexes of Pro-Apoptotic siRNAs and Carbosilane Dendrimers: Formation and Effect on Cancer Cells. *Pharmaceutics* **2019**, *11*, 25. [[CrossRef](#)] [[PubMed](#)]
32. Weber, N.; Ortega, P.; Clemente, M.I.; Shcharbin, D.; Bryszewska, M.; de la Mata, F.J.; Gomez, R.; Munoz-Fernandez, M.A. Characterization of Carbosilane Dendrimers as Effective Carriers of siRNA to HIV-Infected Lymphocytes. *J. Control. Release* **2008**, *132*, 55–64. [[CrossRef](#)] [[PubMed](#)]
33. Tchoryk, A.; Taresco, V.; Argent, R.H.; Ashford, M.; Gellert, P.R.; Stolnik, S.; Grabowska, A.; Garnett, M.C. Penetration and Uptake of Nanoparticles in 3D Tumor Spheroids. *Bioconjug. Chem.* **2019**, *30*, 1371–1384. [[CrossRef](#)] [[PubMed](#)]
34. Jevprasesphant, R.; Penny, J.; Jalal, R.; Attwood, D.; McKeown, N.B.; D'Emanuele, A. The Influence of Surface Modification on the Cytotoxicity of PAMAM Dendrimers. *Int. J. Pharm.* **2003**, *252*, 263–266. [[CrossRef](#)]
35. Tang, L.; Gabrielson, N.P.; Uckun, F.M.; Fan, T.M.; Cheng, J. Size-Dependent Tumor Penetration and in Vivo Efficacy of Monodisperse Drug-Silica Nanoconjugates. *Mol. Pharm.* **2013**, *10*, 883–892. [[CrossRef](#)]
36. Dronina, J.; Samukaite-Bubniene, U.; Ramanavicius, A. Towards Application of CRISPR-Cas12a in the Design of Modern Viral DNA Detection Tools. *J. Nanobiotechnol.* **2022**, *20*, 41. [[CrossRef](#)]
37. Dronina, J.; Samukaite-Bubniene, U.; Ramanavicius, A. Advances and Insights in the Diagnosis of Viral Infections. *J. Nanobiotechnol.* **2021**, *19*, 348. [[CrossRef](#)]
38. Qi, X.; Wei, W.; Li, J.; Zuo, G.; Hu, X.; Zhang, J.; Dong, W. Development of Novel Hydrogels Based on Salecan and Poly(N-Isopropylacrylamide-Co-Methacrylic Acid) for Controlled Doxorubicin Release. *RSC Adv.* **2016**, *6*, 69869. [[CrossRef](#)]

Oświadczenia współautorów

Łódź, dn. 01.06.2022.....

Mgr Kamila Białkowska
Katedra Biofizyki Ogólnej
Instytut Biofizyki, Uniwersytet Łódzki,
ul. Pomorska 141/143, 90-236 Łódź

Oświadczenie

Oświadczam, że w pracy:

- “Spheroids as a type of three-dimensional cell cultures – examples of methods of preparation and the most important application”, **Kamila Białkowska**, Piotr Komorowski, Maria Bryszewska, Katarzyna Miłowska, *International Journal of Molecular Sciences* (22, 7097; DOI: 10.3390/ijms22137097) mój wkład w powstanie pracy polegał na napisaniu i sprawdzeniu tekstu, przygotowaniu rysunków i literatury, korespondencji z edytorem, przygotowaniu odpowiedzi na recenzje.

Mój wkład oceniam na 80%.

- “Interaction of cationic carbosilane dendrimers and their siRNA complexes with MCF-7 cells”, **Kamila Białkowska**, Katarzyna Miłowska, Sylwia Michlewska, Paulina Sokołowska, Piotr Komorowski, Tania Lozano-Cruz, Rafael Gomez-Ramirez, Francisco Javier de la Mata and Maria Bryszewska, *International Journal of Molecular Sciences* (22, 7097; DOI: 10.3390/ijms22137097) polegał na opracowaniu koncepcji pracy, zaplanowaniu eksperymentów, wykonaniu części eksperymentalnej, przygotowaniu próbek do obrazowania mikroskopowego, opracowaniu i analizie wyników, napisaniu i sprawdzeniu tekstu, przygotowaniu figur, korespondencji z edytorem, przygotowaniu odpowiedzi na recenzje.

Mój wkład oceniam na 55%.

- “Interaction of Cationic carbosilane dendrimers and their siRNA complexes with MCF-7 Cells cultured in 3D spheroids”, **Kamila Białkowska**, Piotr Komorowski, Rafael Gomez-Ramirez, Francisco Javier de la Mata, Maria Bryszewska, Katarzyna Miłowska, *Cells* (11, 1697; DOI: 10.3390/cells11101697) polegał na opracowaniu koncepcji pracy, zaplanowaniu eksperymentów, wykonaniu części eksperymentalnej, przygotowaniu próbek do obrazowania mikroskopowego, opracowaniu i analizie wyników, napisaniu i sprawdzeniu tekstu, przygotowaniu figur, korespondencji z edytorem, przygotowaniu odpowiedzi na recenzje.

Mój wkład oceniam na 70%.

Białkowska

Łódź, dn. 30.05.2022 v.

prof. Katarzyna Miłowska
Katedra Biofizyki Ogólnej
Instytut Biofizyki, Uniwersytet Łódzki,
ul. Pomorska 141/143, 90-236 Łódź

Oświadczenie

Oświadczam, że w pracy:

- “Spheroids as a type of three-dimensional cell cultures – examples of methods of preparation and the most important application”, Kamila Białkowska, Piotr Komorowski, Maria Bryszewska, **Katarzyna Miłowska**, *International Journal of Molecular Sciences* (22, 7097; DOI: 10.3390/ijms22137097) mój wkład w powstanie pracy polegał na współdziale w tworzeniu koncepcji pracy oraz pomocy merytorycznej przy pisaniu pracy i interpretacji wyników badań.

Mój wkład oceniam na 10%.

- “Interaction of cationic carbosilane dendrimers and their siRNA complexes with MCF-7 cells”, Kamila Białkowska, **Katarzyna Miłowska**, Sylwia Michlewska, Paulina Sokołowska, Piotr Komorowski, Tania Lozano-Cruz, Rafael Gomez-Ramirez, Francisco Javier de la Mata and Maria Bryszewska, *International Journal of Molecular Sciences* (22, 7097; DOI: 10.3390/ijms22137097) mój wkład w powstanie pracy polegał na współdziale w tworzeniu koncepcji pracy oraz pomocy merytorycznej przy pisaniu pracy i interpretacji wyników badań.

Mój wkład oceniam na 10%.

- “Interaction of Cationic carbosilane dendrimers and their siRNA complexes with MCF-7 Cells cultured in 3D spheroids”, Kamila Białkowska, Piotr Komorowski, Rafael Gomez-Ramirez, Francisco Javier de la Mata, Maria Bryszewska, **Katarzyna Miłowska**, *Cells* (11, 1697; DOI: 10.3390/cells11101697) mój wkład w powstanie pracy polegał na współdziale w tworzeniu koncepcji pracy oraz pomocy merytorycznej przy pisaniu pracy i interpretacji wyników badań.

Mój wkład oceniam na 10%.

KMiłowska

Łódź, dn. 03.06.2022.....

dr inż. Piotr Komorowski
Laboratorium Biofizyki Molekularnej i Nanostrukturalnej
„Bionanopark” sp. z o. o.,
ul. Dubois 114/116, 93-465 Łódź

Oświadczenie

Oświadczam, że w pracy:

- “Spheroids as a type of three-dimensional cell cultures – examples of methods of preparation and the most important application”, Kamila Białkowska, **Piotr Komorowski**, Maria Bryszewska, Katarzyna Miłowska, *International Journal of Molecular Sciences* (22, 7097; DOI: 10.3390/ijms22137097) mój wkład w powstanie pracy polegał na sprawdzeniu i edycji tekstu.

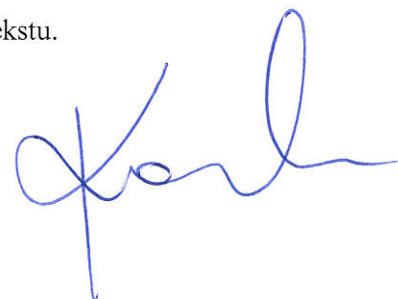
Mój wkład oceniam na 5%.

- “Interaction of cationic carbosilane dendrimers and their siRNA complexes with MCF-7 cells”, Kamila Białkowska, Katarzyna Miłowska, Sylwia Michlewska, Paulina Sokołowska, **Piotr Komorowski**, Tania Lozano-Cruz, Rafael Gomez-Ramirez, Francisco Javier de la Mata and Maria Bryszewska, *International Journal of Molecular Sciences* (22, 7097; DOI: 10.3390/ijms22137097) mój wkład w powstanie pracy polegał na nadzorze nad wykonaniem części badań, konsultacją wyników badań oraz sprawdzeniu i edycji tekstu.

Mój wkład oceniam na 5%.

- “Interaction of Cationic carbosilane dendrimers and their siRNA complexes with MCF-7 Cells cultured in 3D spheroids”, Kamila Białkowska, **Piotr Komorowski**, Rafael Gomez-Ramirez, Francisco Javier de la Mata, Maria Bryszewska, Katarzyna Miłowska, *Cells* (11, 1697; DOI: 10.3390/cells11101697) mój wkład w powstanie pracy polegał na nadzorze nad wykonaniem części badań, konsultacją wyników badań oraz sprawdzeniu i edycji tekstu.

Mój wkład oceniam na 5%.



Łódź, dn. 02.06.2022 r.

prof. Maria Bryszewska
Katedra Biofizyki Ogólnej
Instytut Biofizyki, Uniwersytet Łódzki,
ul. Pomorska 141/143, 90-236 Łódź

Oświadczenie

Oświadczam, że w pracy:

- “Spheroids as a type of three-dimensional cell cultures – examples of methods of preparation and the most important application”, Kamila Białkowska, Piotr Komorowski, **Maria Bryszewska**, Katarzyna Miłowska, *International Journal of Molecular Sciences* (22, 7097; DOI: 10.3390/ijms22137097) mój wkład w powstanie pracy polegał na sprawdzeniu tekstu.

Mój wkład oceniam na 5%.

- “Interaction of cationic carbosilane dendrimers and their siRNA complexes with MCF-7 cells”, Kamila Białkowska, Katarzyna Miłowska, Sylwia Michlewska, Paulina Sokołowska, Piotr Komorowski, Tania Lozano-Cruz, Rafael Gomez-Ramirez, Francisco Javier de la Mata and **Maria Bryszewska**, *International Journal of Molecular Sciences* (22, 7097; DOI: 10.3390/ijms22137097) mój wkład w powstanie pracy polegał na sprawdzeniu tekstu.

Mój wkład oceniam na 5%.

- “Interaction of Cationic carbosilane dendrimers and their siRNA complexes with MCF-7 Cells cultured in 3D spheroids”, Kamila Białkowska, Piotr Komorowski, Rafael Gomez-Ramirez, Francisco Javier de la Mata, **Maria Bryszewska**, Katarzyna Miłowska, *Cells* (11, 1697; DOI: 10.3390/cells11101697) mój wkład w powstanie pracy polegał na sprawdzeniu tekstu.

Mój wkład oceniam na 5%.



Łódź, dn. 05.06.2022.....

dr Sylwia Michlewska
Pracownia Obrazowania Mikroskopowego
i Specjalistycznych Technik Biologicznych
Uniwersytet Łódzki,
ul. Banacha 12/16, 90-237 Łódź

Oświadczenie

Oświadczam, że w pracy:

- “Interaction of cationic carbosilane dendrimers and their siRNA complexes with MCF-7 cells”, Kamila Białkowska, Katarzyna Miłowska, **Sylwia Michlewska**, Paulina Sokołowska, Piotr Komorowski, Tania Lozano-Cruz, Rafael Gomez-Ramirez, Francisco Javier de la Mata and Maria Bryszewska, *International Journal of Molecular Sciences* (22, 7097; DOI: 10.3390/ijms22137097) mój wkład w powstanie pracy polegał na wykonaniu obrazów mikroskopowych (mikroskop konfokalny) i sprawdzeniu tekstu.

Mój wkład oceniam na 5%.



Łódź, dn. 03.06.2022.....

dr Paulina Sokołowska
Zakład Farmakologii i Toksykologii,
Katedra Farmakologii Ogólnej,
Klinicznej i Toksykologii
Uniwersytet Medyczny,
ul. Żeligowskiego 7/9, 90-752 Łódź

Oświadczenie

Oświadczam, że w pracy:

- “Interaction of cationic carbosilane dendrimers and their siRNA complexes with MCF-7 cells”, Kamila Białkowska, Katarzyna Miłowska, Sylwia Michlewska, **Paulina Sokołowska**, Piotr Komorowski, Tania Lozano-Cruz, Rafael Gomez-Ramirez, Francisco Javier de la Mata and Maria Bryszewska, *International Journal of Molecular Sciences* (22, 7097; DOI: 10.3390/ijms22137097) mój wkład w powstanie pracy polegał na opisanu części dotyczącej testu XTT.

Mój wkład oceniam na 5%.

P. Sokołowska

Madrid, May 19th 2022

Dr. Tania Lozano-Cruz
Department of Organic and Inorganic Chemistry
University of Alcalá
e-mail: tania.lozano@uah.es

Statement

I hereby declare that my contribution to the considered papers entitled:

- “Interaction of cationic carbosilane dendrimers and their siRNA complexes with MCF-7 cells” by Kamila Białkowska, Katarzyna Miłowska, Sylwia Michlewska, Paulina Sokołowska, Piotr Komorowski, **Tania Lozano-Cruz**, Rafael Gomez-Ramirez, Francisco Javier de la Mata and Maria Bryszewska in *International Journal of Molecular Sciences* (22, 7097; DOI: 10.3390/ijms22137097) consisted of synthesis of dendrimers and manuscript proofreading.

My contribution is estimated at 5%.



Dr. Tania Lozano-Cruz

Madrid, May 19th 2022

Prof. Rafael Gomez-Ramirez
Department of Organic and Inorganic Chemistry
University of Alcalá
e-mail: rafael.gomez@uah.es

Statement

I hereby declare that my contribution to the considered papers entitled:

- “Interaction of cationic carbosilane dendrimers and their siRNA complexes with MCF-7 cells” by Kamila Białkowska, Katarzyna Miłowska, Sylwia Michlewska, Paulina Sokołowska, Piotr Komorowski, Tania Lozano-Cruz, **Rafael Gomez-Ramirez**, Francisco Javier de la Mata and Maria Bryszewska in *International Journal of Molecular Sciences* (22, 7097; DOI: 10.3390/ijms22137097) consisted of synthesis of dendrimers and manuscript proofreading.

My contribution is estimated at 5%.

- “Interaction of Cationic Carbosilane Dendrimers and Their siRNA Complexes with MCF-7 Cells Cultured in 3D Spheroids” by Kamila Białkowska, Piotr Komorowski, **Rafael Gomez-Ramirez**, Francisco Javier de la Mata, Maria Bryszewska and Katarzyna Miłowska in *Cells* (11, 1697; DOI: 10.3390/cells11101697) consisted of synthesis of dendrimers and manuscript proofreading.

My contribution is estimated at 5%.



Prof. Rafael Gomez-Ramirez

Madrid, May 19th 2022

Prof. Francisco Javier de la Mata
Department of Organic and Inorganic Chemistry
University of Alcalá
e-mail: javier.delamata@uah.es

Statement

I hereby declare that my contribution to the considered papers entitled:

- “Interaction of cationic carbosilane dendrimers and their siRNA complexes with MCF-7 cells” by Kamila Białkowska, Katarzyna Miłowska, Sylwia Michlewska, Paulina Sokołowska, Piotr Komorowski, Tania Lozano-Cruz, Rafael Gomez-Ramirez, **Francisco Javier de la Mata** and Maria Bryszewska in *International Journal of Molecular Sciences* (22, 7097; DOI: 10.3390/ijms22137097) consisted of synthesis of dendrimers and manuscript proofreading.

My contribution is estimated at 5%.

- “Interaction of Cationic carbosilane dendrimers and their siRNA complexes with MCF-7 Cells cultured in 3D spheroids” by Kamila Białkowska, Piotr Komorowski, Rafael Gomez-Ramirez, **Francisco Javier de la Mata**, Maria Bryszewska and Katarzyna Miłowska in *Cells* (11, 1697; DOI: 10.3390/cells11101697) consisted of synthesis of dendrimers and manuscript proofreading.

My contribution is estimated at as 5%.



Prof. Francisco Javier de la Mata